UNIVERSIDAD COMPLUTENSE DE MADRID

FACULTAD DE FARMACIA

Departamento de Química en Ciencias Farmacéuticas

TESIS DOCTORAL

DISEÑO Y DESARROLLO DE NUEVAS BIOTINTAS Y ESTRATEGIAS DE BIOIMPRESIÓN PARA PRODUCIR EQUIVALENTES SIMPLIFICADOS DE TEJIDOS HUMANOS, PARA SU USO EN LA TIERRA Y EN MISIONES EXPLORATORIAS ESPACIALES

("Design and development of new bioinks and bioprinting strategies to produce simplified equivalents of human tissues, for earth and space exploration applications")

NIEVES CUBO MATEO

Tutora: María Victoria Cabañas, QUICIFAR, UCM

Director: Luis Rodríguez-Lorenzo, ICTP-CSIC

Memoria presentada para
aspirar al grado de DOCTORA
en Madrid, Septiembre de 2020

UNIVERSIDAD COMPLUTENSE MADRID

DECLARACIÓN DE AUTORÍA Y ORIGINALIDAD DE LA TESIS PRESENTADA PARA OBTENER EL TÍTULO DE DOCTOR

D./Dña. Nieves Cubo Mateo,
estudiante en el Programa de Doctorado en Farmacia (D9BI),
de la Facultad de Farmacia de la Universidad Complutense de Madrid, como autor/a de la tesis presentada para la obtención del título de Doctor y titulada:

Diseño y desarrollo de nuevas biotintas y estrategias de bioimpresión para producir equivalentes simplificados de tejidos humanos, para su uso en la tierra y en misiones exploratorias espaciales

y dirigida por: Luis Rodríguez Lorenzo
(Tutora UCM: María Victoria Cabañas)

DECLARO QUE:

La tesis es una obra original que no infringe los derechos de propiedad intelectual ni los derechos de propiedad industrial u otros, de acuerdo con el ordenamiento jurídico vigente, en particular, la Ley de Propiedad Intelectual (R.D. legislativo 1/1996, de 12 de abril, por el que se aprueba el texto refundido de la Ley de Propiedad Intelectual, modificado por la Ley 2/2019, de 1 de marzo, regularizando, aclarando y armonizando las disposiciones legales vigentes sobre la materia), en particular, las disposiciones referidas al derecho de cita.

Del mismo modo, asumo frente a la Universidad cualquier responsabilidad que pudiera derivarse de la autoría o falta de originalidad del contenido de la tesis presentada de conformidad con el ordenamiento jurídico vigente.

En Madrid, a 12 de septiembre de 2020

Fdo.: CUBO MATEO NIEVES - 11866399D

Firmado digitalmente por CUBO MATEO NIEVES - 11866399D
Fecha: 2020.09.12 21:02:57 +02'00'

Esta DECLARACIÓN DE AUTORÍA Y ORIGINALIDAD debe ser insertada en la primera página de la tesis presentada para la obtención del título de Doctor.

"DESIGN AND DEVELOPMENT OF NEW BIOINKS AND BIOPRINTING STRATEGIES TO PRODUCE SIMPLIFIED EQUIVALENTS OF HUMAN TISSUES, FOR EARTH AND SPACE EXPLORATION APPLICATIONS"

NIEVES CUBO MATEO

A research about Materials Science and Engineering, Biology, Tissue Engineering, Space Exploration, Bioprinting and Future

PHD THESIS

FACULTAD DE FARMACIA
Universidad Complutense de Madrid

In collaboration with ICTP-CSIC and TU Dresden

September 2020

SUPERVISED BY:

Tutor: María Victoria Cabañas, QUICIFAR, UCM

Director: Luis Rodríguez-Lorenzo, ICTP-CSIC

International supervisor: Michael Gelinsky

LOCATION:

Madrid, Spain

Dresden, Germany

TIME FRAME:

October 2016 - September 2020

Nieves Cubo Mateo: *"Design and development of new bioinks and bioprinting strategies to produce simplified equivalents of human tissues, for earth and space exploration applications"*. A research about Materials Science and Engineering, Biology, Tissue Engineering, Regenerative Medicine, Space Exploration, Robotics, Bioprinting and Future, PhD Thesis, September 2020.

"Sic Itur Ad Astra"

(...so we go to the stars...)

— Jacques Etienne Montgolfier

"Nothing in life is to be feared, it is only to be understood.
Now is the time to understand more, so that we may fear less."

— Marie Curie

Dedicated to all the people who made it possible

2012* – 2020

ABSTRACT [EN]

Fifty years after the first human landed on the Moon mankind has started to plan the next steps for manned space exploration missions. When the time required to return to Earth exceeds 400-500 days (as in travels to Mars), the level of independence that the crew must possess is highly increased. To ensure the survival and good living conditions of this future explorers, new developments regarding medical infrastructure and resources must be carried out.

In this work, the topic of this study was to investigate how 3D printing and bioprinting can be of use to improve the autonomy of the crew when facing the most probable clinical scenarios that can occur in long-term space exploratory missions. The printing parameters of thermoplastics, such as polycaprolactone (PCL), that can be used as a possible support material along bioprinting were studied, including the use or not of alternate layers or the printing starting point. For bioprinting, and taking bone constructs as the tissue of study, a new bioink based on human plasma (which potentially could be derived from the injured astronaut who needs the treatment), alginate, and methylcellulose (that can be grow and used in isolated areas) was designed. An inverted bioprinter was designed and built to be able to test the work capacity of this biomaterial in altered gravity conditions.

As result, it was observed that the use of alternated layers involves the generation of more anisotropic structures, as the z-axis pore is limited to the layer height, while the x and y-pore size can be tailored to specific needs. The defects created because of the alignment, or the lack of it, at the new layer starting point, significantly affects the mechanical behavior of the scaffolds.

The cooling down rate, or even printing speed, can be modified to obtain more chaotic micropatterns including nanofibers without the need of using further technologies. A plasma-based bioink was successfully designed and combined with hydroxyapatite-forming CPC which resembles the native mineral phase of bone. The results have shown that the plasma-based bioink and CPC form a synergistic system supporting adhesion, proliferation, and osteogenic differentiation of bone cells.

Thanks to the inverted bioprinter, it has been demonstrated that the developed bioinks and support materials, like CPC, are suitable for extrusion (bio)printing. They are so adhesive that they can even be printed upside-down and therefore, against Earth's gravity. Therefore, they could be used at altered gravity conditions on space exploration missions.

RESUMEN [ES]

Cincuenta años después de que el primer ser humano aterrizara en la Luna, la humanidad ha comenzado a planificar los próximos pasos para las misiones de exploración espacial tripuladas. Cuando el tiempo necesario para regresar a la Tierra supera los 400 - 500 días (como en los viajes a Marte), el nivel de independencia que debe poseer la tripulación aumenta considerablemente. Para garantizar la supervivencia y las buenas condiciones de vida de estos futuros exploradores, se deben realizar nuevos desarrollos en cuanto a infraestructuras y recursos médicos.

En este trabajo, se estudió cómo la impresión 3D y la bioimpresión pueden ser de utilidad para mejorar la autonomía de la tripulación ante los escenarios clínicos más probables que pueden ocurrir en misiones de larga duración. Para ello se estudiaron algunos parámetros de impresión de termoplásticos, como la policaprolactona (PCL), que pueden utilizarse

como posible material de soporte a lo largo de la bioimpresión (ejemplo de parámetros: uso o no de capas alternas o la alineación del punto de partida de la impresión en cada capa). Para la bioimpresión, y tomando las construcciones óseas como tejido de estudio, se diseñó un nuevo material compuesto a base de plasma humano (que puede ser obtenido de los astronautas), alginato y metilcelulosa (que se puede obtener y utilizar en áreas aisladas). Se diseñó y construyó una bioimpresora invertida para poder probar la capacidad de trabajo de este biomaterial en condiciones de gravedad alterada.

Como resultado se obtuvo que el uso de capas alternas implica la generación de más estructuras anisotrópicas, ya que normalmente el poro del eje z está limitado a la altura de la capa, mientras que el tamaño de los poros x e y se pueden adaptar a necesidades especıificas. Los defectos creados por la alineación, o la falta de ella, en el punto de inicio de la nueva capa, afectan significativamente al comportamiento mecánico de los andamios. La velocidad de enfriamiento, o incluso la velocidad de impresión, se puede modificar para obtener micropatrones más caóticos, incluso nanofibras, sin necesidad de utilizar tecnologías adicionales. Se diseñó con éxito una biotinta a base de plasma y se combinó con un cemento de fosfato cálcico formador de hidroxiapatita, que se asemeja al mineral nativo del hueso. Nuestros resultados mostraron que la deposición combinada de la biotinta basada en plasma y la pasta de CPC para dar lugar a constructos celularizados, forman un sistema sinérgico que apoya la adhesión, la proliferación y la diferenciación osteogénica de las células óseas.

Gracias a la bioimpresora invertida desarrollada, se ha podido demostrar que la biotinta desarrollada y los materiales de soporte, como el cemento óseo de fosfato cálcico autoajustable, son aptos para la (bio)impresión extrusión. Son tan adhesivos que incluso se pueden imprimir al revés y, por lo tanto, contra la gravedad de la Tierra, pudiendo usarse en condiciones de gravedad alterada.

ABOUT THE AUTHOR & BACKGROUND

This work is result of the curiosity and the evolutive study that started in 2012 by Nieves Cubo-Mateo, who is a passionate advocate for 3D printing and the sharing of knowledge.

She was a **Bachelor student in Industrial Electronics and Automation Engineering** (UC3M, Sept 2009- Oct 2013) when she started working with **3D Printers.** Since the beggining, she saw the huge potential of this open-source technology, and started working on the development of new libraries [1] and printable parts to create new extruders and improve printers and educational robots.

At the end of her Bachelor's, she contacted different departments of her university asking for a collaboration to develop a new type of printer capable of working with different materials. This way, she enrolled in a **Master in Materials Science and Engineering** and started to work with the **Bioengineering and Aerospacial Engineering Department** in the development of what was considered "**the first bioprinter capable of creating functional dermo-epidermal skin equivalents**".

This was her first contact with biology and the Tissue Engineering field, and where she started working with human plasma. Since then, she has studied the application of this natural material for the design of bioinks, developing protocols and open-source machines to create accesible technologies, applicable also in isolated areas with low resources.

This PhD thesis was partly motivated by the needs for novel, improved medical treatment options for far-distant space exploration missions as defined by a call from the European Space Agency (ESA). This call on "3D Printing of Living Tissue for Space Exploration" (PLT-Space, call No. AO/1-9028/17/NL/BJ/gp) was published in 2017 and the related study started in May 2018. Main contractor for ESA in this project was the German company OHB System SE (Bremen) which collaborated with the lab of Prof. Michael Gelinsky at TU Dresden (Germany), acting as a sub-contractor of OHB (contract No. 4000123640/17/NL/BJ/gp/TUD).

During her time at TU Dresden Nieves Cubo-Mateo was part of the team, working within this sub-contract on the PLT-Space study. Although this study has ended December 31, 2019 ESA continues to work on this topic and currently is planning to build a bioprinting and 3D cell culture module for the European Laboratory at the International Space Station (ISS).

She, as part of PLT-Space team, defendend parts of the work, presented in this thesis in different closed meetings at ESA.

Some ideas and figures may have appeared previously in the following publications, focused on 3D printing of human skin, before the start of the PhD thesis.

1. Bachelor's final project - October 2012: "Design, construction and evaluation of a cellular deposition system for its use in 3D printers". Author: Nieves Cubo Mateo.
2. ESB Conference - September 2015 **(Oral presentation awarded by the European Society of Biomaterials as best oral presentation.)** - Talk 176 (Sesion 36, Hall 4A, Advance Manufacturing 2: "3D Bioprinting of Functional Fibrin-Based Skin Equivalents".

The rest of the publications related with the work here presented can be found at Appendix C.

RELATED MEDIA

1. **25 - Jan - 2017** [International media, from Uc3M press release]: 3-D bioprinter produces functional human skin 'suitable for transplant'. More information available at: https://www.medicalnewstoday.com/articles/315452.php

2. **20 - Nov - 2018** [ESA bulletin and press release]: 3D printing skin bone and body parts under study for future astronauts. More information: https://www.esa.int/Our_Activities/Space_Engineering_Technology/3D_printing_skin_bone_and_body_parts_under_study_for_future_astronauts

3. **09 - Jul - 2019** [ESA boletin and press release]: Upside-down 3D-printed skin and bone for humans to Mars. More information: https://www.esa.int/Our_Activities/Space_Engineering_Technology/Upside-down_3D-printed_skin_and_bone_for_humans_to_Mars

CONTENTS

LIST OF FIGURES

LIST OF TABLES

ACRONYMS

3D	Three dimensions / three dimensional
3DBP	3D Bioprinting
3DP	3D Printing
alg	Alginate
AEMPS	Agencia Española del Medicamento y Productos Sanitarios
AM	Additive Manufacturing
AT	Advance Therapies
ATMP	Advanced Therapy Medicinal Products
BD	Bone densitometer
CAD	Computer Aided Design
C.C.S-A	Creative Commons Share Alike (License)
CPC	Calcium Phosphate Cement
CT	Computerized Tomography
d	days, used following a number
DEXA	Dual-Energy X-ray Absorptiometry
DIY	Do It Yourself, self made
DMEM	Dulbecco's Modified Eagle's Medium
EC	European Commission
ECM	Extracellular Matrix

EMA	European Medicines Agency
ESA	European Space agency
ESTEC	European Space Research and Technology Centre
FDA	Food and Drug Agency
FDM	Fused deposition modelling
FRSM	Fund for Medical Scientific Research
FNRS	National Fund for Scientific Research
FTIR	Fourier-transform Infrared Spectroscopy
G	Standard value of acceleration due to gravity, 9.81 $m.s^{-2}$
GMP	Good Manufacturing Practice
HBSS	Hanks' Balanced Salt solution
HEKn	Human Epidermal keratinocytes (=hKC)
hFB	Human fibroblasts
hKC	Human keratinocytes
hTERT	Human telomerase reverse transcriptase
HUVEC	human umbilical vein endothelial cells
ISS	International Space Station
ISECG	International Space Exploration Coordination Group
LVR	Linear Viscoelastic Region
mc	Methylcellulose
MDR	Medical Device Regulation
MSC	Mesenchymal Stem Cells
MSG	Microgravity Science Glovebox

OCT	Optical Coherence Tomography
PBS	Phosphate Buffered Saline
PCL	Polycaprolactone
RP	Rapid Prototyping
RGD	Arginine, Glycine, and Aspartate (Arg-Gly-Asp) tripeptide
RDM	Re-distributed Manufacturing
STL	Standard Tessellation Language
TE	Tissue Engineering
TEP	Tissue Engineering Product
TERM	Tissue Engineering and Regenerative Medicine
TSP	Tissue Sharing Program
w/v	Weight/Volume percentage concentration. Grams of solute per 100 mL of solvent

Part I

BACKGROUND AND RESEARCH OBJECTIVES

- **Chapter 1. Introduction**
  - Introduction and motivation of the work
  - Research hypothesis and objectives

Space exploration started with humans looking up into the night sky, looking for answers to questions like "Why are we here?", "Why do we have seasons, or day and night?", "Are we alone?", "What else is out there?".

In this first part, the main reasons for space exploration and the needs that it entails will be discussed, along with the requirements for the next steps on this exploratory travel, where bioprinting can be a key enabling technology.

To finalise the introduction, the main objectives of this dissertation will be listed.

1

INTRODUCTION & OBJECTIVES

Humans are continuously pushing the boundaries of science and technology to overcome the limitations they can find along their journey. The main reason for this behaviour can be found in our curious nature that drives us to explore and challenge our own limits. We need to understand the origin of the things and how they work. But we also want to know what is ahead, how the future will change our lives and how should we adapt to optimize that prospective scenario.

Space exploration is driven by the advances in technology and science carried out on the Earth. However, it must be remarked that also many of those advances used in the outer space, are then transferred back to the Earth. We cross every day with materials that have been developed for space applications: the Velcro pads that keeps our coats close, the scratch-resistant material that protects our glasses, some shock-absorption materials employed in artificial limbs, some enriched baby food, etc[1].

The farther we go into space, the higher is the complexity of the missions as it will entail longer travel times and long exposure of humans to space environmental conditions (as high levels of radiation or altered gravity). When the distance to the Earth increases, no fast return in case of emergency is possible. Crews on such missions have to be self-sustaining, not only concerning nutrition, oxygen supply or waste removal but also with respect to medical treatment. In addition, the health risks, illnesses or injuries that humans face on the Earth are also present in space.

1 Information obtained from nasa.gov, accesses the 24.06.2019.

Because of this, life support systems on-board of space crafts or at extra-terrrestrial human settlements, must be reliable and must cover as many clinical scenarios as possible, while keeping their simplicity, as the available space on-board is limited and very valuable.

Therefore, multi-purpose machines and tools are preferable. Also tools and materials that can be obtained on demand will allow the crew to reduce the amount of initial materials required to be launched. In this regard, it has been already established that 3D printing can be of use on-board for the creation of personalized tools when needed [9].

What if this technology can also be used in the same way to create personalized human tissues along space exploration missions?

1.1 MOTIVATION

The focus of this Thesis is to analyse and try to demonstrate if 3D printing of living tissues (bioprinting) is of interest for the scenarios described below (space exploration missions) and whether it can be translated to space conditions.

Prior to establish the objectives and hypotheses of this work, it is necessary to understand a little bit further the 3 main pillars of this study:

- Space exploration aims and challenges: which are the main clinical scenarios ahead?
- 3D printing, as an accessible, flexible and reproducible technology: can it be used as a multi-purpose tool at isolated areas with limited space and materials?
- Tissue engineering (TE), regeneration of human tissues: where are we? What do we need to achieve to consider success? What is needed to transfer TE technology into space exploration conditions?

1.1.1 *Exploratory missions*

Space exploration started thousands of years ago, with humans looking up into the night sky, looking for answers to questions like "Why are we here?", "Why do we have seasons, or day and night?", "Are we alone?", "What else is out there?".

"The Earth is the cradle of humanity, but mankind cannot stay in the cradle forever."

1911, Konstantin Tsiolkovsky

The launch of the first human-made object to orbit Earth was performed by the Soviet Union's Sputnik 1, on 4 October 1957 and four years layer (1961) on April 12, Russian Yuri Gagarin became the first human to orbit Earth in Vostok 1. Apollo 11 was the first manned mission to land on the Moon, on 20 July 1969. Since then, many other landers and orbiters have been launched to the Moon and recently, to Mars.

Twenty years after the first man touched the Moon, at the Apollo 11 20th Anniversary Celebration at the National Air and Space Museum, President Bush declared: *"I'm proposing a long-range continuing commitment: First, for the coming decade, for the 1990's, Space Station Freedom [...]; and next, for the new century, back to the moon, back to the future, and this time, back to stay. And then a journey to another planet, a manned mission to Mars."* That is how at the end of the 20th century, the International Space Station (ISS) was launched into orbit (1998).

Figure 1.1: Space agencies involved in the ISS coordination group.

All this efforts are driven by the pursue of humans to discover new life, to understand how everything started, to identify new resources, to inspire and educate. Knowing more about the outer space we can protect ourselves better from possible space threats, extend human presence deeper into the solar system and ensure a better future.

Since the beginning of the 21^{st} century, when the first astronauts arrived, the ISS serves as a microgravity and space environment research laboratory in which crew members conduct experiments in biology, physics, astronomy, etc. It serves as the first stage on the journey to Mars, as it provides a platform to test and study factors as human health and deconditioning in weightlessness.

"Every vision is a joke until the first man accomplishes it; once realised, it becomes commonplace."
1920, Robert H.Goddard

Although the Moon does not present the characteristics required to establish permanent camps there (mainly because of the moon dust hazard [10]), it serves as a good precursor and as a training platform for Mars exploration and settlement [11]. However, when thinking about further planets as Mars, the technical requirements of the mission increase as the crew will face more adversities and because of the long distances, they need to be autonomous, even in cases of accidents.

In this regard, 3D printing can support the generation of tools and other objects under demand, allowing the crew to manufacture tailored elements when required and in an automatic way. As they work with thermoplastics, the possibility of recycling is high, which is also an advantage for them, as it would fit in the sustainability engagement that is needed in a close live system (like at circular economy).

Which are the main clinical scenarios that astronauts will have to face in the proposed exploratory missions? Is there a need of new technologies and methodologies?

1.1.2 *3D Printing - Accessible technology*

Additive manufacturing (AM), also known as 3D printing, includes today a wide range of advanced manufacturing techniques where the material is added layer-by-layer, offering promising solutions for tailored, short-production runs. AM was initially termed as Rapid Prototyping (RP) and the expression was used in industry to describe a group of processes for rapidly creating a system or the physical representation of a part before its final release to the market. It was emphasized that the goal of this group of processes was to quickly create an object and that the outcome would be used as a prototype, which future models or parts will derive from. However, today it use has spread, and now final products are also build with these technologies.

Besides the obvious benefit of a manufacturing approach that can operate in an autonomous manner, increasing production and reducing cost, one of the major advantages that AM has to offer is the ability to directly deliver physical assets free from any geometrical limitation, i.e. complex replacement parts. Therefore, at least in theory AM can be used in situations where a structure with special topology or tailored porosity is needed. These physical objects can be obtained directly from Computer Aided Design (CAD) models or - in case of patient-specific, anatomical objects - from 3D medical data (CT or MRI), obtaining a digital data sheet that defines the final dimensions of the object [12].

This technology has spread widely in the last years, making itself room in different industries as machine building, architecture, clothes, food, education, aerospace and also medicine. In the latter, devices as prostheses, orthoses, or individual polymer casts for fracture stabilization can be made using different AM technologies. Also personalized anatomical models and guides for surgery have been introduced, as well as patient-specific implants, leading to more precise surgeries while saving time in the operating room and costs [13].

In combination with proper materials, AM can also provide clinicians and medical students with 3D models (phantoms) that can be used for training as they give back tangible information of anatomic and pathological models that can be used to plan/train surgeries or as educational resources [14].

How can this flexible technology be of use in space / extra terrestrial settlements? What is required for the translation? Can we simulate those conditions on Earth for testing?

1.1.3 *From Tissue Engineering to Bioprinting*

In the last decades the gap between available donor organs for transplantation and patients urgently needing new organs increased continuously. Mostly because of this, researchers from different fields are trying to join efforts to achieve new methodologies in order to obtain human tissue and organ equivalents, suitable for implantation. That is how tissue engineering (TE) started.

The first successful tissue-engineered skin products were made in the late 1970s and early 1980s [15]. Most would agree that this is when modern tissue engineering really started, although the term "tissue engineering" was coined later, around 1987 [16]. Regarding space, TE experiments with classical methods started in the late 80's, showing that microgravity might benefit TE by promoting cell-cell association while minimizing turbulence and shear stress. Indeed, cells in suspension tend to aggregate when exposed to microgravity [17, 18] which can nowadays be used for inkjet printing or for magnetic levitation. For bone and cartilage tissues, it has also been demonstrated that cartilage constructs flown in space are mechanically inferior to constructs grown on Earth while those generated in rotative wall vessel (RWV) bioreactors are quite similar in both composition and mechanical strength to natural cartilage [19].

From a general perspective, tissue engineering describes the formation of

living tissue outside of a living organism (*ex vivo*), i.e., in a tissue culture lab (*in vitro*). In most cases, a natural or synthetic volumetric matrix (*"scaffold"*) is seeded with cells and then further cultivated until the maturation of the tissue occurs (Figure 1.2). But when a clinical application is intended, these constructs should consist of a biodegradable material that will act as temporal support only, but then give space for the formation of a new biological extracellular matrix (ECM) and ingrowth of new tissue after implantation.

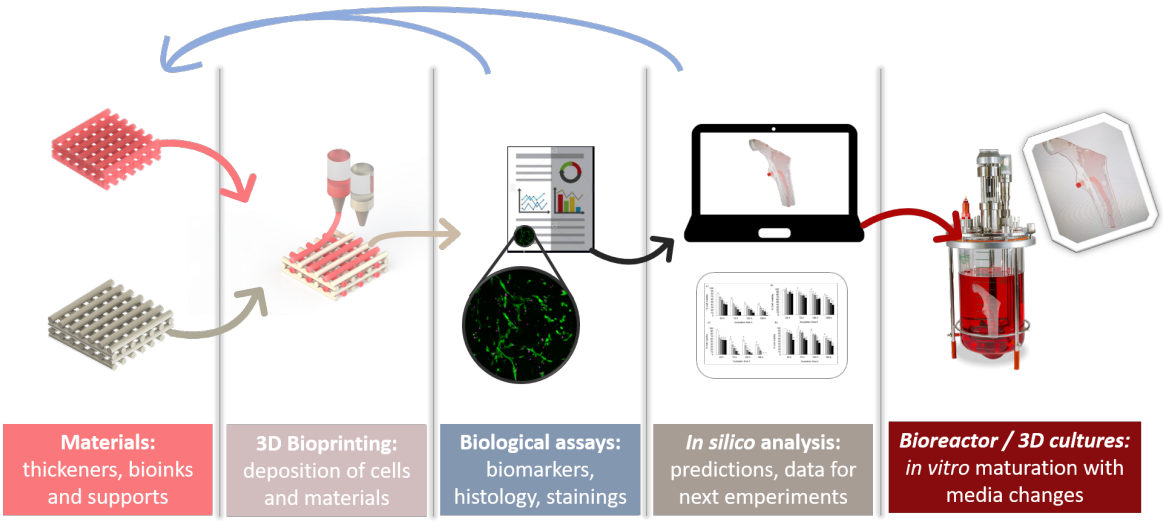

Figure 1.2: Steps required for the development of matured tissues from bioprinted constructs.

These engineered tissues can be built principally following two different strategies:

- Manufacturing porous scaffolds with classical methods (as gas foaming, solvent casting, fibre bonding, phase separation, particulate leaching and freeze drying [20]) or printing inert, acellular scaffolds onto which cells are seeded posterior **(Tissue Engineering, TE)**.

- Creating cell-containing constructs in one step, embedding cells inside the deposited biomaterials in a controlled way (Figure 1.2) **(Bioprinting)**.

The limitations of the traditional methods are that in all these techniques,

acellular scaffolds were created first and seeded subsequently. Because of this, only one cell type (or a homogeneous mixture of cells) can be introduced into the scaffold, either by gravity or with a forced flow, mostly leading to uneven cell distributions. The limitation to one cell type (or homogeneous cell mixtures) prevents fabrication of complex tissues or organs, always consisting of several cell types, spatially arranged in a highly controlled manner.

In contrast, in the second approach derived from AM, 3D bioprinting offers the possibility of fabricating tissue equivalents or even organ-like constructs, either autologous or allogeneic, by printing multiple cells, soluble factors and biomaterials simultaneously, following a precise predesigned pattern. Utilization of AM technologies in both approaches - scaffold fabrication for conventional TE as well as 3D bioprinting - opens up the possibility to manufacture constructs, patient-specific in size and shape.

Can bioprinting be used in altered gravity conditions to create tissue substitutes? Where can the materials be obtained?

1.2 RESEARCH HYPOTHESES AND OBJECTIVES

Research ► hypotheses

The aim of this thesis is to answer the following **research hypotheses**:

- Which are the main clinical scenarios that crew will face on the Moon, Mars or in a low Earth orbit (LEO) mission - as at the ISS station or the Deep Space Gateway - and how bioprinting can be a technology of interest for such missions?
- Is it feasible to translate this technology to altered gravity environments? How can we demonstrate it on Earth?
- Which are the materials that fit better to the technical requirements obtained? Can we develop a bioink for the bioprinter based on them

(to create the selected tissue of interest)?

As final experimental result, the aim is to develop a proof of concept (POC) of printed human tissues (skin/bone) that can be potentially manufactured under space conditions. To achieve this goal, and given the multidisciplinary nature of this task, a wide research in the state of the art of different fields is first required. Some of this topics are space exploration and its conditions, 3D printing, bioprinting, tissue engineering and biomaterials.

The work to perform along this project will entail activities belonging to areas of knowledge as diverse as:

◄ ***Fields involved:***

- Engineering

- Space Sciences

- Computer sciences

- Biology

- Material sciences

- **Industrial Engineering:** mechanical design and calculations.
- **Space Sciences:** to understand which are the needs and the technical requirements to be faced in the outer space and on the targeted planetary bodies.
- **Computer Sciences:** programming of the printer (firmware) and creation of the deposition paths (G-Codes) trought scripts (Python).
- **Material Sciences and Technology:** biomaterial selection and test.
- **Biology:** tissue regeneration strategy selection, cell culture methodologies and characterization of the results.

The final aim of this project wass to answer some research hypothesis related with the use of bioprinting under space environmental conditions. Also, the development of a proof of concept (POC) of a printed human tissue that can be potentially manufactured under such conditions wass desired.

1.2.1 *Specific objectives*

► ***Specific objectives***

To fulfil the above mentioned aim, different steps and developments are required. The specific objectives or milestones proposed for the current study are:

1. Research and drafting of an **updated State of the Art** in the current topic (space medicine) with special attention to the use of 3D printing and bioprinting.
2. **Study** of the possible **mission scenarios** and the **clinical cases**, selecting the **tissues of interest** for the study.
3. **Selection** of already available **biomaterials** to be used as a bioprinting matrix (**bioink**) for the generation of the chosen tissue/s demonstrators and study of the 3D printing process to create biphasic constructs.
4. If possible, the **design and development of new biomaterials/bioinks** to create volumetric, size relevant tissues (using bone as model), that can be use in space contidions, procuring a good cell viability.
5. **Design and manufacture of a paste extruder** adaptable to a DIY 3D printer that **works under the desired gravity conditions**, adapting also the firmware for the 3D printer electronics.
6. **Biological assays** to test the biocompatibility and functionality of the proposed materials and strategies, and to characterize the tissue evolution *in vitro*.

1.2.2 *Outline*

For a better understanding of the current document, it has been separated in 4 main parts. The first one, where this outline is included, is an introduction to the topic of the Thesis, where the main research

problems and hypothesis are contained. Afterwards, the theoretical part of the study has been included, covering space exploration scenarios and focusing on 3D printing and bioprinting. To continue, three chapters covering the development and test of the bioinks, support materials and the space condition POC workbench, can be found. Finally a closure chapter of conclusions, to summarize the work and the contributions derived from it, has been added.

To simplify the experimental data and protocols to the reader, the information regarding materials and methodology has been included as an appendix for both, the technical and the scientific experiences, at the end of Part iii. For a more detailed reading, also the related publications and supplementary information have been attached.

In summary, the rest or the document has been separated into the following chapters:

◀ *A summary of the document structure*

- **Chapter 2 - State of the Art on Exploratory missions:** Which are the possible scenarios we will have to face in the next missions due to the main health hazards entailed and which technical requirements are raised. Here the technologies that will be used along the project are selected.
- **Chapter 3 - Design of the experiment:** case study of the main clinical scenarios, and study of how 3D printing and bioprinting can be of use in the planned missions.
- **Chapter 4 - Development of a new construct for bone regeneration:** step-by-step development of the plasma-based bioink and how it has been combined to other existent materials (as polycaprolactone or calcium phosphate cements) to obtain reinforced mineral structures.
- **Chapter 5 - Development of a proof of concept workbench for space conditions, the inverted bioprinter:** development of the setup that

will allow to carry out the proof of concept, when printing in altered gravity, on Earth.

- **Chapter 6 - Research procedures and protocols**: detailed information from the experimental part.
- **Chapter 7 - Answers to research hypothesis and questions:** related with the initial goals and research hypothesis.
- **Chapter 8 - Conclusions:** brief conclusions for each part of the thesis.

Part II

STATE OF THE ART

- **Chapter 2. State of the ART**
  - Medical approaches in space environments
  - 3D Printing as a tool for tissue engineering
  - 3D Printing/bioprinting in Space

Before starting the study, an exploratory research is required to understand what is already done, which are the main limitations to overcome and where can we find the technical specifications for our development. For that, the medical approaches used in space environments will be reviewed, along with the use of 3D printing and bioprinting.

2

STATE OF THE ART: SPACE MEDICINE, 3D PRINTING AND BIOPRINTING

◀ *Obj. 1*

SOTA Research

In this chapter a brief review with the current medical treatments performed out of the Earth, and the state-of-the-art of 3D printing/bioprinting for skin and bone is included. To finalize, joining this two topics, a study regarding which 3D printing / bioprinting experiments have been already carried out at the ISS is also included.

2.1 MEDICAL APPROACHES IN SPACE ENVIRONMENTS

The considered diseases and health incidents have been assessed and statistically gathered in studies, such as the HUMEX study [21] or Human Health and Performance Risks of Space Exploration Missions [22]. They refer to incidents that happened during space missions in the past, such as medical events during space shuttle programs, on Mir, on the ISS, etc. But also, terrestrial analogues are considered, such as submarine patrols or Antarctica research missions.

The most common incidents involved injuries, such as bruises, sprains etc., skin issues, such as burns or cuts, and heart problems, such as arrhythmias. Generally, these medical events have been harmless and could be treated onboard with drugs. However, although they are rare, the most catastrophic health incidents leading to mission abortion and/or dead of one of the astronauts have to be taken into account. These include severe

injuries, electrical or chemical burns, organ damage, such as appendicitis, heart attacks, strokes etc.. Only recently the latest Mars simulation activity HI-SEAS mission VI had to be interrupted because one of the team members has been injured and needed medical attention, [23]. Thus, it is of great importance for future space exploration missions, which can not rely on medical infrastructure on Earth by a fast return, to treat such serious medical events autonomously or with a communication link to Earth.

Before actually considering the medical treatment procedures, it is worth spending some time on mitigation strategies which minimize the risk of such health incidents. In order to reduce the risk coming from radiation exposure, a radiation shield is needed and a radiation threshold for human beings shall be defined based on the maximal exposure of blood forming organs (BFO). The threshold value can be based on experiences from previous missions on the ISS, but also from people who work with radioactive material in their jobs. Then the consequences from reduced gravity, such as bone demineralization or decreased exercise capacity, can be confronted with physical training during the astronauts permanence in space.

In order to mitigate the risks of health issues during an EVA, the astronauts need training under similar conditions, such as wearing space suits etc.. In case of an emergency, the astronaut has to be quickly returned to the planetary base station, so that a first medical treatment can be done. Thus, it is useful to have a permanent communication link to the lander or the orbiter, which orbits the corresponding planet permanently. In order to avoid general health risks, a sophisticated selection of astronauts is necessary. This means, the age, inherited diseases in the family, diseases during childhood etc. have to be taken into account. Flashy safety warnings in the space ship, the orbiter, the lander module and the exploration vehicle are required. Special training with equipment and protection measures have to be implemented as well.

2.2 3D PRINTING AS A TOOL FOR TISSUE ENGINEERING

3D printing emerged in the field of Tissue Engineering as a new approach to overcome the main limitations present at classic assembly methodologies. Up to now, the manufacturing of biological constructs, to replace or improve damaged biological tissues, was based in self-assembly and the development of scaffolds where cells could be seeded subsequently.

In this process, each layer is of a definite thickness that depends on the level of resolution the machine operator has selected: finer layers will lead to dimensionally more accurate parts but require also longer built times. A complete AM process chain consists of a set of 8 basic stages, starting from the first one, which is the CAD representation of the model, ending to the application of the manufactured part. The 8 basic steps of an AM process according to Gibson *et al.* [2] are briefly reflected in Figure 2.1.

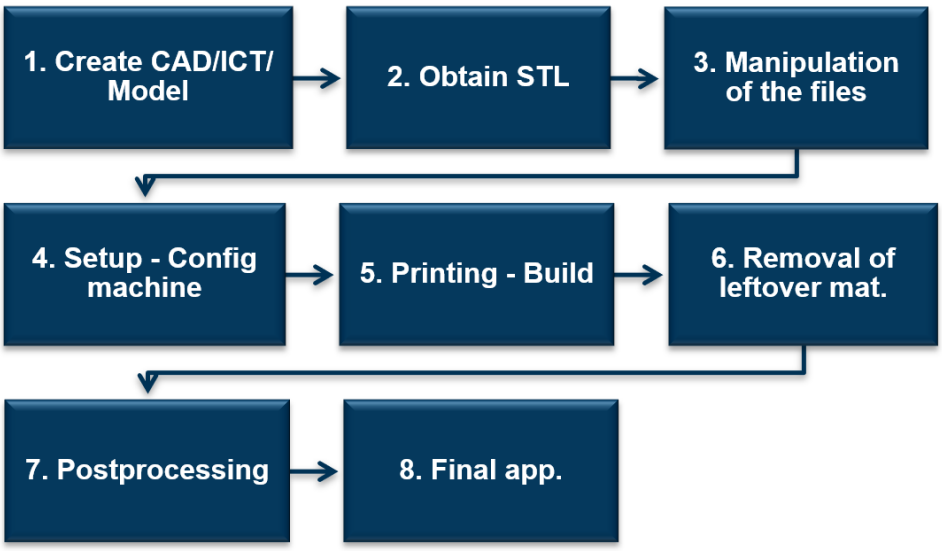

Figure 2.1: AM process from 3D model to final application. Scheme based on a figure previously published [2].

Nowadays a lot of technologies can be found in the field of AM [12]. However, only those that are related to or can be translated to bioprinting are discussed.

They can be distinguished between:

- **Extrusion:** Viscous materials (as melted thermoplastics, soft polymers, ceramic pastes, etc.) are pushed through a small orifice (nozzle) and deposited as strands following the desired pattern. Commonly some physical or chemical process is required to change the phase of the material, stabilizing the structure. This can be triggered by the addition of ions, the variation of temperature or pH, evaporating the solvents, or photo-crosslinking, etc.
- **Inkjet:** Droplets of low-viscous liquids (inks) are directly deposited onto a substrate. When working with powders the ink is normally a resin that act as binder.
- **Laser assisted:** In selective laser sintering (SLS) or selective laser melting (SLM), ceramic, polymer or metal particles are sintered/melted together with a laser beam. The beam is directed across a powder bed to increase the local temperature and cause particle fusion in the heated area along the laser path. Applied in bioprinting: Laser-induced forward transfer (LIFT). Here an ultra-short laser pulse induces the vaporization of a metal film that acts as a mask protecting cell from high power beam, resulting in the formation of a droplet, which is then deposited on the receiving substrate.
- **Stereolithography/ Photopolymerization:** Similar to SLS but instead of powders the laser beam is used to locally polymerize organic monomers. In case of 2-photon stereolithography the laser can write 3D structures inside a monomer solution, realizing even resolutions in the sub-micrometer range.

  As 3D printing is basically used for scaffolding, where cells will be seeded after the printing and post-printing process, the techniques and materials that can be used are not as limited as in bioprinting.

2.3 BIOPRINTING, EMBEDDING CELLS

Bioprinting involves the deposition of layers of a bioink that after crosslinking will form a hydrogel matrix to provide structural support to the cells and other extracellular components embedded within [3, 24, 25]. Therefore, when compared with 3D printing, the difference is the simultaneous deposition of the base material and the cells to form tissue constructs.

It is important to remark that a bioprinted construct is not a tissue or an organ. It requieres an *in vitro* culture period, which depends on the tissue generated and is required for tissue differentiation, for remodelling and maturation. Then the printed tissue or organ construct can potentially be applied to replace the function of damaged natural tissue.

Another advantage of bioprinting, is that it allows the inclusion of multiple cell types in the same layer or in different regions of the construct while maintaining a high spatial resolution. For that, cells are commonly mixed and embedded into their respective biomaterial prior to printing (bioinks). During the AM process, therefore, biomaterials and cells are positioned together, enabling the fabrication of complex tissue constructs. As a side effect, very high seeding efficiency is guaranteed as the cells are immobilized in the scaffold material during manufacture.

Depending on the nature of the deposition, three main classes of techniques can be distinguished:

- (1) Deposition of discrete spherical cell/biomaterial droplets or cell aggregates used as building blocks [26].
- (2) Continuous extrusion of bioinks where cells are suspended and deposited in a strand-like fashion [27].
- (3) Arrangement of cells without physical support through magnetic fields or acoustic waves [28, 29], altough it is not always considered as bioprinting.

The following schematic (Figure 2.2) shows the probably most important AM technologies in bioprinting: the left and central one belong to the group in which cells or biomaterials are deposited in a discrete manner whereas the method shown on the right side demonstrates continuous extrusion.

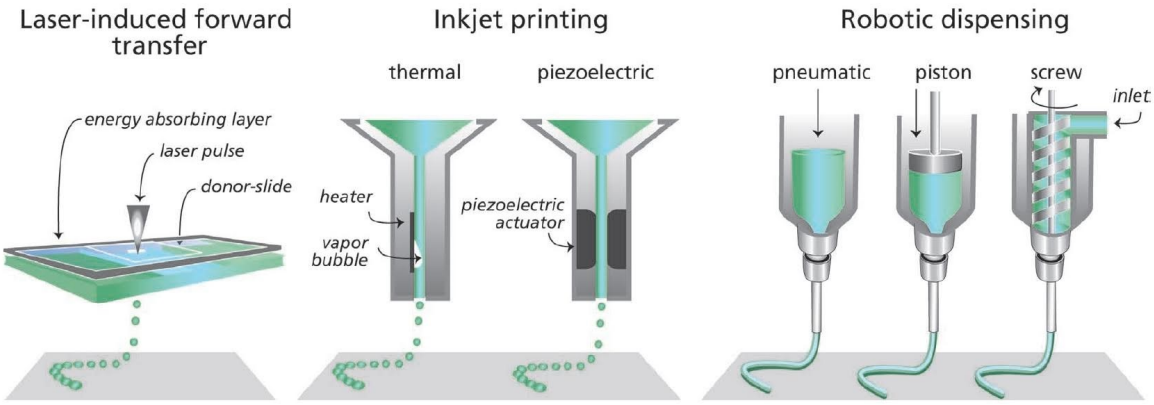

Figure 2.2: Scheme of the main technologies used in 3D bioprinting. Reused with permission of the Copyright Clearance Center from [3].

The main characteristic of the first group is that bioinks are released in small discrete droplets. Nowadays, several technologies can be used to achieve this non-continuous deposition (thermal, acoustic or piezoelectric control, microvalves, laser-induced, etc.). If cells are released in small droplets of low-viscous inks, this process commonly is called inkjet bioprinting. But if cell aggregates, also known as cell spheroids, are deposited in most cases no biomaterial is involved as such aggregates, commonly with ca. 100 µm in diameter, tend to fuse spontaneously when being in direct contact to each other.

For this AM technology the term "bioassembly" has been coined to demonstrate that it is more an assembly-based than printing-like process (Figure 2.3).

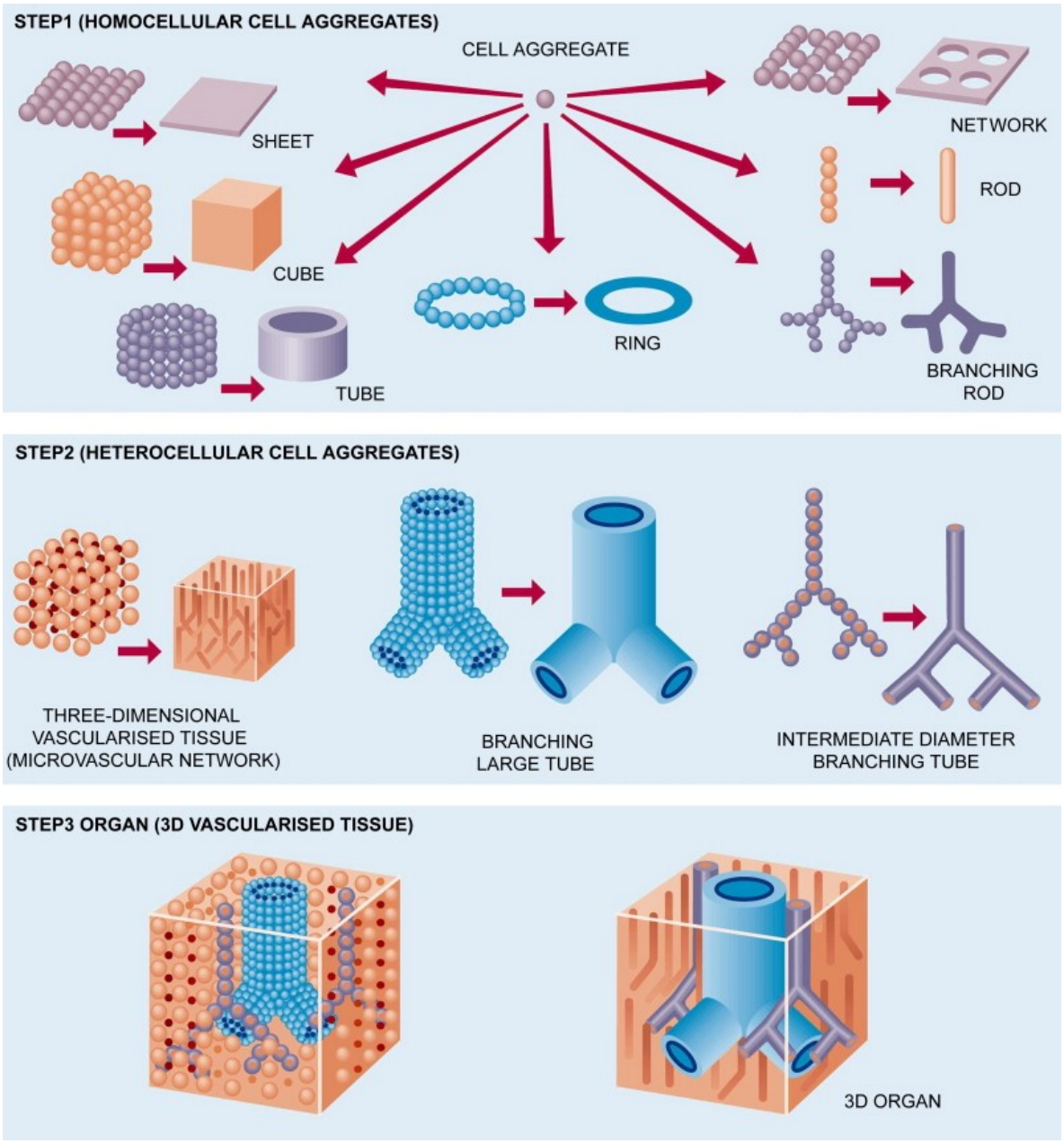

Figure 2.3: Left: Bioassembly process of 3D structures from discrete cell aggregates. Reused with permission of the Copyright Clearance Center from [4].

Another method to deposit small volumes of cells and respective biomaterials is the so-called laser-induced forward transfer (LIFT) technology. In contrast to all other technologies here a sheet-like

cell/matrix layer has to be fabricated first from which then small volumes are transferred to a new substrate. This 2-step-procedure makes LIFT more time consuming and elaborate than other bioprinting methods.

For the second group of technologies, where a continuous deposition of the bioink is aimed, different robotic dispensing methodologies have been traditionally used. The most common are normally known as *syringe-based extrusion* or *3D bioplotting* and the release of the material can be achieved through diverse mechanical methods (Figure 2.2). Advantage of extrusion-based bioprinting is the commonly high speed of deposition and the compact architecture of the respective printers.

As an example, Figure 2.4 shows the GeSIM BioScaffolder 3.1 as one of the typical devices used for extrusion printing and bioprinting.

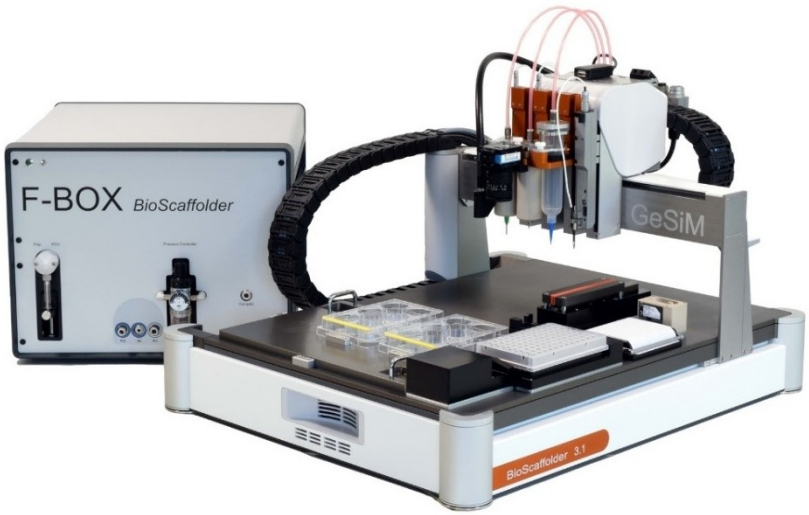

Figure 2.4: BioScaffolder 3.1 GeSIM (Germany,) a typical extrusion-based (bio)printer. Picture provided by the manufacturer.

Extrusion-based bioprinting is a very versatile technology and it could be demonstrated that mixtures consisting of many different human cell types and a variety of synthetic and natural biomaterials can be utilized

successfully. Figure 2.5 shows a typical workflow, using two different cell-laden bioinks, polycaprolactone as additional structural support and pluronic as sacrificial material for achieving open macropores. The bioprinted construct has the shape and size of a human ear.

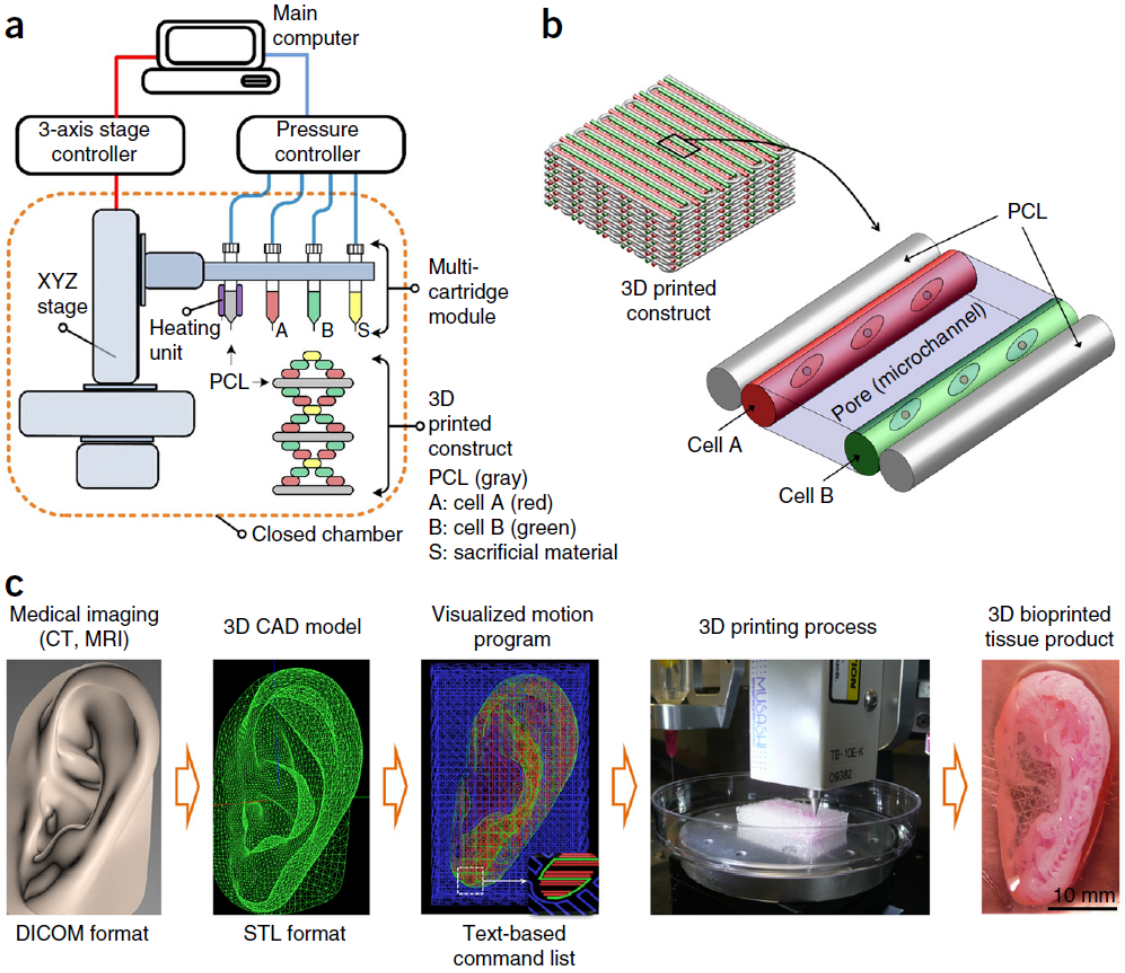

Figure 2.5: Schematic of the workflow of complex extrusion-based 3D bioprinting. Reused with permission of the Copyright Clearance Center from [5].

Some years ago, a new technology addressed as *3D screen bioprinting* was announced. However, still no scientific paper about the process or its results have been published. A patent application was released in January 2019 [30].

Finally, following the autoassembly strategy, other techniques that do not

require the deposition of physical supports (viscous bioinks) are also under investigation. Such technologies are mainly focused on spatial cell arrangement to promote cell-cell interactions that will lead into the formation of a natural ECM. To achieve this spatial control, other approaches are currently under development: utilization of acoustic waves [28] and magnetic fields [29].

As summary, it should be highlighted that all the groups of technologies have advantages and disadvantages, as reflected on table 2.1.

The main disadvantage of the inkjet-based methods is that hardly macroscopic objects can be fabricated as they would be needed for most medical applications if cell suspensions are utilized for the printing process. In addition inkjet bioprinting uses either single cells, suspended in low viscous liquids such as cell culture media, which is not suitable for fabrication of three-dimensional tissue constructs or spherical cell aggregates are printed (assembled), more or less without additional biomaterials (*"scaffold-free"* approach).

In contrast, the utilization of cell spheres as building blocks (*bioassembly*) requires extremely high cell numbers, which remain difficult to achieve - but allows manufacturing of macroscopic and really three-dimensional objects. For extrusion-based printing, suitable soft hydrogels (*bioinks*) are applicable for 3D scaffold fabrication as well as protecting the cells during the printing process and allowing further cell growth afterwards [3]. The main recognized drawback of extrusion-based printing, beside its low resolution, is the risk of nozzle clogging. Furthermore, as cells cannot be kept alive *ex vivo* in concentrated or highly crosslinked gels, in most cases a second, stiffer material is required to provide mechanical stability of the construct. This supporting material can be a thermoplastic polymer like polycaprolactone [31] or an additional, but highly concentrated hydrogel [32]. Other posible strategies for bioprinting of macroscopic cell-laden constructs recently have been reviewed [33].

Table 2.1: Classification of the main bioprinting technologies based on their deposition process. Advantages and disagvantages have been reviewed, along its main features of each technology. Table previously presented by OHB 2019 to ESA (contract No. 4000123640/17/NL/BJ/gp/TUD). Reused with permision of OHB System AG, 2020.

	Process	Technology	Main features/ Characteristics	Advantages	Disadvantages
Physical support: bioink deposition	Discrete	**Inkjet**	Deposition of single cells in low viscous inks.	High precision positioning single cells in two dimensions.	No volumetric constructs can be achieved because of the lack of mechanical stability of the low density bioinks employed.
		Bioassembly	Final constructs will assemble in 3D by themselves from individual cell aggregates.	Close cell-cell interactions.	High number of cells required to form the cell aggregates or spheroids for the printing process.
		LIFT	High energy lasers are used to deposit.	High accuracy. Once the materials are prepared (pre-printing) the deposition is faster than in bioassembly.	Complex pre-printing process is required to seed and arrange cells in the matrix. Mask materials are needed to avoid cell damage.
	Continuous	**Extrusion BP (syringe-based extrusion)**	Cells are suspended in a viscous, polymeric solution (bioink) and extruded as strands.	Less cells are required.	Low resolution, defined by the nozzle diameter. As cells are diluted in the bioink formation of cell-cell contacts is hindered.
		3D Screen BP	Use the transference of materials from prearranged sheets of hydrogels and bioinks.	Big areas can be deposited fast. Shear stress might be smaller than in extrusion bioprinting.	Pre-printing arrangements are needed to create the screens and maybe several of them are needed to complete a layer.
No physical support	Spatial cell arrangement	**Acoustic waves**	Sinusoidal and stationary acoustic waves are used to control the position of cells and to form aggregates.	No physical scaffold is required to keep cells together during the fusion process, while cells generate their own ECM.	As it is based on mechanical waves (sound) it requires a physical medium to propagate.
		Magnetic levitation	Like acoustic waves but using magnetic fields, that do not require a physical medium to propagate.	Will probably work also in the absence of gravity (first experiments are currently planned).	Cells or cell aggregates have to be magnetic and therefore must be coupled with magnetic nanoparticles.

It is important to highlight that similarly to the AM process, in bioprinting different steps can be found: pre-printing, bioprinting, and post-printing, as shown in Figure 2.6. It is important to understand them as well as the requirements and limitations of each to translate this technology to locations outside of Earth:

1. **Pre-printing:** In this phase, the main objective is to multiply the number of available cells, commonly obtained from a little biopsy. This is usually the bottleneck of the process because despite presenting an exponential growth, the start is always with a very limited number of cells from the patient. For this phase, incubators or cells culture bioreactors would be needed.

2. **Tissue printing:** The deposition of the cells and the biomaterials that will form the initial artificial extracellular matrix as a suitable space to grow and develop. More materials can be added at this step to improve the mechanical properties of the scaffold or the biological activity. In this step, a sterile bench with the bioprinter would be needed. Also, to carry the cells from the cell cultures to the cartridges of the machine and to prepare the bioinks in sterile conditions.

3. **Post-printing and maturation:** of the constructs, to prepare them for their normal function when implanted into the patient. Post-printing processes, like the crosslinking of the freshly printed construct, can be controlled by researchers while the maturation phase is mostly driven by cells and only some external parameters as culture conditions or mechanical stimulation can be modulated. For this, specific machines (tissue bioreactors) should be developed to simulate the physiological environment for each kind of cells and that allows the maturation of the tissues for their later introduction into the body. It is especially important for musculoskeletal and cardio-vascular tissues to be mature when transplanted, otherwise, they could fail.

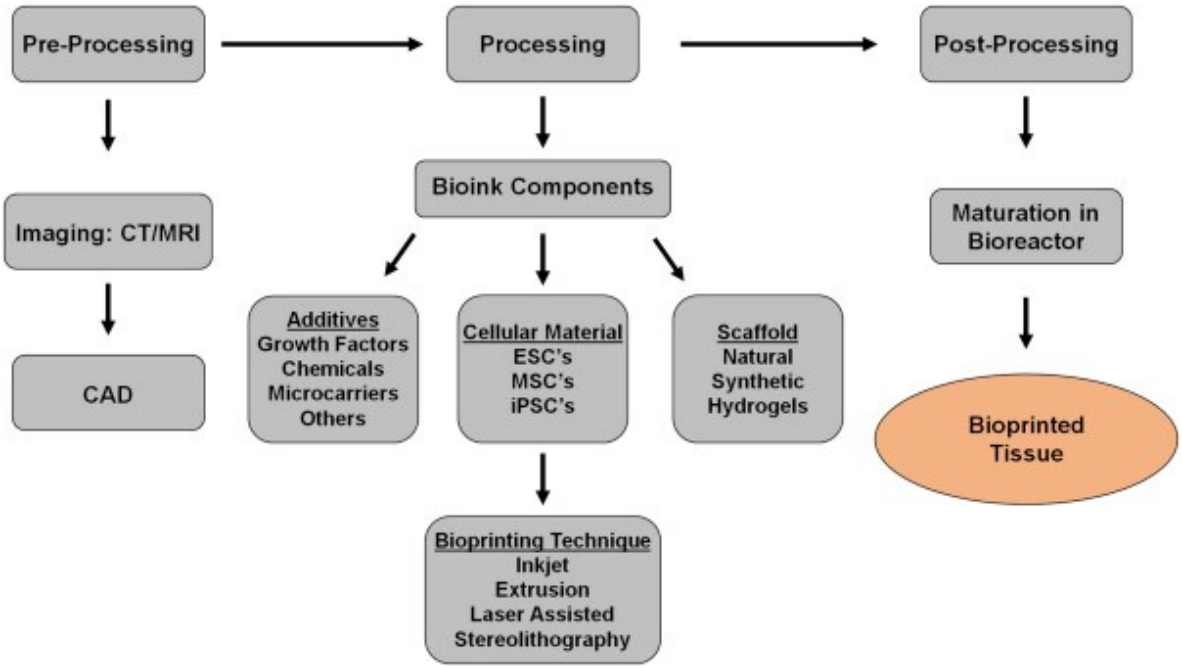

Figure 2.6: Bioprinting workflow, including previous and posterior process. Image licensed under Creative Commons CC-BY-NC-ND, by [6].

2.3.1 *Main challenges to overcome*

As shown in the previous section, the use of 3D printed scaffolds for its use as physical structure for biological constructs, entails some technical limitations. That is why the simultaneous deposition of living cells together with the structural materials (bioprinting) is so important.

In one hand, the combination of the material extrusion and the deposition of different living cells and biological material allows the creation of more complex structures, overcoming one of those critical points.

On the other hand, the presence of living cells creates a new set of requirements to ensure their viability along the process, and afterwards. As now one should work on physiological conditions (temperature, pressure, pH, salt and sugar concentrations, oxygen levels, etc.), the range of materials that can be use is more limited.

Bioprinting looks like a promising technology for tissue regeneration. However, it is still a long way to go until complex, vascularized tissues or even complete human organs can be built as only miniaturized ones, or basic tissues, have been achieved so far. That is mainly due to the complexity of the natural structures to mimic where in most of the cases the biology beneath is still not fully understood. Also, there are some critical issues regarding technology and materials that researchers still must overcome.

Regarding materials, the main limitation found nowadays is how to create volumetric structures that present the required mechanical properties while providing cells with the environment and vasculature they need to regrow the original tissue. Technologically, more precise machines and faster process (not inducing high shear stress) are needed to better mimic the natural structures and to increase cell viability.

2.3.1.1 *Earth requirements and limitations*

As summary, the main challenges which still have to be solved are:

- **Material restriction:** Most common materials employed in 3D printing, because of their easy processability and recycling, are thermoplastics [34]. However, they are not widely used in combination with cells because of their high melting points. For bioprinting, soft hydrophilic polymer hydrogels offer the best environmental characteristics for human cells. However, their mechanical properties are very poor and sometimes they are not able to maintain their shape because of posterior swelling and fast degradation [35].
- **Mechanical properties and size:** There is always a compromise between stiffness and cell behaviour [36]. Hard materials will be more resistant and will provide the desired stiffness; however, cells will not proliferate and differentiate correctly within this environment.

Nowadays, researchers can create miniaturized and simplified tissue constructs (organoids) that are able to partially mimic the function of natural tissues [37]. For example, Organovo (USA pioneer company on bioprinting) is developing such small bioprinted tissue models for testing of new drugs. However, this would not be enough to resemble complete functional organs.

- **Viscosity of bioinks:** Because of the lack of gravity, low viscosity materials (normally used with inkjet technologies) should be avoided in space. Also on Earth, such materials will lack the required consistency to be printed without a fast reaction (normally chemical crosslinking) than change its state from liquid to gel or even solid. But too dense materials would present problems to be extruded and their biological properties can be affected because of a reduction of the micropore size and mechanical stress produced while printing [38]. Therefore, more shear-thinning bioinks have to be developed to provide higher cell viability for different tissues.

- **Process speed and cell viability:** 3D printing is known to be a slow process because of its layer by layer processing, which is further decreased when working with high resolution. For bioprinting, this is also an important element to have in mind, as for complex biological structures it would be needed to work at micrometre resolution. Another issue to solve is how to maintain cell viability and the required physiological conditions while avoiding cells to attach to the different surfaces along all the process when working with long tubes as in screw deposition, where a lot of death volumes are also found [38].

- **Maturation:** To create functional tissues from autologous cells and materials, new machines that simulate the appropriate cellular environment and mechanical conditions are required [39]. This apparatus, commonly know as bioreactors, are also important in

space to simulate Earth's conditions as close as possible (1-G, oxygen concentration, humidity, etc.).

– **Vasculature:** To obtain larger and more complex constructs, a complete micro and macro vasculature that allows oxygen and nutrient diffusion as well as waste removal is needed. Different approaches have been developed for this purpose, as the use of sacrificial materials while printing, coaxial extrusion to create tubular structures and the use of angiogenic materials but a fully functional vascular supply system which can be connected microsurgically to artery and vein of a patient are still not available [40]. It will be quite complicated to manufacture such systems as they would need to cover several length scales.

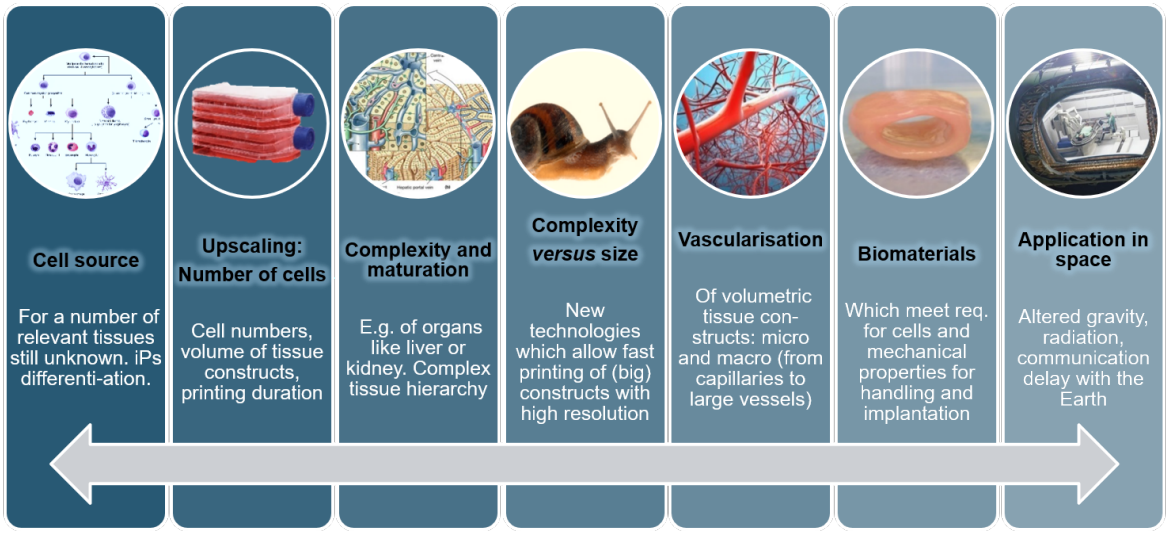

Figure 2.7: Main research and technological needs to overcome in bioprinting. A pictured based on a figure previously release from OHB 2019 to ESA (contract No. 4000123640/17/NL/BJ/gp/TUD). Reused with permision of OHB System AG, 2020.

2.3.1.2 *Space requirements and limitations*

In addition, exploration bioprinters should overcome some present limitations:

– **Microgravity (μG):** The reduction in gravitational forces results in decreased buoyancy-driven flows, rates of sedimentation and hydrostatic pressure. In general, fluid dynamics are also altered, and there is a near absence of convection [41]. In this sense, both 3D printing and bioprinting can be deeply influenced. For example, 3D printing technology Fused Filament Fabrication (FFF) is less affected because of the fast solidification of thermoplastics, whereas the soft and less viscous materials used in bioprinting will be difficult to handle. Microgravity would also affect manipulation of liquids like cell culture medium in general, needed to keep the constructs alive until implantation. In this regard, viscosity can be a function of temperature and may be altered by shear thinning effects and therefore needs to be adjusted for different environmental conditions. Also, to be mixed with cells, bioinks need to be in a liquid or gel phase. Finally, not all biomaterials are printable and those which are may not be applicable in a wide range of processing parameters. Bioinks having a viscosity in the range of $30.6 \cdot 10^7$ mPa s are reported to be best printable via extrusion printing [42]. Under reduced gravity it might be advantageous to use bioinks with higher viscosity to guarantee sufficient stability and also cohesion between the different layers already during printing (= layer-by-layer deposition) and therefore before crosslinking or other stabilization steps. But to obtain also vital tissue constructs in microgravity conditions, it is mandatory to find a compromise between high viscosity and high cell viability.

– **Radiation:** While there is a large body of existing literature on the effects of low linear energy transfer (LET) radiation such as gamma and X-rays on biological samples, including data from long-term animal studies, clinical studies and others, the information on radiation of the kind encountered in space (e.g., protons and high-LET radiation such as heavy charged ions) is less well-defined [41]. Radiation became at this point a critical issue as it will strongly

influence electronics, (bio)materials and cells and might as well be quite harmful to bioprinted tissues *in vitro*.

– **Ambient gas and pressure:** Pressure, humidity and temperature are determinant factors for bioprinting and 3D printing as well. Pressure can affect not only cells but also the biomaterials used and how they are manufactured. Some other parameters, as the diameter of the strand, the density, hydrogel swelling behaviour and some geometrical aspects of the constructs, can be affected. But as in spacecrafts, space stations as well as human settlements on other planets Earth-like atmospheric conditions have to be provided for the astronauts this might be a less important aspect.

2.4 REGULATIONS AND LAW FRAME

The final aim of bioprinting is to develop complete organs from patient own cells. The dreamed work flow for that would be to obtain cells directly from a biopsy along the surgery and build the organ with a machine hosted inside the hospital operating theatre. However, this is not possible, as cell expansion, printing and maturation process require long times and all these steps are necessary before implantation for a successful result.

Therefore, as cells must travel from the surgery room to different facilities along the process to accomplish the final assembly, a very strict and good manufacturing practice (GMP) must be carried out to follow all the persons, places, procedures and transportations to which the sample has been subjected. Without such guidelines any resultant product will be invalid and not applicable for the clinics.

An example of a possible process line can be found on the schematics below (Figure 2.8), where the steps required to create a temporal cellularized scaffold to replace nose cartilage is shown. Of course, all the involved materials should be approved by the European Medicines Agency

(EMA), the Food and Drug Administration (FDA) or the respective other agency/ and all the machines employed should have the CE marking.

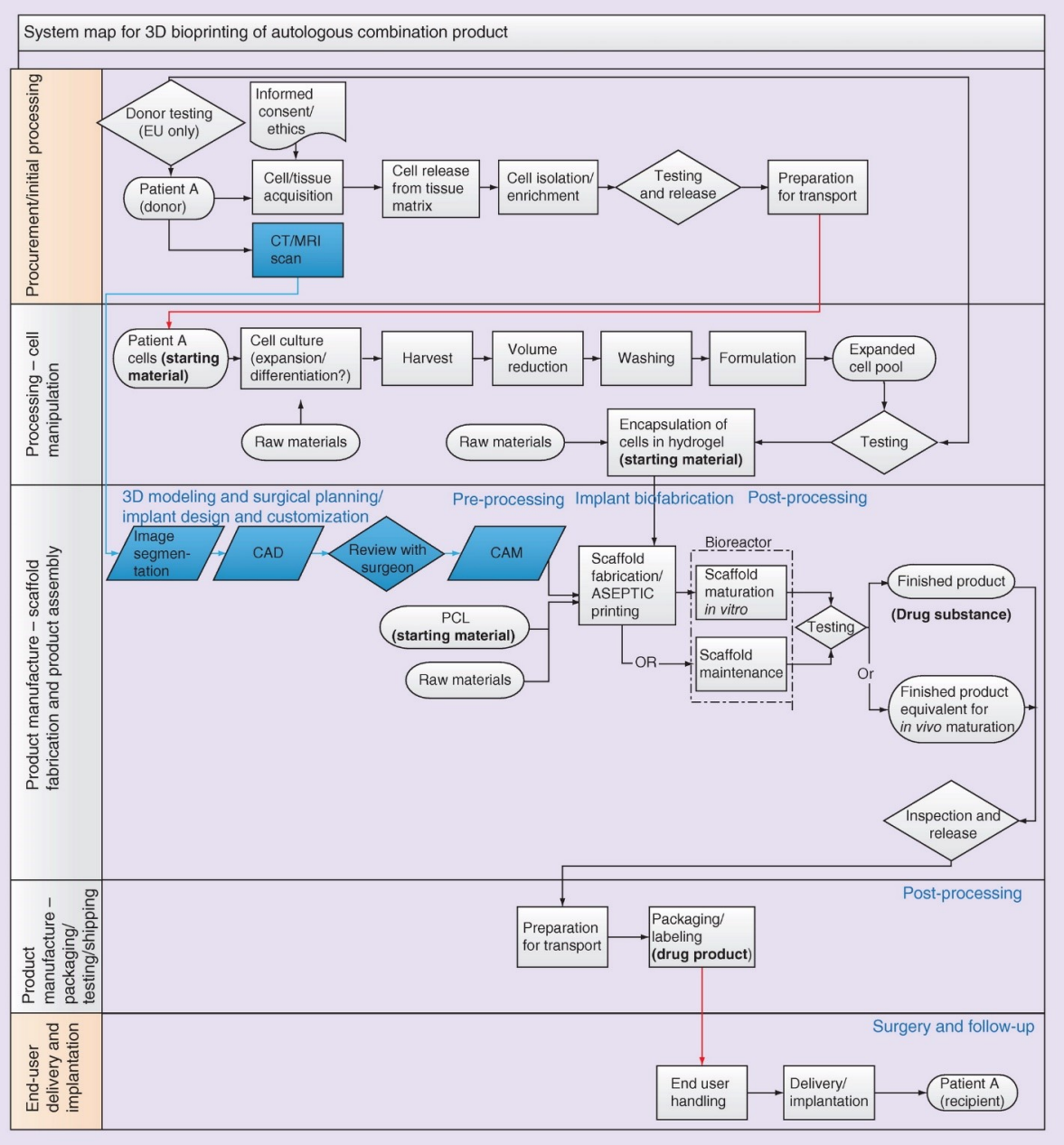

Figure 2.8: Cross-functional flow diagram of the manufacturing process for the centralized industrial production of a personalised autologous 3D bioprinted combination product for total replacement of the nose after tumour removal. Image licensed under the Attribution-NC-ND 4.0 Unported License, by [43].

As 3D - bioprinting is also considered for medical applications in space, the regulation of this technology in the field of medicine would be also discussed here. In any case, both technologies are relatively new and therefore still no specific regulations have been released, neither in Europe nor the U.S. Therefore, the most similar legislation available belongs to the fields of Regenerative Medicine and Tissue Engineering, contemplated inside the group of Advanced Therapies (AT).

In the case of bioprinting, there is still no specific regulation for this new technology. However, the Medical Device Regulation (MDR) - published and came into force on May 2017 - may be applicable to stablish the requirements that the machines must fulfil to work inside hospitals and to handle human cells and tissues, even at different stages of production [44].

In a general way it can be covered by the law as a Tissue Engineered Product (TEP). Beside others, in this group can be found:

- Skin cells embedded in sheet-like matrices/scaffolds (TE: skin equivalents).
- Osteoblasts or bone-marrow-derived stem cells combined with ceramic based scaffolds or biomaterials (TE: bone equivalents).

EMA classifies TEP into the family of "Advanced Therapy Medicinal Products" (ATMP), treated by Regulation (EC) 1394/2007 [art. 2(1) b], that amends Directive 2001/83/EC and Regulation (EC) No 726/2004 (Figure 2.9).

Also Tissue and Cells Directive 2004/23/ES should be applied when working with not engineered cells and Blood Directive 2002/98/EC when working with blood or its components (as plasma) independently of its final function. This should be highlighted in this work, as plasma will be proposed as autologous material for cell support on bioprinting Chapter 4.

The requirements to comply with an individual medical prescription for a custom-made product for an individual patient are (Article 28, ATMP

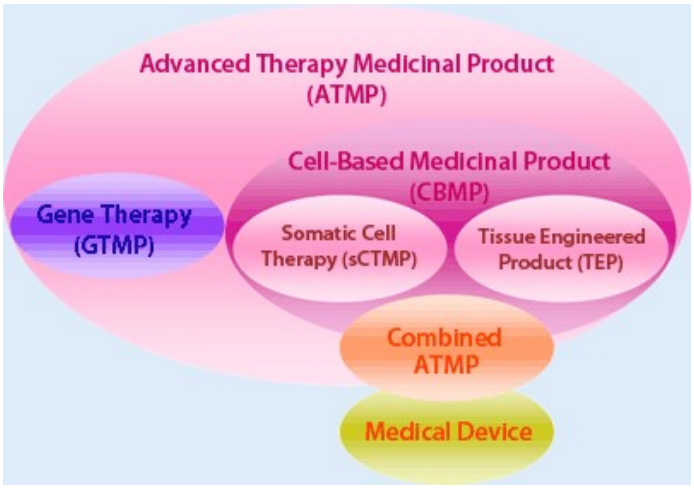

Figure 2.9: Reflection paper on classification of advanced therapy medicinal products. Reused with permission of the Copyright Clearance Center from [7].

Regulation - (EC) No. 1394/2007):

- Manufacturing to be authorised by the Member State (MS) competent authorities.
- National traceability and pharmaco-vigilance requirements.
- Specific quality standards as on the Community level (not dealt within the Community legislation: Regulation (EC) No 726/2004 of the European Parliament and of the Council of 31 March 2004 laying down Community procedures for the authorisation and supervision of medicinal products for human and veterinary use and establishing a European Medicines Agency.

As it was introduced at the beginning of the section, 3D bioprinted constructs are normally manufactured and processed along several technical stages at multiple sites. Therefore, they also must comply with the "re-distributed manufacturing (RDM)" process law. It covers the procurement and initial processing, processing and cell manipulation, scaffold fabrication and product assembly, packaging, testing, shipping, and end-user delivery and implantation. For a scaffold matrix with

embedded cells, the classification and thus the legislation into which the product fits is determined by the way in which the finished product achieves its intended medical purpose, the claimed mode of action (MoA), the characteristics of the active substance and the way in which it is combined in the finished product. This means the manufacturer would need to determine several critical characteristics that will define the product under development before being able to classify the finished product [43].

2.5 3D PRINTING/BIOPRINTING IN SPACE

As stated in the previous section, one of the challenges that 3D bioprinting has to face is the presence of a continuous force that pulls down the materials, making them to collapse if the stiffness of the material is not high enough. That force is the gravity. Therefore, the use of bioprinting in an environment where this force is reduced or even almost annul, offers new possibilities to researchers.

Russian scientists from 3D Bioprinting Solutions (3dbio) sent a magnetic bioprinter (Organ.Aut) to the ISS in 2018, which allows 3D assembly of tissue structures in micro-gravity [45]. This device uses magnetic levitation technology in zero gravity, so that the object is not created in layers, as in conventional 3D printers, but volumetrically, from all sides at the same time. With this machine, the crew onboard were able to bioprint bone tissue in space by growing fragments of bone structure in zero-gravity conditions. During experiments on the ISS, tissue samples were made from calcium phosphate ceramics, which were populated with living cells. These samples are now currently being comprehensively studied on Earth [46].

This technology, despite been claimed as a bioprinter, belongs to the bioassembly technologies, as it uses magnetic levitation forces to keep cells together, and does not use the layer-by-layer concept characteristic of the 3DP. Due to the magnetic forces that aggregate cells in a focal point, it can

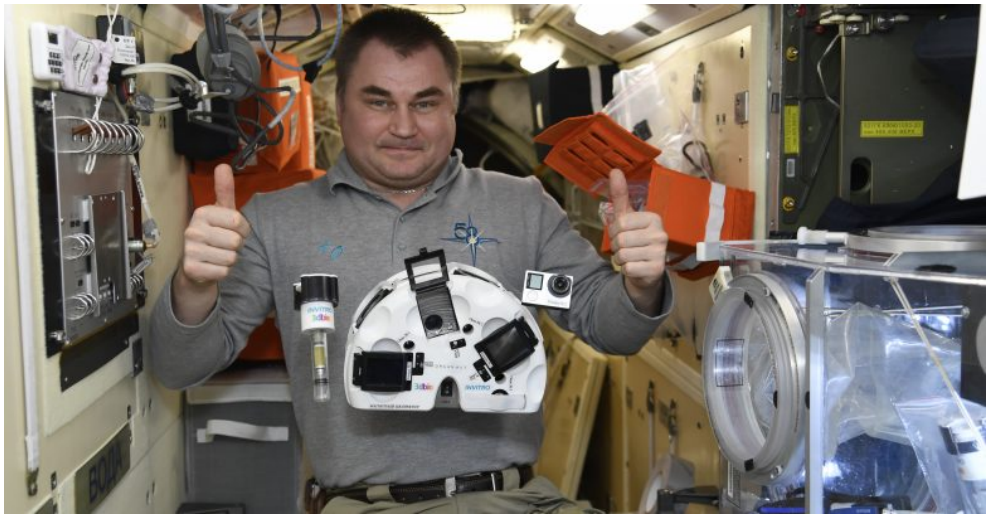

Figure 2.10: 3D Bioprinting Solutions (3dbio) magnetic bioprinter (Organ.Aut) at ISS. Picture obtained from Nasa.gov website. Credit: NASA.

generate spheroids and when the cells grow their own extracellular matrix, organoids. However, because of this aggregation methodology it is difficult to shape the generated structures or to create tissues with different cell types and distributions.

Also onboard, a BioFabrication Facility (BFF)[1] owned by an American company (TechShot, in collaboration with nScrypt), containing between others a bioprinter, was set up in 2019 at the ISS. Media reported that "it has successfully printed a large volume of human heart cells aboard the International Space Station (ISS) U.S. National Laboratory"[2]. However, there is still no information available or published with the results. The roadmap of this research is to increase the thickness of the printed cardiac-like tissues along the next two years approximately. In december 2019, the news stated 'each print measured 30 mm long by 20 mm wide by 12.6 mm high. The BFF printed inside a Techshot-developed cell culturing cassette that strengthens the assemblage of cells over time; to the point

1 More info available at: https://techshot.com/bioprinter/

2 https://www.medicaldesignandoutsourcing.com/how-3d-bioprinting-in-space-could-ease-donor-organ-shortage/

where they should become a viable, self-supporting tissue-like structure expected to remain solid once back in Earth's gravity"[3].

It is known that the lack of gravity can affect the biological behaviour of cells, folding the enhancement of cell proliferation, altering the direction in which fibers are grown or inhibiting some gene regulations, for example [21, 47, 48].

3 https://www.prnewswire.com/news-releases/success-3d-bioprinter-in-space-prints-with-human-heart-cells-300982759.html

Part III

STUDY OF CLINICAL SCENARIOS, DESIGN OF NEW MATERIALS AND PRINTING STRATEGIES. DESIGN OF WORKBENCH AND CASE STUDY

- **Chapter 3.** Design of the experiment: Tissues of interest, Proof of concept (POC) & materials.
- **Chapter 4.** Development of new constructs for bone regeneration.
- **Chapter 5.** Design and development of the proof of concept workbench for space conditions.
- **Annex .P** Research procedures and protocols, detailed information.

The experimental part carried out as the core of the current PhD Thesis, is developed in this part.

First, based on the SOTA, a theoretical study was performed to choose the tissues of interest and the kind of materials that will be available on such exploratory missions. With that, a new bioink based on autologous materials that can be used for different applications, was developed. In this case, it was combined with a mineral material to obtain bone.

Finally, to demonstrate if this approach is translatable to the space conditions, it was necessary to develop a workbench platform to perform a series of tests and simulate those conditions, on Earth.

3

DESIGN OF THE EXPERIMENT: TISSUES OF INTEREST, PROOF OF CONCEPT (POC) & MATERIALS

As it was previously stated at the introduction, the human tendency of going further from Earth makes it necessary to restate the possible clinical scenarios that the crew will face in the next exploratory missions.

In this chapter, the possible clinical scenarios that the crew can face, along the main health hazards that come along, will be studied. Also, the main technical requirements that such medical scenarios will generate are contemplated, along with the possible uses for 3D printing and bioprinting under these conditions and environments.

A version of this chapter was partially submited by OHB to ESA previously, under the framework of the PLT-Space project.

3.1 POSSIBLE CLINICAL SCENARIOS

◂ *Obj 2. & Research question 1.1:*

Which are the main clinical scenarios that crew will face[...]?

On exploratory missions, as astronauts venture farther from Earth and for longer periods of time, the probability of experiencing a serious injury or falling ill increases notably. Until now, most common medical problems faced in environments as ISS were motion sickness, headaches, back pain, skin conditions, burns and dental emergencies.

The risk of an astronaut developing a serious illness and needing intensive care is small, but still a possibility. As it was highlighted previously, the

crew number will increase proportionally with the operation's distance and duration. Therefore, in case of long-term distant to Earth-space exploration missions, e.g. mission to Mars, the number of crew members would increase and with it the probability of illness and intensive care needs.

However, due to the long distance to Earth the application of health care methods encounters several challenges. First, the communication is limited since a delay is introduced. For example, the time delay each way when communicating from Mars to Earth is up to 22 minutes. This avoids fast medical assistance and precludes the use of teleoperated robots, like the "da Vinci" Surgical System. Therefore, fully automated robots would be required, if needed, for surgery interventions with endoscopic systems.

During these kinds of space missions, there is no option for the crew to return to Earth within a reasonable amount of time to treat a medical emergency. Thus, there would be a need for smarter and more autonomous medical devices, medications with a much longer shelf life, therapies focused on regenerative medicine (instead of temporal artificial replacements) and more extensive medical training for the crew.

3.1.1 *Main health hazards*

At a space exploration mission, astronauts are exposed to health hazards, which can cause injuries and organ damage that must be treated to save the astronaut's life. Major environmental risk factors for human health in space are the impact of radiation and altered gravity levels. Isolation can play a major role too, as it can lead to psychological disorders and then, to physical issues. For the development of this section, the HUMEX studies on the survivability and adaptation of humans to long-duration exploratory missions, for the Moon [21] and Mars [47] was used.

► **Radiation:** Depending on mission scenarios, this environment consists of varying combinations of primary galactic, solar, and trapped radiation

components, each of which being mixtures with vastly differing radiobiological effectiveness (Radiation doses (Sv) can be consulted at [47, 21]). This can directly affect crew health and life expectancy. Late effects, such as enhanced morbidity or the apparition of malignant cancers occurring up to 20 and more years after exposure must be considered as well as early effects which may comprise morbidity such as anorexia, fatigue, nausea, diarrhoea, and vomiting (the symptoms of the so called prodromal syndrome) or cataract formation and erythema and early mortality within days to a few weeks from failures of the haematopoietic, the pulmonary and the gastrointestinal system.

Astronauts will be exposed to high radiation levels during space exploration missions, as out of the Earth's atmosphere - and when travelling to Mars, out of the Van Allen belt too - radiation coming from the energetic particles of sun irradiation, galactic cosmic rays and others are stronger than here. Also, it must be considered that some planets may have their own radioactive environment. Therefore, the risk of developing cancer or any other kind of cell damage is increased.

► **Altered gravity:** Unrestricted adaptation to microgravity leads to physical deconditioning such as loss of muscle and bone mass, a reduced cardiovascular and physical capacity, and changes in motor skills. Lack of gravity can also cause body fluids to shift upwards, which may cause swelling, high-blood pressure and vision and organ problems. In these cases, nutrition and exercise become very important and special measures like medications and body cuffs aim to reduce the risk of long-term medical problems associated with muscle and bone wastage.

► **Isolation - Psychological issues:** Living and working in a space habitat involves chronic exposure to many different stressors related with factors as microgravity, alterations of usual dark-light cycle, limited facilities and supplies for personal hygiene, elevated noise level, elevated CO_2 concentration in the ambient air, isolation of family and friends, lack

of privacy, restricted and enforced interpersonal contacts, etc. Exposure to these different stressors can be assumed to induce different behavioural stress responses of the individual astronaut or the entire space crew which can even lead to impairments of cognitive performance and perceptual-motor skills.

3.1.2 *Medical treatments: classical and new approaches*

After the main health hazards have been identified, it is important to consider the different medical treatment options and analyse which are available for the different mission scenarios. In the following, three selected medical treatment scenarios are briefly described:

1. Full medical treatment without surgery.
2. First medical care and return to the Earth for further treatment (e.g. surgery).
3. Full medical treatment including surgery.

The first scenario considers medical events that can be treated by medical procedures without surgery, e.g. bandaging cuts, medication of organ or heart function disorders, etc. The required equipment for conducting these procedures have to be either brought along and replaced by shuttle flights from the Earth on a regular basis or, if limited or no regular flight connection is available, produced on site using, for example, 3D printing technology.

The second scenario considers medical events that must be treated by surgery, like skin or organ transplantation, difficult fracture treatment and the introduction of stents or bypasses, between others. If the mission is close to the Earth and the return is possible, the crew gives first aid and stabilizes the injured person for the travel. Further treatment, such as surgery, is then provided by specialists on the Earth. For distant mission scenarios this medical option is not available, since no fast return (< 1 week) is possible.

Consequently, in cases with no fast return option, full medical treatment including surgery must be available on site in order to protect and secure the crew's health. As no flight connection and only limited communication link to Earth is available, a medical infrastructure which can work autonomously has to be established.

3.2 TISSUES OF INTEREST

◀ *Obj 2. cont*

Research question: *Which are the main tissues of interest?*

As described above, all these risk factors can have severe impact in different tissues, and the effect can be quickly seen on skin, bone and cartilage, muscles and some organs. Exercise can ameliorate muscle, bone and cartilage loss and small fractures can be handle with immobilization cast. However, when a severe bone fracture is occurring - or part of it must be removed because of a tumour presence - new therapies must be applied to fix and regenerate it. Skin is easier to replace thanks to its superficial localization, when removed after severe burn accidents. In the case of internal organs, disease detection and diagnosis are more complicated, and the treatment required a posteriori depends on the pathology and the organ of interest, so no general solution can be pointed out. Therefore, despite general visceral organs would be analysed, the future applications of bioprinting for skin, bone and cartilage will be highlighted, as they are normally the more expose and damaged tissues.

3.2.1 *Skin*

Skin, which is the outer covering of the body, has a protection function: it avoids excessive water loss and prevents pathogens to enter our system [49]. It also regulates body temperature and contains several types of glands and sensors (nerve endings) that allow us to feel objects and to secret toxins. As we grow older, our skin becomes more fragile, thin and requires longer periods to heal from injuries.

Astronauts lose more skin cells and their skin age faster during space flight. A common complaint of astronauts is cracking skin and rashes or itchiness. Apart from itching and dryness of the skin (possibly partly due to the special skin care being used in the ISS), a thinning of the skin and increased sensitivity combined with delayed healing of wounds and an increased tendency to skin infections have been reported during and after a long stay in space. These data have been obtained from three experiments carried out on the ISS regarding tissue development in space of humans and mice.

A brief review of these projects has been summarized below. No numerical data is given due to the amount of graphs and stadistics required to show the changes along these experiments. In addition, some data is given in arbitrary units and just used for comparation to obtain first conclusions. However, the papers with all the experimental research methods and results is cited for further consultation.

- **SkinCare (ISS/ESA - 2006 - IP: Michael Massow, Ph.D., ISS Lab Ruhe GmbH, Dortmund, Germany):** For this investigation, researchers measured skin hydration, trans-epidermal water loss, elasticity, and the fine structure on predetermined skin areas before, during, and after flight. One area was treated daily with a skin care emulsion. Measurements showed: decreased skin elasticity, decrease in density of the skin fibre, thinning of the top skin layer, and prolonged moulting of base layer cells, while the emulsion-treated area showed improved hydration (more data avilable at [50, 51]). Furthermore, the measured increase in the trans-epidermal water loss reflected an impairment of the barrier function of the outermost skin layer. It seemed the astronaut underwent an accelerated skin ageing process in space [52].
- **Skin-B (ISS/ESA - 2013-16/16-17 - IP: U. Heinrich, University of Witten/Herdecke, Witten, Germany):** The Skin-B investigation

contribute to a better understanding of skin ageing mechanisms which are slow on Earth (therefore nearly impossible to study efficiently) but very much accelerated in weightlessness. It showed that significant changes of the epidermis as well as of the dermis occurred. A thinning of the epidermis was observed in ISS crew members [53]. The thinning is likely due to a decreased turnover of epidermal cells, which means skin cell metabolism may be gravity dependent. Additional skin measurements on astronauts are required before long-duration space exploration beyond low Earth orbit (LEO) can begin [51].

– **MDS (ISS/ESA/FRSM/FNRS - Aug-Nov 2009):** The Mice Drawer System (MDS) used for the International Tissue Sharing Program (TSP) was the longest rodent space mission ever performed. It provided 20 research teams with organs and tissues collected from mice having spent 3 months on the International Space Station (ISS). The impact of such prolonged exposure to extreme space conditions on mouse skin physiology was studied [54]. The data obtained suggest that a prolonged exposure to space conditions may induce skin atrophy, its premature ageing and deregulate hair follicle cycle.

Figure 3.1: Skin studies performed aboard the ISS. Picture obtained from Nasa.gov website. Credit: NASA.

3.2.2 *Bone and cartilage*

Bones provide general structure and support for the whole body, enable mobility, protect the various internal organs, are the location of red and white blood cell production, act as buffer system and store minerals. It is a complex dynamic tissue undergoing a continuous remodel-ling process. Gravity, as a physical force, plays an important role in the remodelling and contributes to the maintenance of bone integrity.

A common problem of bone loss in the elderly is shared by all astronauts who lose up to 1% of their bone mass each month in space [55], resulting in an osteoporosis-like bone structure. Obviously, this is worrying for longer missions to far-away planets or celestial bodies as it can lead to pathologic fractures (which are mostly difficult to treat comminuted fractures) and other long-term health problems.

Several studies have been carried out in space to check for these parameters [21, 47, 56, 57, 58]. However, this tissue is not as easy as skin to study, and it is only accessible through densitometers or other non-invasive medical imaging techniques. The ISS is equipped with a bone densitometer (BD) that measures bone density using Dual-Energy X-ray Absorptiometry (DEXA).

In the TSP introduced above, bone tissues were also studied. They revealed a bone loss during space-flight in the weight-bearing bones, where a decrease on the trabecular number as well as an increase of the mean trabecular separation was observed after flight. Trabecular thickness did not show any significant change and non-weight bearing bones were not affected [59].

Humans have three different types of cartilage: elastic (in external ear flaps and in parts of the larynx), hyaline (all joints (there called also articular cartilage), nose, ears, trachea, parts of the larynx and smaller respiratory tubes), and fibrous cartilage (intervertebral discs and menisci).

As cartilage is a non-vascularised tissue, its self-healing capacity is limited. With damaged/injured, inflamed and/or worn articular cartilage movement of the respective joint becomes painful and finally impossible; in case of spinal discs damage of the fibrous cartilage may lead to disc herniations which can cause severe pain and paralyses. Recently a study showed increased risk of cervical and lumbar intervertebral disk herniations in astronauts which might be caused by swelling of the disk under unloaded condition during space flight [60]. In contrast, articular cartilage erosion might be reduced under reduced gravity conditions.

3.3 TECHNICAL REQUIREMENTS FOR 3D (BIO)PRINTING AND CONSTRUCTS

Research question ◀ 1.2: [...] and how bioprinting can be a technology of interest for such missions?

As stated in several occasions before, besides the environmental conditions, the main challenge that humanity will face on long-term exploration missions is the fact that the crew can not depend on the Earth after taking off. This fact raises several technical aspects, making it mandatory for the crew to be as much autonomous as possible.

When developing a technology or a material that needs to be functional under such conditions, we should cover some specifications regarding:

- Environmental factors: altered gravity and radiation.
- Limited space and payload: close life systems.
- Delayed communication and no fast return available: autonomy.

Inside the framework of this project, the given general specifications can be translated into technical requirements necessary for the selection or development of the demonstrator's biomaterials (objective stated at section 1.2.1).

3.3.1 *Altered gravity and radiation*

On Earth, gravity is an important force that has a strong influence in physical phenomena when working on macro scale. However, in an orbiting spacecraft or at celestial bodies where this force is diminish, other forces as surface tension, adhesion, cohesion or capillarity become more important, even at the macro level [61].

In the present study, this fact is important for the development of the biomaterials that will be printed as the tissue support at altered gravity conditions.

Bioinks ► requirements

For bioinks to be useful under such conditions, they should present:

- A proper **adhesion** with the base material (e.g.: plastic/glass tissue culture dish) to avoid detachment of the scaffold/construct.
- Strong **cohesion** between the molecules of the fluid to generate a continuous strand and allow the generation of complex geometries, where even bridges may be present.
- **Fast gelation** to increase shape fidelity, avoiding the deformation that can be produced by the physical forces.

Those specifications are also sought on Earth, however under altered gravity conditions, the direction and module of the forces applied to the system can vary and therefore, constructs should be stable under a wider (and higher) range of external forces. The values will be different if we consider a travelling or an orbiting spaceship, or even a stable planetary base (each Planet will have a different gravity). In this case, the range of interest is from 0 to 9.8 m/s^2, so from microgravity to gravity. At zero gravity (zero G), the scaffold won't be subjected to any force, so it would remain stable. Therefore, the maximun aceleration that will be studied is G, with the samples and printer over a base (compression stress) or hanging down (tensional stress).

Regarding radiation, cells will be exposed to higher levels of cosmic and gamma radiation on space. The bioink where cells are embedded, can be used to reduce the intensity of the energy that impacts them, creating a shield effect. It is known that water acts as a good shield, as the part of the molecule that blocks part of cosmic rays is the nuclei, and as water is made by three small atoms, has a bigger nuclei density that other materials, as for example, metal [62, 63]. But, as we consider the presence of human beings (who need the tissue replacement), a global shielding should be included, and therefore this issue **(radiation) will not be further investigated along the present study.**

3.3.2 *Open surgeries*

It is also important to have in mind that to introduce in the body the tissue equivalents generated, a surgery is required. At present, operations would be impractical in micro gravity, because blood and fluids would leak out of the patient's body, float around creating a biohazard that can infect other astronauts and contaminate the spacecraft. Also, the tendency of organs to eviscerate has also been reported. In addition, the bias of floating bowel to abut the abdominal wall can cause a risk of instrumental perforation [64].

However, researchers have already started to work on this problem. For example: Scientists in the U.S. (a collaboration between NASA, the University of Louisville, Carnegie Mellon University and Baylor College of Medicine) have developed a method that consists on a transparent dome that can be placed over a wound and gets filled with fluid, such as physiologic salt solution, to stem the blood flow [65]. It could stop the bleeding or give a surgeon time to seal the wound while operating. This is now a work in progress and they have started to try it in microgravity. This team is also working on new tools for endoscopic equipment that includes a fibre-optic camera and light source to visualize the operating field, and a variety of surgical tools to hold, manipulate, cauterize, cut or suture tissue. In space, laparoscopic surgery is the obvious solution to contain the organs and reduce biological contamination.

From a spacecraft-engineering point, also a rotating medial operation module on a space vessel can be considered to create enough g-forces to circumvent this problem entirely. For this rotation, as well as for planetary bodies the g-level threshold needs to be defined to be sufficient for adapting operational procedures, without needing new tools/devices.

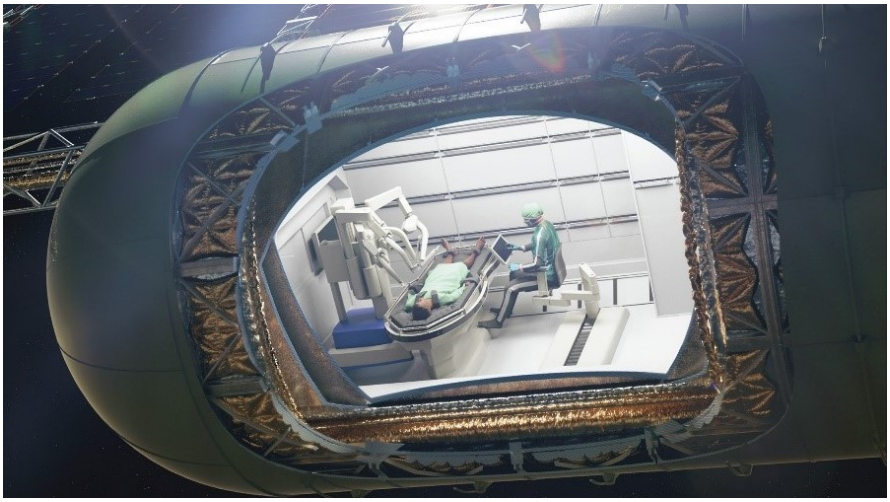

Figure 3.2: Rendered image of a surgical isolated module. Illustration by T. Trapp (CC BY-SA), published at [8].

In microgravity, at open or laparoscopic surgeries, the patient and the surgeon must have to be fixed on place to work safely along the procedure to be successful. Because of this, NASA is also considering to use specialized robots as surgeons. One of them, Robonaut 2, is already on board the ISS and the aim is that it performs basic medical functions which can be remotely controlled from Earth [66]. For medium and long distance missions a remote control from Earth is not possible, thus the ultimate goal is that it could be programmed to carry out complicated procedures in an autonomous way.

To recap all the exposed clinical scenarios exposed on previous sections, how they can be treated on Earth and on Space, and how Bioprinting can help on each situation, a table summarizing all it can be found below (Table 3.1). Also some of the main limitations or requirements for each case have been included.

Table 3.1: Summary of clinical scenarios and treatments on Space on Earth. Table previously submited by OHB 2019 to ESA (contract No. 4000123640/18/NL/BJ/gp). Reused with permision of OHB System AG, 2020.

Damaged tissues / Type of injury		Medical Treatment on Earth	Possible Translation to Space	3D - printing / Bioprinting Application	Limitations / Requirements
Skin	**Small burns (1st - 2nd deg.) or superficial injuries**	Not required, only on special cases or complications	Same treatment	N/A	-
	Extensive/ severe burns (3rd - 4rd deg.) or deep injuries	Skin grafting	Same treatment (may require an operating room, OR)	Bioprinting (BP) can create autologous skin	Adapted bioprinter and basic operating room as skin grafting is not as complex as open body surgeries
Bone & Cartilage	**Small fractures**	Immobilization with cast (normal plaster materials or 3D printed)	Same treatment	3D Printed tailored cast	A 3D printer is required – The materials should resist the mechanical loads
	Complex fractures and bone defects	Removal of the injured bone segment and replacement (metal, ceramic, autologous. or TE bone)	Same treatment (O.R.)	Bioprinted autologous bone and/or 3D printed cast for posterior immobilization	OR and adapted bioprinter and required tools for microgravity. Optional: surgical robots
	Articular cartilage defects	- Focal: cell therapy or TE - General: Replacement by artificial joint	Same treatment (O.R).	BP can facilitate fabrication of TE constructs; 3D Printing for prosthesis	OR and adapted bioprinter; cartilage has limited self-healing capacity in general
	Intervertebral disc hernia-tion/rupture	Severe cases: surgical discectomy or spinal fusion	Same treatment (O.R.)		
Organs	**Damage**	Partial replacements using artificial patches	Same treatment (O.R.)	BP can generate autologous partial replacements	OR, Cell availability and adapted bioprinter for autologous patches
	Failure	Transplant: full replacement	Same treatment, when organs are available (O.R.)	BP will allow the creation of full functional organs	OR, Healthy compa-tible organs must be available; long term: bioprinting of whole organs,
	Malfunction	Use of drugs to replace the organ function	Same treatment	BP can be used to create organoids *in vitro* to produce the required biolo-gical substances	Adapted bioprinter and bioreactors

3.3.3 *Closed life-support systems and autonomy*

Space limitations, and the fact that humans will need to be sustainable by themselves when established in other planets or far stations, creates the need of closed life-support systems and autonomous machines.

Those closed systems do not rely on matter exchange with any part outside the system. For that, waste products of any kind must be converted into raw materials for other production system/species (like oxygen, CO_2, water, minerals or other food supply). It can apply concepts of the green chemistry, where recycling and reuse are the keys for sustainability.

As shown in Figure 3.3 different processes are required to exchange gases, recycle waste, grey and black waters.

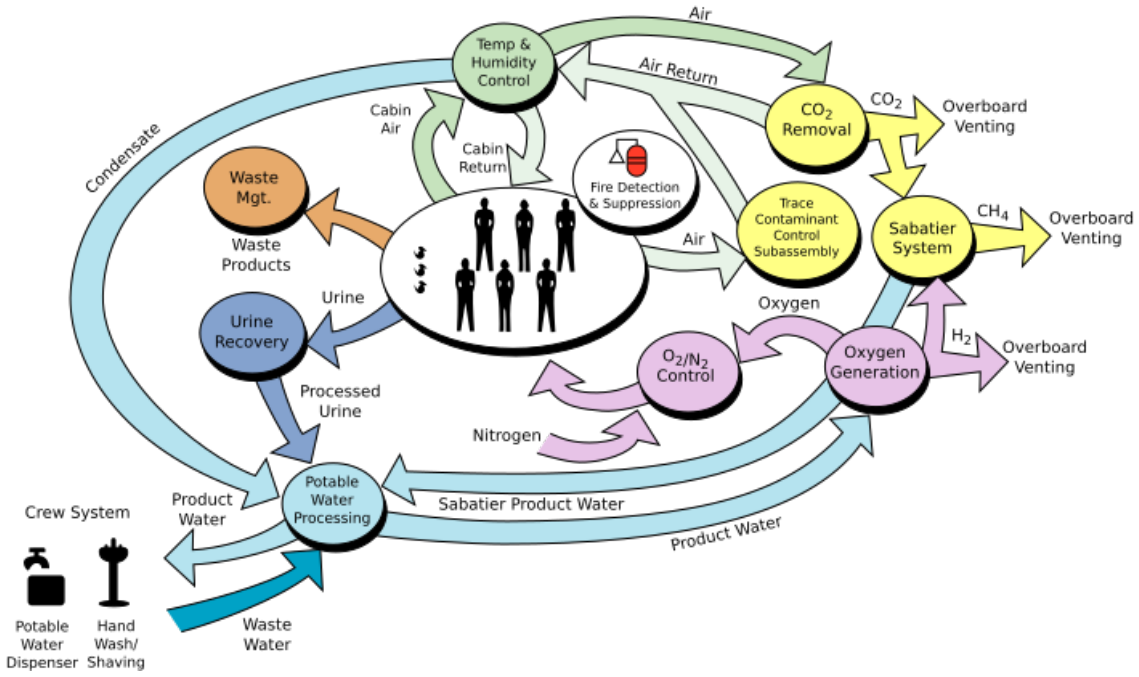

Figure 3.3: A flowchart diagram showing the interations between the different segments of the International Space Station's Environmental Control and Life Support System. Original version: NASA. Derivative version: AntiNeo, http://science.nasa.gov/headlines/images/ecls-air/cycle.gif; Public Domain at Wikimedia.

Some of the common used species that can take part in this cycle are plants and algae. They can be used as food, to clean the air or as raw materials.

For us, they can be also a base material for the generation of hydrogel bases and thickeners for the production of bioinks. Also natural materials from the own body must be considered (blood, hair, nails).

Regarding autonomy, because of the communication delays that exist (bigger as we go further from Earth), machines can not rely on teleoperation manoeuvres. Therefore, humans need machines that are capable of developing pre-programmed routines in real time, taking parameters from the own crew if necessary. 3D (bio)printers allow the generation of several objects, including tissues and prosthesis. It will require a basic technical training, but will work in an autonomous way once programmed.

4

DEVELOPMENT OF NEW CONSTRUCTS FOR BONE REGENERATION

Bone is the most commonly transplanted tissue after blood and the most attempted to replicate after skin. However, no fully functional equivalents have yet been achieved with functional vascularization and that fully integrate inside the body [67]. The complexity of bone including the mechanical, anisotropic, nonlinear, heterogeneous, viscoelastic properties and complex vasculature of bone tissue, is thought to be directly related to the fails of the attempts made to fabricate artificial tissue up to date [68].

Also, tissue engineering (TE) strategies are perceived by clinicians and patients as a time-consuming and expensive process as a result of the necessity of multiple stages of scaffold fabrication (Figure 4.1), cell harvest, culture expansion and reimplantation that discourage their application in real clinical scenarios.

Scaffolds are described as artificial structures used to support three dimensional (3D) tissue ingrowth [68]. Their role is not only structural but functional. They should be used as delivery devices, to provide biological cues for accelerating tissue ingrowth, and also as drug delivery systems, to prevent infections for having an opportunity to succeed as bone engineering devices. Considerations for the manufacturing of scaffolds comprise:

- Material composition and processabiliy.
- Superficial characteristics (roughness, protein adhesion, cell atachment, porosity, etc.).

– Internal designed porosity and architecture

– Degradation kinetics and byproducts.

– Mechanical performance changes over the time.

The first requirement for the selection of a material for bone regeneration is the cytocompatibility. Ideally, it should also be osteoinductive but at least it should be considered osteoconductive and biodegradable. Another requirement is that the biodegradable products (byside products) are not toxic.

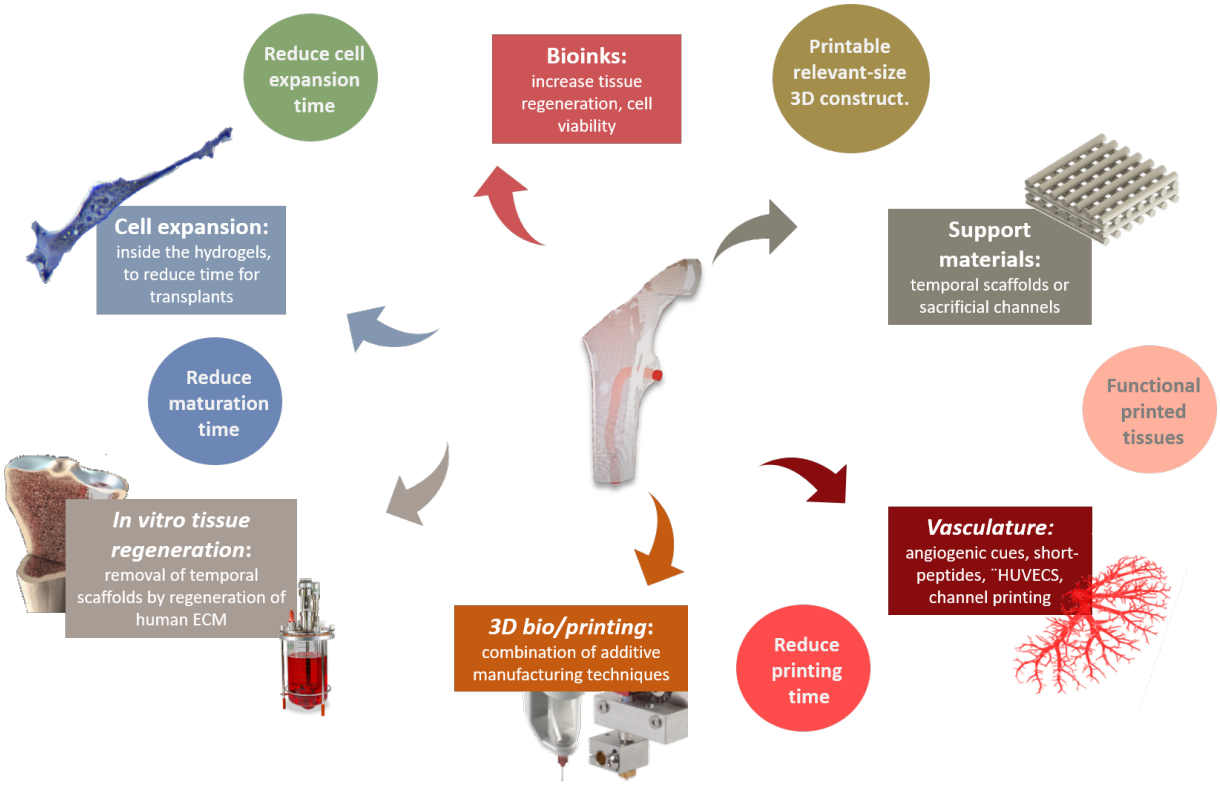

Figure 4.1: Requirements of the biomaterials and devices that must be developed to achieve an effective bone regeneration.

Many different approaches have been tried to develop composite materials for bone regeneration. The most common approaches used up to now for the development of bone scaffolds are the use of calcium phosphate cements (CPC), that present a self-setting behaviour with a

phase change that produces hydroxyapatite, and the use of thermoplastics (as polycaprolactone (PCL) or polilactic acid (PLA)), commonly used in the last years as ceramics carriers for 3D printing and bioprinting.

As stated above, the processability of the material should be considered. The selection of the technology to be used for the manufacturing process will come determined by the processability of the chosen materials. When thinking about bioprinting, because of the material requirements to obtain a layer deposition (as the need of high temperatures for melting) or its behaviour when set (drastic pH changes or exothermic reactions), not easy combination with living cells is attainable.

◀ *Obj 4.*

Research question: *Design and development of new bioinks*

In this work, and according to the previous general understandings, three main points or requirements were considered:

1. Bone constructs should contain mineral phases providing a physico-chemical and mechanical **similarity to native hydroxyapatite** [69, 70, 71].
2. For clinical relevance, the engineered grafts should be **scalable to volumetric size** (>10x10x10 mm^3) [33].
3. Cells in the center of a volumetric tissue need nutrient and oxygen supply and therefore tissue engineered constructs should **contain macropores** to allow **good cell vitality** in the center of the bioprinted construct and potentially also ingrowth of blood vessels after implantation [72, 73].

An additional requirement to extend the validity of these materials and constructs to space exploration missions is that the **biological materials** employed in the development of bioinks **can be obtained from the own crew (cells, proteins, serum) or grown from plants**, safe bacteria or fungi [74, 75]. The mineral components for the pastes could be obtained from animal bones and shells.

It has been published that the combination of CPC and soft hydrogels based on alginate and methylcellulose allow the fabrication of bone precursors [76, 77]. However, there is an important decrease of the cell viability in the points of contact between the hydrogel and the cement. Although still no further studies have been published regarding this effect, the most probable causes are a local pH change provoked by the CPC when transforming to hydroxyapatite, or a local toxicity effect created by the carried liquid of the cement paste[1].

Research question 3 ►
Design and development of new biomaterials/bioinks to create volumetric, size relevant tissues [...]

Therefore, a new bioink that avoids or cushions the death rate of the cell embedded into it, and that covers the points specified above, was required to print along this calcium phosphate cement. More information about the CPC employed can be found at Section 4.1.5.

4.1 SELECTION OF THE MATERIALS

Obj 3. ►

Research question:
Selection of the materials for the demonstrators

To pursue the autonomy of the crew at the exploratory missions, the base materials employed to bioinks must be easy to obtain. Therefore, natural sources like algae or plant derivatives, and materials coming directly from the human body are preferred.

One of the easiest and available materials to obtain in any manned mission is human plasma. It can be isolated through mechanical separation (centrifugation) from blood. As it is the largest component of blood, a normal donation of blood (almost 500 mL that can be donated every 56 days, so 250 mL monthly) will give 137.5 mL of plasma, which for bioprinted constructs would be sufficient for more than 800 cm^2 of artificial skin or for 50 cm^3 of bone equivalent (base calculations can be found at Figure 4.2).

1 More test are already ongoing regarding this effect. For the pH, nanoparticle sensors are introduced inside the paste and the pH change is studied. This is still a work in progress. Similar published work [78]

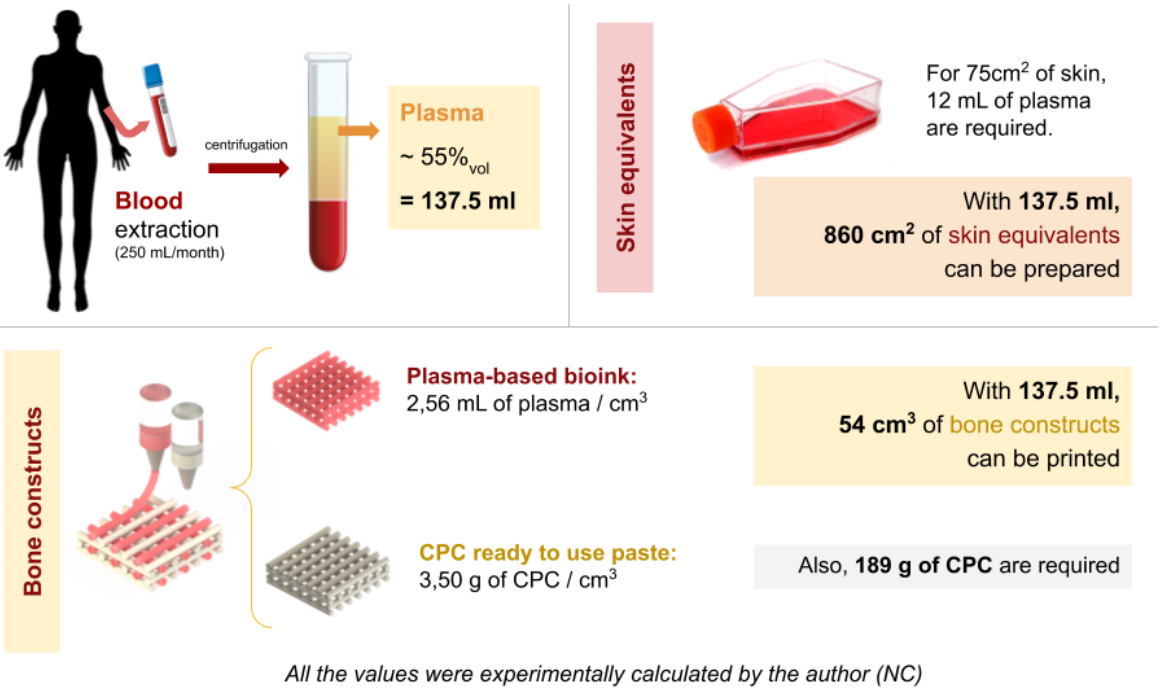

Figure 4.2: Calculations for skin and bone equivalents, with 250 mL of plasma, the amount that a human can donate monthly without risk.

Plasma contains many proteins and growth factors that promote cell activity and wound healing. This mimics the natural healing process that happens inside the body after injuries, while the blood coming from the damaged areas clots thanks to the platelets and coagulating factors present in plasma. Afterwards, the surrounding cells will invade the clot and start the regeneration of the damaged area. However, as the consistency of plasma is similar to that of water and as it requires long times to form a clot depending on the donor, it will not be a good material for bioprinting when used alone or in altered gravity conditions.

For this reason, and following the strategy mentioned above, a **new bioink based on fresh-frozen human plasma plus other two natural materials** coming from algae and plants (to improve its printability and stability) was developed within this project.

Briefly (as shown in Figure 4.3), the first plant derived modifier used,

that allows plasma to become printable, is methylcellulose (mc). It can be synthesized easily from cellulose which is extracted from plants. Based on rheological analyses and previous works with these materials, mc (M0512, Sigma, USA, molecular weight $\approx$ 88.000 Da, 4.000 cP) was dissolved in plasma in a concentration of 90 $mg.mL^{-1}$ (9% w/v). The second component, used to obtain a faster stabilization as it is easily crosslinkable, was alginate (disolved with a concentration of 30 $mg.mL^{-1}$ (3% w/v)). It is derived from brown algae which may be cultured under altered gravity conditions.

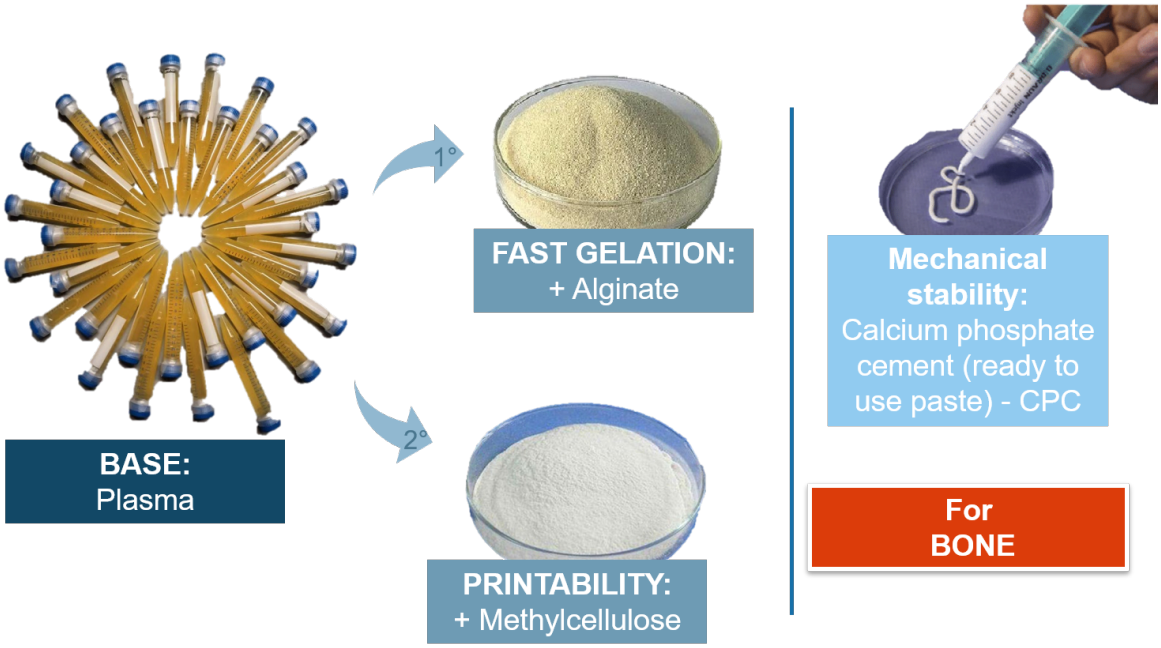

Figure 4.3: Components of the plasma-based bioink and the ready-to-use CPC used for biphasic constructs. PCL can also be used as mechanical support.

Both mc and alginate can be also used for nutritional purposes as they are approved as a food additive (E461 and E400-405, respectively). In addition, the use of algae and plants can be of help to produce also oxygen and to purify water.

In the next subsections, the experimental work carried out to develop the new bioink and select the proper biomaterials will be explained in further detail, step by step. It will cover (Figure 4.4):

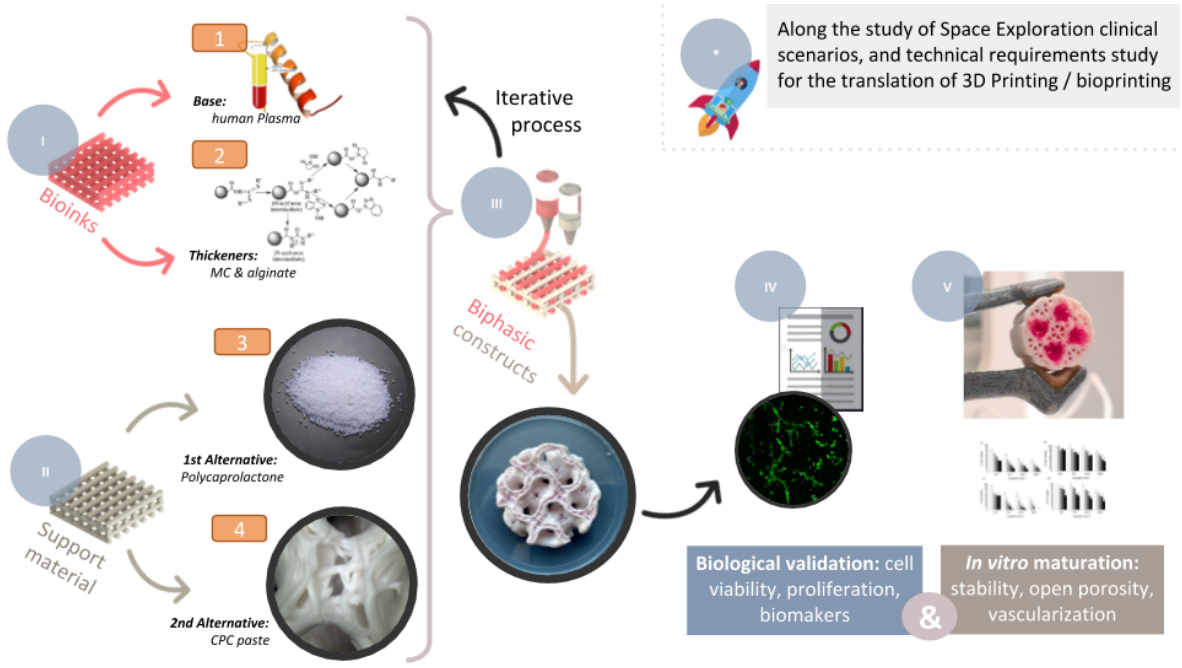

Figure 4.4: Summary of the experimental work developed for bone: plasma-bioink, support materials, biphasic constructs, biological and mechanical test.

- The development of the plasma-based bioink.
- The selection of the support materials. For bone two different approaches were contemplated to improve the mechanical strength of the construct: the use of a extrudable thermoplastic polymer (polycaprolactone) and a self-setting calcium phosphate cement (CPC).
- The fabrication of the biphasic constructs.
- And finally all the biological and mechanical testing performed to validate this materials.

4.1.1 *Plasma derivatives*

As stated above, plasma is the largest component of blood and makes up about 55% of total blood volume; it contains over 700 proteins (as fibrinogen,

fibronectin or albumin) and other substances. It has been widely used as base material for tissue engineering to treat skin, bone, muscles, nerves, eye lesions, etc., as it promotes the natural process of wound healing, resembling the induced conditions when a tissue is injured.

In this work, the amount of fibrinogen (2.26 $mg \cdot mL^{-1}$ in the pooled plasma, using the Clauss fibrinogen assay [79]) and the protein content was analyzed, as they might influence the response of cells to a plasma-based bioink. Experimental procedures can be found on p. 115. Results for the 10 highest expressed angiogenic proteins are shown in Figure 4.5.

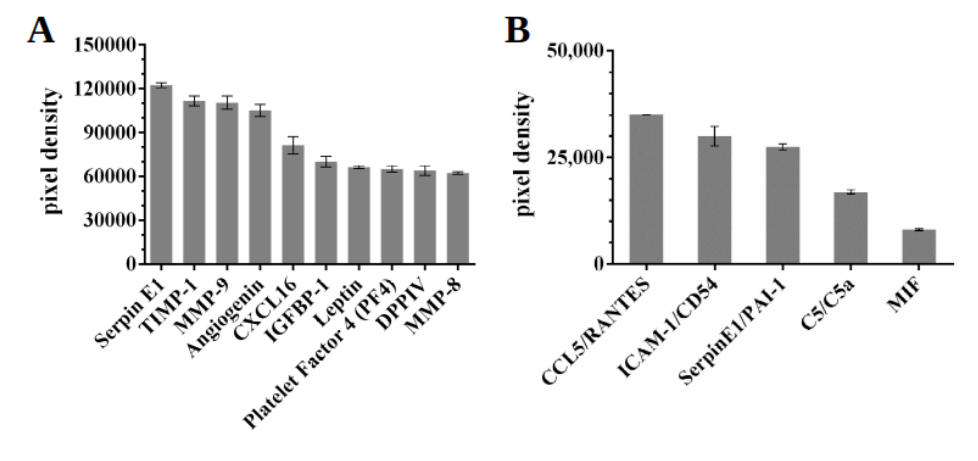

Figure 4.5: Characterization of growth factors included in the pooled plasma. Exemplarily displayed are the most highly expressed proteins. The used protein arrays showed (A) angiogenic proteins and (B) cytokines/chemokines.

The array revealed a total of 28 angiogenic factors, which could contribute actively to vascularization of bioprinted grafts. Moreover, these proteins might provide pro-inflammatory and anti-inflammatory cues, as well as support for the proliferation of endothelial cells and the sprouting of angiogenic progenitors, such as angiogenin [80]. Also serpin E1 (an inhibitor of fibrinolysis [81]) and leptin (impacting bone metabolism [82]) were detected, which might be influential for bone tissue development.

Also, five cytokines that play a role in inflammation and mediate the

crosstalk between cells, especially of the hematopoietic system, could be detected (Figure 4.5 B).

Overall, the plasma pool contained a large variety of proteins and growth factors that might function together more effectively than single proteins can impact the response of cells to the bioink.

"For a successful technology, reality must take precedence over public relations, for Nature cannot be fooled"

Prof Richard Feynman

Plasma was chosen, because as stated above, it is easy and cheap to obtain, and always present in a manned mission. In addition, it allows us to send the wound healing signals that would be present in a real body injury. The natural process is as follows:

1. Blood is the main transportation system in the human body, it circulates through the endothelium, which is the tissue that lines the inside of all blood vessels, including those of the heart.
2. Although the transport and supply of oxygen to tissue cells is carried out by specialized cells, other vital components such as nutrients, metabolites, electrolytes, and hormones are carried over into the non-cellular fraction of blood, plasma.
3. When a blood vessel breaks, a blood clot forms as part of haemostasis, which is the body's physiological response to stop bleeding.
4. During haemostasis, a primary haemostatic plug, consisting of platelet aggregates and a fibrin clot, forms at the site of the injury.

The formation of the fibrin network is the process by which soluble fibrinogen in the blood is converted into insoluble fibrin by the action of thrombin and transglutaminase or factor XIIIa. This process comprises three main stages: proteolysis of fibrinogen by the action of thrombin, polymerization of fibrin monomers and stabilization of fibrin by factor XIIIa [83, 84].

Injury to the endothelium activates the blood coagulation cascade (Figure 4.6), which ultimately activates thrombin (which in turn activates fibrinogen

polymerization in fibrin) and factor XIII that binds the strands of fibrin monomers to form a clot. stable. The blood coagulation cascade is made up of a series of enzymes, which are inactive until a previous enzyme in the cascade activates their action. Other proteins (Factor V and Factor VIII) serve for protein binding, assembling factor complexes at the site of injury [85].

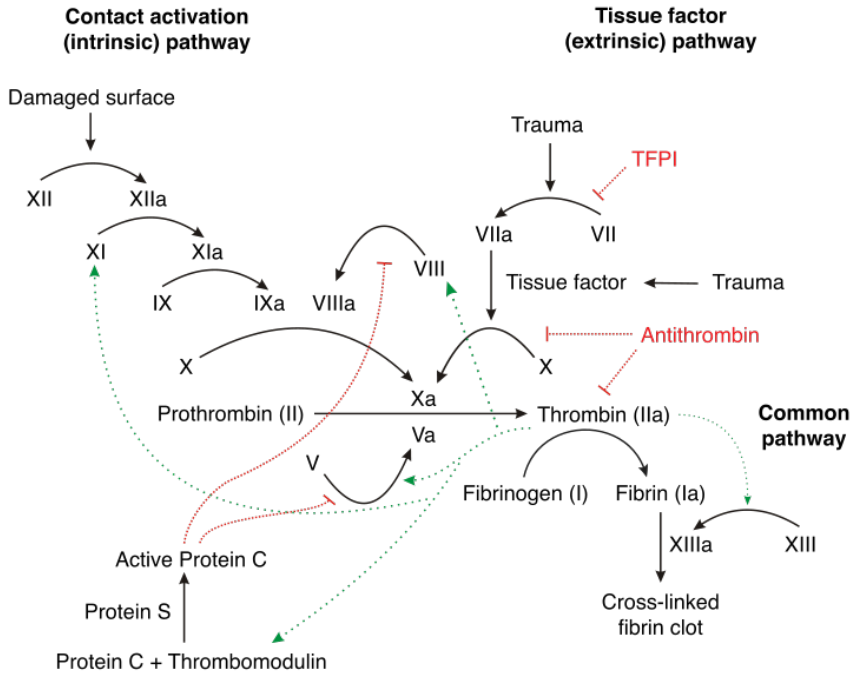

Figure 4.6: Schematic overview of the coagulation cascade. Coagulation factors are indicated by Roman numerals, with suffix "a" indicating the activated form. TFPI = tissue factor pathway inhibitor. Picture from: Joe D, Wikimedia C.C. S-A. 3.0.

The author of this thesis, worked previously with plasma to create skin equivalents through 3D bioprinting [49]. However, in that case, plasma was deposited as flat sheets, and no 3D structure was required. In that occasion, plasma gelation started inmediatly before deposition, so the deposited bioink was more viscous than pure plasma, allowing the material to remain in its place. However, it would not allow the deposition of stacked layers until complete gelation, which could take up to 2 hours [49].

However, for bone constructs with open pores, the low viscosity of plasma would not allow printing of strands with enhanced shape fidelity. Because of this, it was blended with two natural and easy to obtain biopolymers: alginate for enhancement of viscosity and fast and cytocompatible gelation with divalent ions, and methylcellulose, which was shown in several studies to increase the viscosity of a bioink tremendously [86].

4.1.2 *Sodium alginate (alg)*

Alginate (alg) is a linear polysaccharide composed of homopolymeric units of 1,4-linked (-D-mannuronic acid) (M) and (-L-guluronic acid) (G) (Figure 4.7). M block segments posses a linear and flexible conformation; whereas the (1 - 4) linkages to guluronic acid introduce a steric hindrance around the carboxyl groups. For this reason, the G block segments provide folded and rigid structural conformation that is responsible for a pronounced stiffness of the molecular chains. High M content alginates are also immunogenic and more potent in inducing cytokine production as compared to high G content alginates. Alginates extracted from different sources have different M and G contents along with the length of each block, influencing the properties of the material [87].

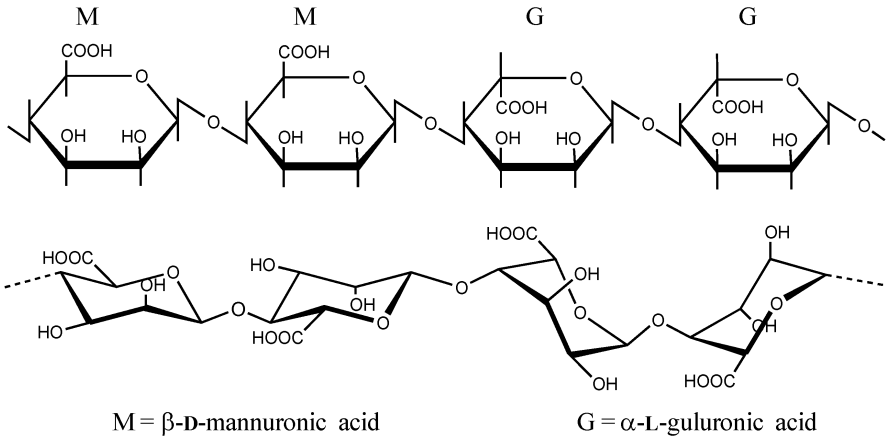

Figure 4.7: Sodium alginate chemical structure. Image license: public domain.

The alginate used in this work was purchased to Sigma-Aldrich (Merk), Germany. The M/G ratio was experimentally obtained by an international collaborator of the ICTP Lab (Aurora C.Hernández-González)., by FTIR using the Filippov and Kohn method [88] and with RMN [89]. It has been extensively investigated and used in biomedical applications due to its biocompatibility, low toxicity, and gel formation in the presence of divalent cations such as Ca^{2+} [87].

In this work, alginate is used a as viscosity increasing agent and to decrease the gelation time of our hydrogel (up to 2 h in some cases when working only with plasma), as stated before.

4.1.3 *Methylcellulose (mc)*

Methylcellulose (mc) is a polysaccharide, the methyl ether of cellulose (Figure 4.8). It is non-toxic and biocompatible polymer, with a totally reversible thermo gelling behaviour. It is in sol-state at low temperatures and in gel-state at high temperatures. The gelation temperature, as well as the gel strength, is dependent on the degree of substitution, the concentration and the molecular weight of methylcellulose, as well as on the media electrolyte concentrations [86].

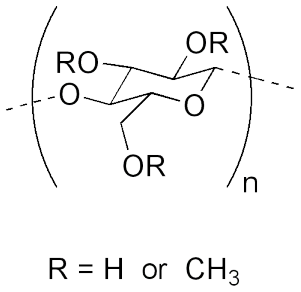

Figure 4.8: Methylcellulose chemical structure. Image license: public domain.

It has been demonstrated that methylcelluse can be released after polymer crosslinking along the maturation/swelling process in cell culture

media or any other buffer. This release is affected by the sterilization method employed, as the mc chains break generating shorter molecules that can scape more easily [90]. This can led to the generation of micropores, which will improve the diffusion of oxygen and nutrients.

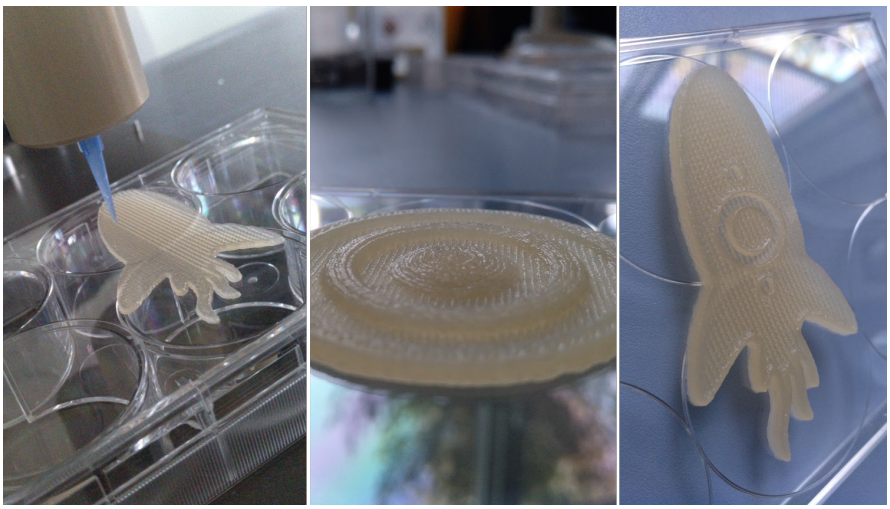

Figure 4.9: Stability of the plasma-alginate-methylcellulose (plasma-alg-mc) hydrogel before crosslinking thanks to the addition of methylcellulose.

As stated above, alginate provided the fast gelation response required to stack layers while printing. However, the concentration of alginate required to make plasma printable, is too high for a practical use. If just alginate would be used to make plasma printable, a concentration higher than the 8% (experimentally tested) will be necessary to make it printable. With this amount of alginate (that does not contains RGD domains), cells have troubles to migrate, spread or proliferate. RGD peptides can be included to improve the biological integration inside the material, or use modified alginates, as those that have been oxided to provide more cell adhesion regions [91].

Therefore, a modification of the alginate or the addition of another material (in our case mc) was required to make the plasma-based bioink printable and biologically attractive.

4.1.4 *Polycaprolactone (PCL)*

One of the most critical conditions that engineered constructs should have to achieve a successfully regeneration of the target tissue, is to present similar properties than the native tissue. For bone regeneration, mechanical properties are fundamental to withstand the natural physiological loading inside the body and send the correct signals to the neighbour cells and tissues. Of course, other properties such us the surface topography and porosity, or the own chemistry of the material will also have a strong influence in the attachment of the cells and into the posterior development of the tissue. In addition, the material degradation kinetics is also a key point for an appropriate tissue regeneration, as the material should degrade in a rate that allows cells to remodel the matrix without endanger the mechanical stability of the construct [67]. Along this process, vascular channels will also need space to invade the new tissue to keep cells alive.

Thus, the materials and the manufacturing processes chosen to develop the desired tissue engineered scaffolds should comply with all those requirements and provide a long-term stability and integration.

Polycaprolactone (PCL) is one of the most used synthetic polymers for tissue engineering and regenerative medicine applications. This is due to the appropriate properties of PCL. These include long-term biodegradability, ease of processing due to the low melting temperature ($\approx$ -60°C), suitable rheological and viscoelastic properties, and thermal stability. Because of its history in drug delivery devices, PCL has also a shorter regulatory path to market than many other polymer systems through the Food and Drug Administration (FDA) and the European Medicines Agency (EMA). As an example, a custom designed airway splint device was printed using PCL, and administered to the patient under the emergency-use exemption from the FDA [92]. Although PCL is not bioactive, the introduction of active biological clues does not require strong synthetic efforts. It can easily be manufactured with properties tailored to suit specific applications [93, 94].

Some groups have already worked also with PCL in combination with living cells to create hybrid constructs for bone or cartilage tissue engineering in real bioprinting efforts [95, 96, 97].

As explained above, bioprinting involves the use of bioinks which combine biological and hosting synthetic materials [49]. Hydrogels are normally used as the hosting material for bioinks but they do not present appropriate mechanical properties for bone or cartilage applications [87]. Bone tissue engineering efforts have been, then, directed to combine bioinks with temporal scaffolds that ensure good stability along the regeneration process before the synthetic device is replaced by natural extra cellular matrix (ECM). However, since thermoplastics used in the manufacture of the temporal scaffolds present a melting point above the physiological temperature of living cells, which endangers cell viability, the most feasible approach consists in the fabrication of scaffolds (3D printing) that can be cell seeded a posteriori [98].

Along the development of this thesis, the influence of parameters of "hidden" importance in the design of PCL (3D4makers.com, Haarlem, Netherlands) scaffolds, such as, number and orientation of layers, cooling rate or positioning of the starting point in the printer, in the porosity and mechanical performance of the scaffolds were studied [99]. These parameters have been named "hidden" because they are not normally provided and, as it can be observed from the results, and discussed above, they may affect dramatically the performance and the reproducibility of thermoplastic scaffolds manufactured through 3D printing for bone tissue engineering.

PCL is still under study and further modifications (introduction of hydroxyapatite with Sr^{2+}) are carried out in parallel, so it was left out of the final application, choosing a ready to use CPC paste as the final support material. However, the conclusions and results obtained along this first approach with PCL can be consulted in section 4.3 and at the publications released [99, 100].

4.1.5 *Calcium phosphate cement (CPC)*

Calcium phosphate cement (CPC), is a bioactive and biodegradable material (paste) that sets with humidity creating hydroxyapatite, which is the mineral phase that can be found in bone and that gives it its rigidity. This pasty material can potentially be replaced with bone after a period of time, as cells (osteoclasts) can degrade it so that osteoblasts over time can rebuild the natural environment.

The CPC paste used is manufactured by INNOTERE GmbH (Radebeul, Germany), has the CE mark for clinical application in Europe and is sterilized by γ -irradiation (25 kGy) before use.

It is based in some precursor powders: α-tricalcium phosphate, calcium hydrogen phosphate anhydrous, calcium carbonate and precipitated hydroxyapatite. As catalyst, potassium hydrogen phosphate is used, and as carrier liquids: Miglyol, Cremophor ELP and Amphisol A [101].

4.2 BIOINK ASSESSMENT

Once the materials have been selected, the ratio between the components must be studied. Literature reports that a 3% of alginate and a 9% of methylcellulose is a good ratio regarding rheology, to ensure the printability of the material [102]. However, as high concentrations of alginate can produce a matrix with very small pores and too stiff for cells to migrate and obtain the nutrients, other smaller percentages had to be tested too. Also rheological test are needed to test the flow, stability and recovery of the bioink.

4.2.1 *Alginate and Methylcellulose concentrations*

As stated above (section 4.1.1), plasma can require long times to gelate, and alginate was added to achieve a fast crosslinking. Trying to reduce the

amount of alginate used in the literature (3%), different concentrations of alginate were studied, with and without plasma as solvent (summary of the sample conditions included in Table 4.1).

Table 4.1: Summary of samples studied, varying the concentration of alginate, methylcellulose and plasma. Qualitative measurement of hydrogel stability and cell spreading capacity.

Exp. n	Plasma/HBSS	Alginate	MC	Stable?	Cell spreading?
1	HBSS	0.39%	-	+	?
2	HBSS	3.00%	-	+++	-
3	HBSS	0.39%	9%	+	?
4	HBSS	3.00%	9%	+++	+
5	Plasma	-	-	-	+++
6	Plasma	0.39%	-	+	++
7	Plasma	3.00%	9%	+++	+++
8	Plasma	0.39%	9%	+	++

When plasma was not the base for the paste, Hanks' Balanced Salt Solution (HBSS) was used instead. PBS was never employed because the phosphates present on it can kidnap the Ca^{2+} (quelant effect), avoiding the gelation of the hydrogel. Because of the variable nature of plasma, even withing the same patient in two different extraction time points, plasma for at least 5 donors was always pooled to obtain an uniform mixture.

Also, mc was added or not to the mixture. When mc was not present, the mixture was liquid (not viscous enough to be printed), and the scaffolds for the study were obtained as cylinders, gelating the combination inside a 24-well plate. When mc was added, the resulting paste cannot flow due to its high viscosity, so a spatula is used to form similar cylinders in a 24-well plate that can be compared. Those disks had an approximate diameter of 15 mm and were 2 mm height.

Before forming the disks, $5{\cdot}10^6$ cells per gram of paste were added to the hydrogel and gently mixed by hand with a spatula to form the bioink. Human telomerase reverse transcriptase-immortalized mesenchymal stem cells (hTERT-MSC) were used in this case.

For the experiments, pictures were taken at day 7 and day 14, studying cell viability (Live/Dead staining) and their morphology once fixed (DAPI-Phalloidin), to see the nucleus and the actin cytoskeleton and microfilaments. With this, it was possible to discriminate which materials would allow the spreading of the cells and their migration. Cell media (DMEM with 1% P/S and 10% FBS) was changed every 2 days.

The first analysis showed that small amounts of alginate, although allowing a better cell spreading, produced non-stable matrices that dissolved in 3-5 days (in HBSS, at 37°C). However, pure plasma matrices made by hand did not show this problem. It is possible that alginate steal calcium ions for its own gelation first. Afterwards, plasma can have a lack of cations, not allowing fibrin to form more stable networks.

If mc was not used, the mixture was too liquid to be printable, with or without plasma. This was expected, as the viscosity of the plasma was similar to water.

The most significative results are summarized in Figure 4.10. Only those stable enough to be handable after 2 weeks (3% alginate) were finally selected. Between those, it was observed that:

- When only alginate is present, cells do not spread and remain in a spherical morphology that won't allow a proper differentiation of the MSC. That is because alginate lacks cell-binding motifs. For its use alone, alginate would require some modification, as the adding of RGD domains.
- The presence of mc fibres inside the alginate network seems to allow a slightly better spreading of the cells, as can be seen when comparing

the two first images.

– If plasma was present, cells were capable of spread (even after some hours), migrate and form networks, already at day 7. After 2 weeks, it was the only one totally covered by cells.

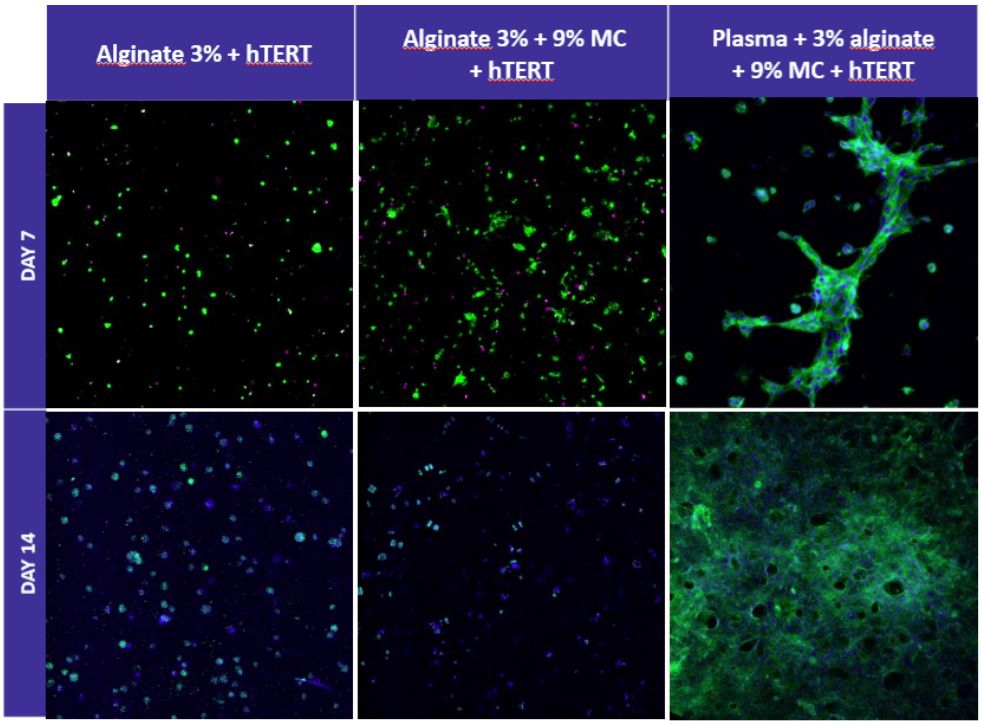

Figure 4.10: Cell staining (DAPI/Phalloidin*) used for a comparative study of hydrogels with and without plasma or methyl cellulose. *The two first images starting at the upper left corner show a Live/Dead staining.

4.2.2 *Rheological test: plasma-based bioink*

To check viscosity and printability properties, plasma, plasma-alg and plasma-alg-mc pastes were evaluated for rheological behaviour, as described on p. 115. When working with Non-Newtonian fluids, the viscosity varies as a function of the applied shear stress/shear rate.

In summary, the following test were carried out (results can be seen in Figure 4.11, and described below):

1. **Shear thinning** (constantly increasing shear rates), to obtain the degree of shear thinning (decrease of viscosity with increasing shear) when printing, predicting the extrusion process success and the cell survival.
2. **Amplitude sweep**, to detect the shear stress range that belongs to the linear viscoelastic region (LVR), were the material shows a visco-elastic behaviour (shear stress and shear rate are proportional).
3. **Oscillatory frequency sweep** tests, to obtain the viscosity, and the storage (G') & loss (G'') modulus inside the LVR.
4. **Shear recovery** tests of plasma-alg-mc, inducing shear stresses of the LVR, to test the capacity of the material to recover (be stable) after being printed.

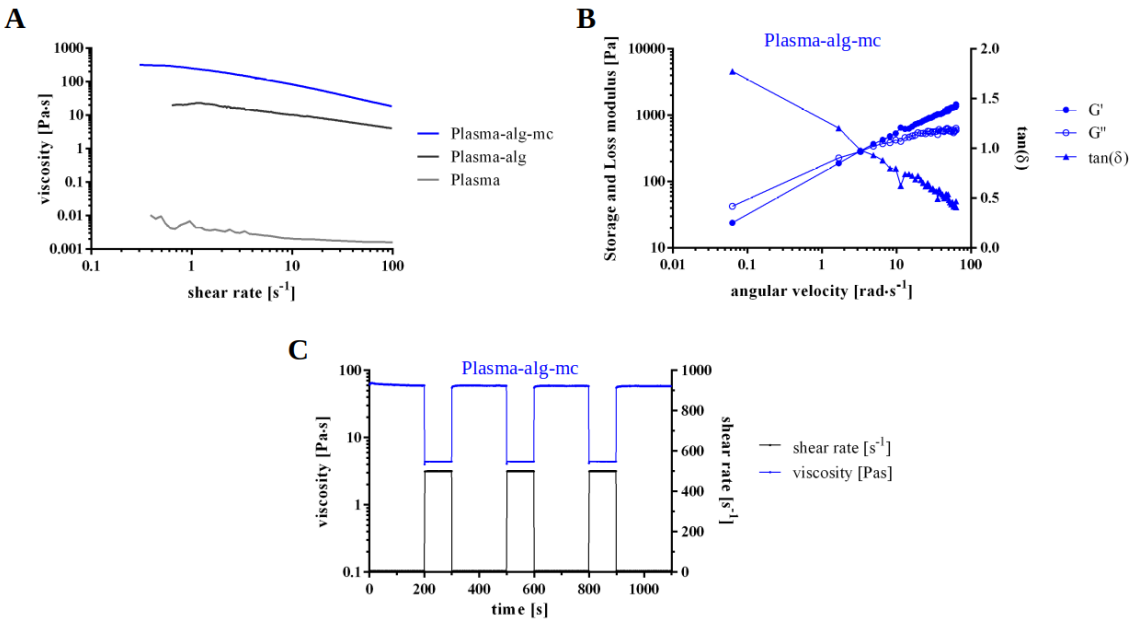

Figure 4.11: Rheological studies performed. Representative curves of (A) shear thinning experiments of plasma, 3 w/v% alginate dissolved in plasma and 3 w/v % alginate-9 w/v% methylcellulose dissolved in plasma; (B) Frequency sweep test of plasma-alg-mc; (C) Shear recovery tests of plasma-alg-mc.

Rheological evaluation of the plasma revealed a low viscosity comparable to that of pure water, as well as a shear thinning behaviour, most probably as

an effect of the contained fibrinogen (Figure 4.11 A). Therefore, **pure plasma could not be plotted as single substance** into macroporous structures, as the strands would fuse together after deposition leading to a complete unporous structure which inhibits diffusion of oxygen and nutrients. Hence, plasma was evaluated for its capability to be blended with biopolymers to enhance its plottability (Figure 4.11 A), as stated in previous sections.

3 w/v% alginate (alg) was dissolved in the plasma solution, resulting in a significantly **increased viscosity**. Furthermore, incorporation of alginate into the bioink would allow fast and cytocompatible crosslinking after fabrication. However, initial plotting tests displayed a collapse of plotted strands in z-direction and macropores were not stable after plotting (data not shown).

Therefore, **9 w/v% methylcellulose** (mc) were added to the plasma-alg solution, resulting in a **significant increase of ink viscosity** (Figure 4.11 A), similarly as already shown for 3% alg dissolved in PBS [102].

A frequency sweep test of plasma-alg-mc is shown in Figure 4.11 B. Both, storage and loss modulus increased with the angular velocity. Until a cross-over point at 3.2 rad·s^{-1}, the loss modulus was higher compared to the storage modulus, indicating that **plasma-alg-mc was not crosslinked in zero-shear state.**

The shear recovery behaviour of plasma-alg-mc (Figure 4.11 C), shows than even after repeated exposure to high shear rates, the paste was able to increase its viscosity in low-shear regions and full recovery, compared to previous cycles. The average **recovery time was determined as 39.1±13s**, which is a rather high value compared to values reported in literature like those for highly concentrated poloxamer 407 inks (25 s) [103] or alginate-carrageenan inks (5-15 s) [104].

The conclusions extrapolated from this experiments were:

- Plasma enhances the spreading and migration of the cells, but because of its low viscosity can not be plotted as single substance.
- Alginate seems to be interacting with the fibrinogen network formation, but is essential for the fast crosslinking of the mixture. Low concentrations produce non-stable matrices.
- Methylcellulose is truly essential to make the paste printable, as plasma-alginate blend strands collapse in z-direction and macropores were not stable after plotting.

4.2.3 *3D plotting of plasma-based bioink*

After the preparation of the bioink (protocol that can be found on p. 115), plasma-alg-mc could be plotted in 0°/90°layer patterns resulting in rectangular macropores between the strands (Figure 4.12 A).

Additionally, **more complex structures** of larger scales were achieved with high accuracy as demonstrated with the logo of the Technische Universität Dresden in which **more than 50 layers** were easily stacked achieving volumetric structures (Figure 4.12 B, C). Moreover, the logo of the Centre for Translational Bone, Joint and Soft Tissue Research with a basic area of approx. 176 cm^2 was successfully plotted (Figure 4.12 D).

In scanning electron microscopy (SEM) images of the surface and the cross section of plasma-alg-mc strands (Figure 4.12 E-G) **no heterogeneous domains were observed,** indicating that alginate and methylcellulose, but also the fibrinogen of the plasma, were homogeneously distributed throughout the entire scaffold. Most crucially, **fibrinogen did not self-assemble to fibrin during the storage in the cartridge** prior to the plotting process, which otherwise would have led to an inhomogeneous

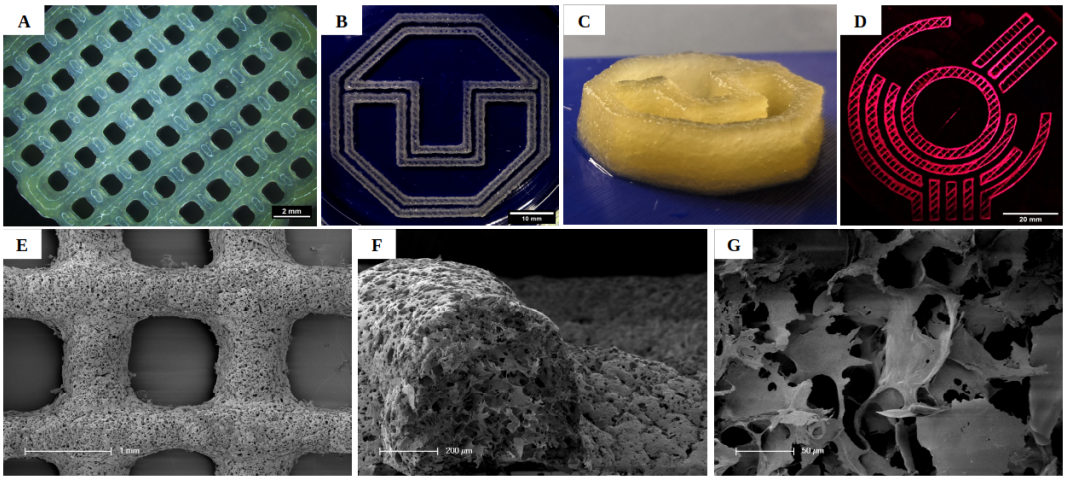

Figure 4.12: Extrusion-based printing of the plasma-alg-mc ink. (A) Stereomicroscopic image of a cubic scaffold plotted with a 0°/90°layer orientation (4 layers). (B, C) Images of a plotted logo of the Technische Universität Dresden (50 layers), (D) image of a plotted large-sized logo of the Centre for Translational Bone, Joint and Tissue Research (4 layers). (E-G) Scanning electron microscopical images of the plasma-alg-mc ink. Scale bars: (A) 2 mm, (B) 10 mm, (D) 20 mm, (E) 1 mm, (F) 200 µm, (G) 50 µm.

material deposition. Additionally, a distinct microporosity of the plasma-alg-mc ink was observed.

4.2.4 *Bioplotting of MSC embedded at the plasma-based bioink*

In order to investigate the applicability of the plasma-alg-mc ink for bioplotting, **human mesenchymal stem cells (MSC) were encapsulated into the bioink** and subsequently plotted and crosslinked before incubation in cell culture medium. As plasma-free control, a bioink with similar concentrations of alginate and methylcellulose but dissolved in PBS was used. The complete detailed protocol can be found on p. 118.

Viability of MSC in the plotted scaffolds, assessed at day 1 by live/dead staining (Figure 4.13 A,B), was s**ignificantly increased in the plasma-alg-mc bioink** (77.6 ± 2.7%) compared to the PBS-alg-mc bioink (49.7 ± 4.7%). In the

case of **PBS-alg-mc,** cell viability increased over time (up to 95%), however, MSC stay roundish, as the ink **lacks binding motifs for cell attachment.**

In contrast, a dense network of MSC was found within the **plasma-alg-mc ink**, as well as **MSC spread over the scaffold** surface after 14 days of incubation (Figure 4.13 C).

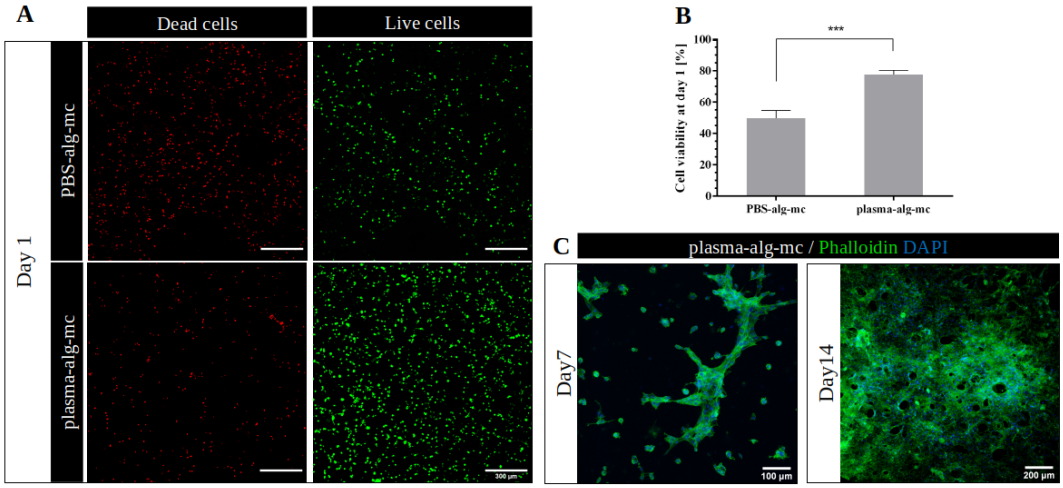

Figure 4.13: Investigations on the behaviour of bioplotted MSC in the plasma-alg-mc bioink, a PBS-alg-mc bioink served as plasma-free control. (A) Representative images of a cell viability staining of MSC (live cells green, dead cells red) at day 1 of cultivation in PBS-alg-mc and plasma-alg-mc. Scale bars represent 300 µ m. (B) Calculated cell viability within the plotted bioinks at day 1 (n=7, mean±SD,***p<0.001). (C) Fluorescence staining of the cytoskeleton (Phalloidin, green) and the nuclei (DAPI, blue) of MSC within the plasma-alg-mc constructs after 7 and 14 d of cultivation. Cells were able to spread and form cell-cell contacts.

4.3 SUPPORT MATERIALS

Once the soft hydrogel that contains the cells is ready, a more robust material that can withstand the loads to which the construction will be subjected, is requiered. For that, an thinking in the current materials available for 3D Printing and aproved by the FDA and the AEMPS,

polycaprolactone (PCL) was chosen for being one of the most used synthetic polymers for tissue engineering and regenerative medicine applications.

4.3.1 *Scaffold design and fabrication with PCL*

Three different configurations were used for the design of the internal structure of the scaffolds, as shown in Figure 4.14; they are: a solid one with alternate layers (0°, 90°), a porous one with 30% infill and alternate layers (0°, 90°) (from now on, ALT) and finally another configuration where 3 layers are piled before changing the orientation (0°, 0°, 0°, 90°, 90°, 90°) also with 30% infill, called non-alternate (n-ALT). All layer patterns were rectilinear and a layer height of 0.25 mm was used, unless stated otherwise.

For the fabrication of the scaffolds, a Hephestos 2 (Prusa i3, BQ, Madrid, Spain) with a heated platform and a double drive gear extruder and a 400 ÎŒm nozzle was used. The nozzle temperature was set to 172°C and the build plate to 40°C. External geometries were designed for each analysis following the ISO normative indicated on each section.

When noted (FAN), an external fan was employed to decrease the cooldown time (forced cool down specimens). The cooling rate with and without the fan was experimentally measured, recording the temperatures obtained in the nozzle every 5 s after switching off the heating current. Without the fan, the cooling rate described a non-linear curve that could be approximated to a second order polynomial (R^2 = 0.999): $0{,}0223x^2$ - 3.5x + 182. Meanwhile, following the same behaviour but with a steeper initial rate, the cooling rate of the system with the use of the external fan was modelled as (R^2 = 0.993): $0{,}0223x^2$ - 3.5x + 182.

Six different pattern probes were obtained from the three original designs (Figure 4.15, Table 4.2): in the alternate configuration, the effect of the starting point position (aligned or random) of the layers was studied; in

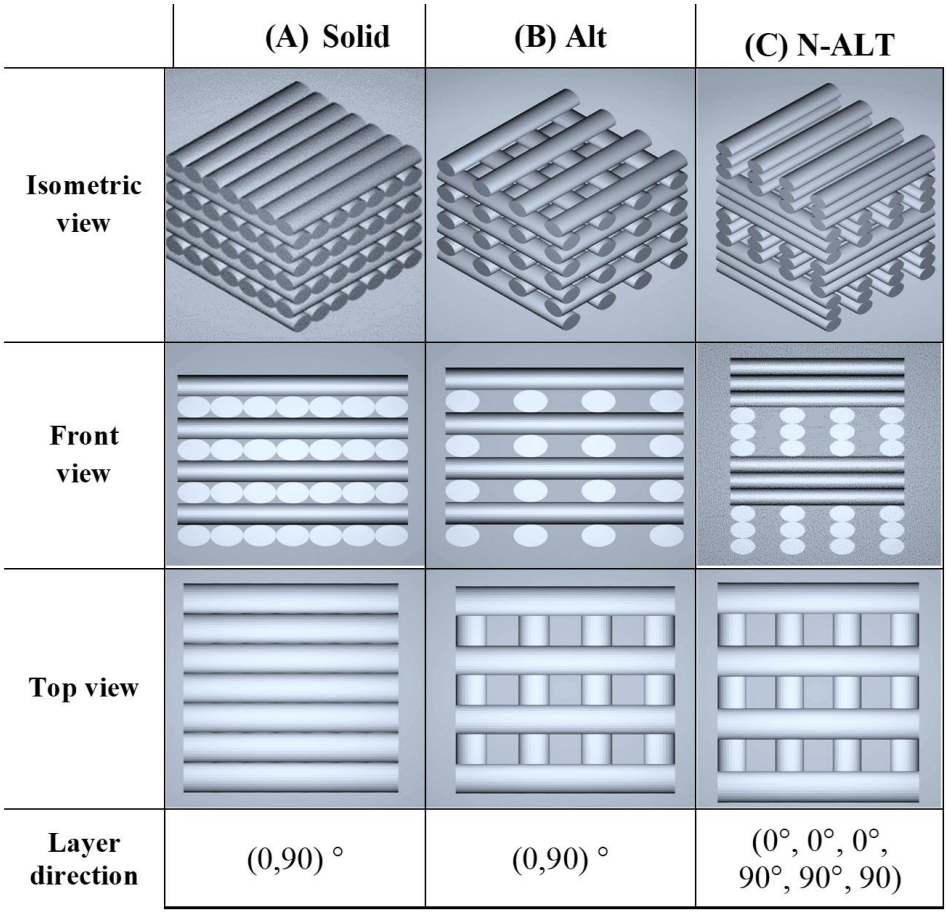

Figure 4.14: 3D models of (A) solid (100% infill), and 30% (B) alternate (ALT) and (C) non-alternate (n-ALT) scaffolds.

the case of the non-alternate configuration, scaffolds were printed first at room temperature (RT) and then with an external fan focused on the printed surface to study the effect of the cooling down speed. Finally, as the non-alternate scaffolds can also be printed in combination with cell-laden hydrogels to create composite materials in bioprinting, a final configuration was created filling the pores a posteriori with a hydrogel. Table 4.2 summarizes the parameters of the six patterns.

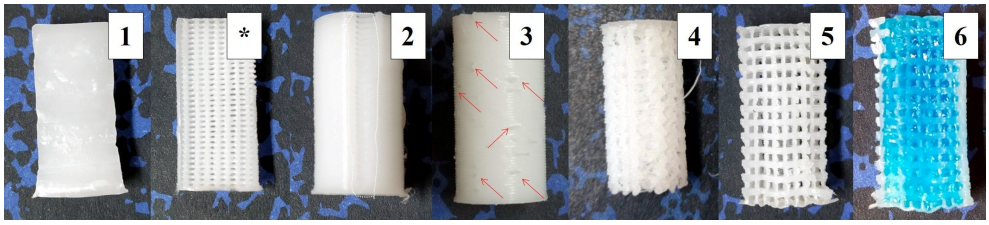

Figure 4.15: Pictures of the six different PCL specimens: (1) Section of solid (100%) infill; *) Section of the 30% alternated scaffolds [2,3]; (2) Aligned seam from fixed starting point at 30% ALT with shell; (3) Random starting point appearance at 30% ALT with shell; nonaligned defects pointed out with arrows; (4) Scaffold resulting from a slow cooling down at 30% n-ALT; (5) Forced cooling down (external fan) of 30% n-ALT; (6) 30% n-ALT filled with the hydrogel and blue colorant for a better contrast (from now 30% n-ALT+hyd).

Table 4.2: Summary of probes configurations (specimens) and their intended features.

n	infill	Layers	Other	Notes
1	100%	solid	solid	Original cylinder for comparison, no pores.
2	30%	ALT	aligned starting point	Porous scaffold, with anisotropy in the Z-axis - Aligned start point (seam)
3			random starting point	Porous scaffold, with anisotropy in the Z-axis - Random start point
4	30%	n-ALT	RT cool down	Porous scaffold, with more isotropy in the Z-axis - Slow cooling down (room temperature)
5			external fan	Porous scaffold, with isotropy in the Z-axis - Forced cooling down (external fan)
6			filled - hydrogel	Porous PCL scaffold, filled with crosslinked hydrogel

4.3.2 *PCL characterization*

The working temperature range for processing the material was studied through thermal analysis, TGA and DSC. T_g, T_f. The TGA assay carried out within a 50 - 600°C range showed a single thermal decomposition step

starting at 392°C and ending at 435°C. Subsequent DSC analysis produced a Tg at -64°C and a melting point at 51°C that agree with literature values and should determine the processing temperature [105]. On the one hand, the PCL filament used has a melting point of 51°C, and degrades above 392°C; on the other hand, the work range of the printer can be set in the range (room temperature -230°C), so the working temperatures to ensure the integrity of both the polymer and the printer, are (51-230°C).

At DMA analysis, PCL shows a prevalent elastic behaviour over 5°C and up to 37°C. Storage modulus decreases with the raise of temperatures. At physiological temperature, once the scaffold has been manufactured, the material holds an elastic modulus of 112.7 MPa (equal to the complex modulus) and a storage (viscous) modulus of 2.90 MPa. It is generally acknowledged that mechanostructural stimuli from the surrounding microenvironments of cells crucially influence cellular functions [106]. Later research focused on the viscous modulus, since the elastic modulus could not fully account for the different cell responses observed to different substrates. It has been found that cells are significantly more sensitive to the fluidic motion of a substrate than to the elastic modulus, especially for biodegradable scaffolds [107], and a minimum in the complex modulus should be the most favourable condition for tissue culturing in these scaffolds as obtained for our printed PCL.

4.3.3 *PCL scaffolds characterization*

SEM images from the alternated (A-B) and not alternated (C-F) scaffolds, obtained from lateral sections of cut samples (A, C and E) or from the top (B, D and F) can be found in Figure 4.16. Image A, that represents the most commonly used z-stack, shows a high anisotropic relation between the pore size in the z-axis when compared with the xy-pore (image B). While C shows a regular and ordered structure, due to a faster cooling down, image E reveals a more chaotic pattern, with some closed pores. The same effect can be observed from the top; in F, the polymer flowed a little bit before setting,

creating flatter and thinner strands, in contrast with more cylindrical ones observed at D.

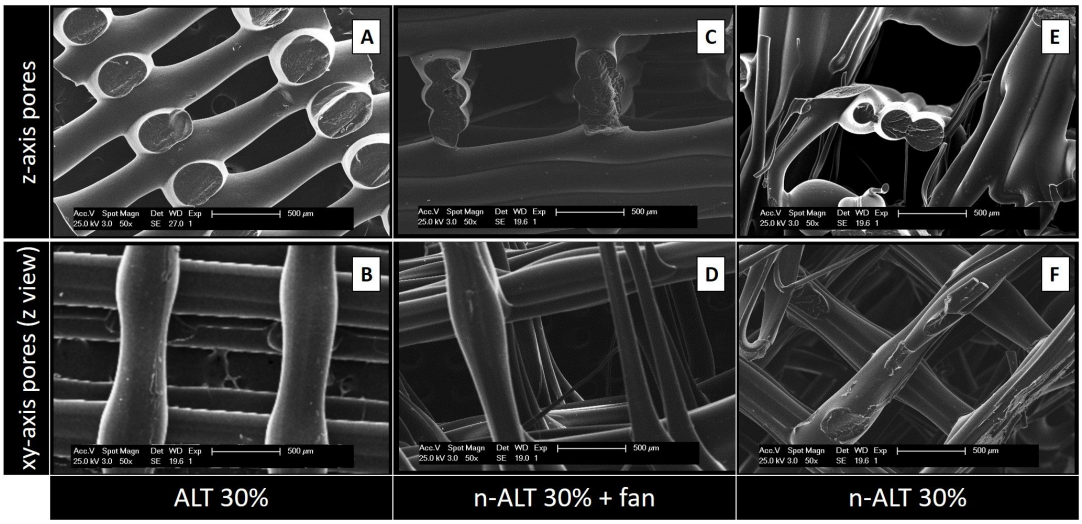

Figure 4.16: SEM images from the alternated (A-B) and non-alternated (C-F) scaffolds, obtained from lateral sections of cut samples (A, C and E) or from the top (B, D and F). E and F represent more chaotic structures due to the slow rate of cooling down, as no external fan was used. Scale bars: 500 µm.

In a more detailed view of the scaffolds with a slow rate of cooling down (30% n-ALT), it can be observed that the presence of random microfibers and pores with different sizes and morphologies (Figure 4.17).

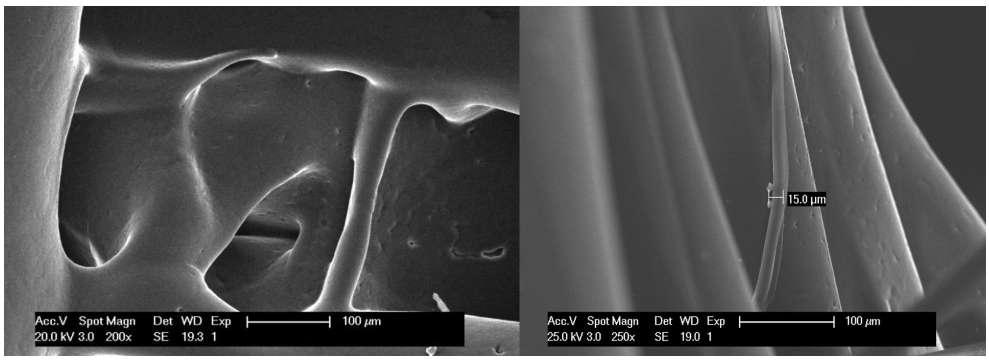

Figure 4.17: Micrograph of macro and micro pores and microfibres created randomly for a slow cooling down (not forced air flow) of the PCL (30% n-ALT). Scale bars: 100 µm.

From the six initial configurations, pores and strand sizes were measured with ImageJ from the obtained SEM images of the three different scaffolds with 30% infill and the results can be found in Table 4.3 and Figure 4.18. No significant differences can be observed between the strand size from ALT to n-ALT, whereas in the case of n-ALT+fan, it is slightly thinner than ALT. When the cooling down is quick, the resulting filament sets faster, generating a more cylindrical strand that results in a regular, open-pore structure.

On the one hand, this is a positive effect as it avoids pore collapsing, generating a more open scaffold with higher shape fidelity. However, it also leads to a smaller surface contact between layers and the fast cooling down of the polymer can also generate a more brittle construction. Scaffolds with alternate strands display lower squared z-pore morphologies, whereas n-ALT specimens possess a higher heterogeneity between specimens.

Table 4.3: Pore and strand size distribution (values represented by its means ± SD, standard deviation) for 30% ALT, n-ALT (room temperature cooling down, RT) and n-ALT forced cool down (+fan). In addition, the coefficient of variation of the results (x%) was included for each measurement.

Sample	z-axis			xy-axis pore size (µm)	Strand diameter (µm)	Homogeneous distribution? (pore and strand)
	pore size (µm)		trans. vs long. ratio			
	transv.	long.				
30% ALT	733 ± 22 (3%)	254 ± 13 (5%)	2.90 ± 0.24 (8%)	816 ± 61 (8%)	361 ± 26 (7%)	✓ - huge anisotropy
30% n-ALT + fan	938 ± 80 (9%)	689 ± 60 (9%)	1.37 ± 0.22 (16%)	542 ± 48 (9%)	290 ± 30 (10%)	✓ - more isotropic pores in z-axis
30 % n-ALT	728 ± 90 (12%)	532 ± 87 (16%)	1.43 ± 0.40 (27%)	930 ± 123 (13%)	314 ± 87 (28%)	✗ - higher variability

(%) = coeff. of variation of results

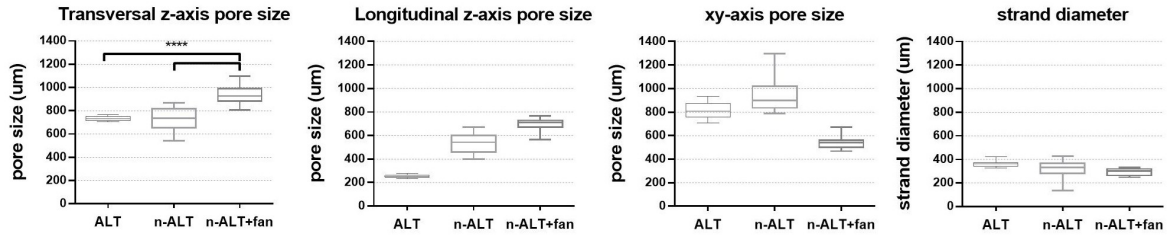

Figure 4.18: Box and whiskers plot for pore sizes measured with ImageJ at z-axis (transversal = horizontal, longitudinal = vertical) and at xy-axis (in any direction between parallel walls), along with the strand diameter. (n = 3 samples with at least 4 measurements per sample, mean ± SD,****p < 0.001).

Compression test results have been summarized and represented in Figure 4.19. As expected, solid samples (100% ALT) showed the highest compressive modulus (18 MPa), with a reduction of more than a half when the infill was reduced to 30%.

Among the samples with a 30% of infill, scaffolds with alternate strands (ALT) held up higher stresses than those where the direction of the strand was changed after three layers (n-ALT). Among the non-alternate configurations (n-ALT), a higher compressive modulus was found when the cooling down temperature was forced by the use of the external fan (n-ALT +fan). Non-alternate structures (n-ALT) have bigger z-axis pores, as they present more transversal strands. Because of this, the n-ALT configuration leads to an easier layer collapse, weakening the scaffold, as can be shown in the reduction in the compressive modulus.

When no fan was used, a less ordered structure was obtained than with forced cool down. When samples with aligned (30% ALT-aligned) and random (30% ALT-random) starting points are compared (Figure 2., samples 2 and 3) a slightly, but significant ($p<0.0002$) difference in the compressive module is found. Finally, when a hydrogel was used to fill the gaps inside the scaffolds (n-ALT +hyd), no significant change (with n-ALT) was observed.

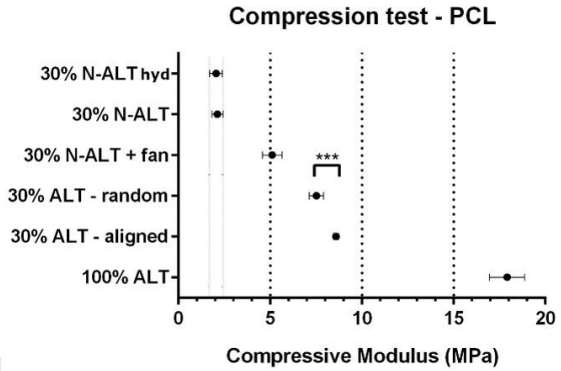

Sample	ALT			n-ALT		
	100%	30% (Starting points)		30%		
	-	aligned	random	-	fan	hydrogel
Module (MPa)	17.92 ± 0.96	8.58 ± 0.14	7.52 ± 0.39	2.12 ± 0.31	5.11 ± 0.54	2.05 ± 0.36
Max. load (N)	492.4 ± 28.9	296.2 ± 5.3	313.7 ± 84.4	55.3 ± 4.8	241.0 ± 63.1	58.8 ± 10.0

Figure 4.19: Summary of the compression test results (± standard deviation) with a comparative graph at the top. (n = 10, mean ± SD, ***p <0.0002). All, but the first two (w and w/o hydrogel), represent significative difference with p < 0.0001.

4.3.4 *Conclusion regarding printing parameters with PCL*

The working range of the PCL should be set in a range that does not compromise the integrity of the polymer or the printer (52-230°C). In this case, 172°C was chosen, as it provided an appropriate polymer fluency during the printing, although it also created the need of an extra fan to obtain a proper cooling rate. Then, in addition of the intrinsic properties of the thermoplastic selected for the manufacturing of the scaffold, cool down conditions and design parameters determine the properties of the printed device.

► An important factor in the final characteristics of the obtained scaffolds, frequently ignored in the literature, is the **cooling down conditions**. When the pictures and micrographs of the scaffolds, shown in Figure 4.16, are compared; E, F for the slow cooled down to room temperature scaffolds, and

C, D for the forced cool down scaffolds, it can be clearly appreciated how scaffolds C, D present a regular and homogeneous pattern, while scaffolds E, F show a rather chaotic structure including some collapsed pores and a major heterogeneity for fibre diameters.

It can be deduced that when the cooling down is quick, the resulting filament sets faster, generating a more cylindrical strand that yields a regular, open-pore structure. On the one hand, this could be something desirable as it avoids pore collapsing, generating more open porosity and higher shape fidelity. On the other hand, it may lead to a smaller surface contact between layers that should yield a more brittle construction. Moreover, it can be observed that when the pore sizes are significantly bigger (Figure 4.16 C, D), this increase in the distance and the reduction in transversal layers leads to a smaller modulus and ultimate strength. However, it is important to notice that although this heterogeneity involved lower mechanical properties, it may be favourable for the biological performance, since it provides a better environment for cell attachment and proliferation [108].

► **The surface and the general texture of the constructs** were also altered due to the fast/slow cooling rate, as it can be appreciated in the SEM images displayed in Figure 4.17. Slow cooling creates different roughness and triggers the apparition of small random internal strands. Although at first view those lines could be considered as defects, it has been described that greater roughness yields better cell attachment and proliferation [109]. This behaviour can be attributed to the rubbery character of PCL at room temperature, since its Tg is -60°C.

Therefore, this phenomenon can be different from other thermoplastic polymers also used for bone engineering, such as poly(glycolic) acid (PGA), Tg 35-40°C or poly(lactic) acid (PLA) Tg (55.2°C) [110] and different copolymers [111]. This suggests that the T_g may have a role to play in the final features of the scaffolds and it must be considered whether to force down the cooling rate in the design of the manufacturing parameters.

► The manufacturing of porous scaffolds for tissue ingrowth also requires that **porosity is interconnected** for the ingrowth of the tissue and vascularization that avoids hypoxia and failure of the constructs [112]. Thus, it is important in the design of porosity along all directions. In this work, infill was set at 30% for being an appropriate porosity percentage for fulfilling these characteristics, and to obtain a similar xy and z-pore size. Moreover, this porosity percentage is described as close to the optimized to obtain a homogeneous cell distribution when seeded [113] and no further experiments were needed. From there, two different approaches can be taken, alternate and non-alternate layers, as can be visualized in Figure 4.14. Alternate scaffolds offer larger pores in x and y directions, increase the space for media and nutrients flow, cell spreading, tissue ingrowth and vascularization, although they have yielded lower mechanical properties and a small pore size along the z-axis can also lead to the collapse of the pores, compromising the flow and tissue ingrowth.

► The **printing starting point**, which in principle should not affect pore or strut size or the properties of the manufactured scaffold, is a parameter that must be set when designing scaffolds. Our measurements indicate that it may have an effect on the compression modulus of the scaffolds being greater when an aligned design is defined. This may explain the better mass distribution in aligned designs than in random set designs. Although at first thought the samples with aligned starting points seem to be the weakest, as they present a preferential path for defect propagation, they hold a higher modulus than those specimens where the starting point was random.

One possible explanation for this would be that the random pattern requires longer movements between layers, which can create oozing (material leaking) and lead to a thinner starting strand or even zones with no polymer deposition. This issue could be optimized by decreasing retraction, but this will also avoid the formation of microfibres. Of course, this effect is more visible when printing with an external shell that will also act as the main supporting load zone.

4.4 BIPHASIC BONE CONSTRUCTS

As stated in the previous section, to be able to create a **bone substitute**, besides the bioink where the cells are embedded for the bioprinting process, a robust materials with **a mineralized phase is also needed**. This will bring cells the minerals required for the regeneration of the ECM and will act as a biological cue for bone regeneration. When cells recognize the materials present in the sourranding area, they will spread better, faster and when working with steam cells, they will be able to differentiate correctly towards the desired cell line.

In this case, as explained before, a ready-to-use paste based on calcium phosphate was used in combination with the developed plasma-based bioink (Figure 4.20). This paste hardens in the presence of water, as there is a change on the phase of the CPC and hydroxyapatite crystals are formed.

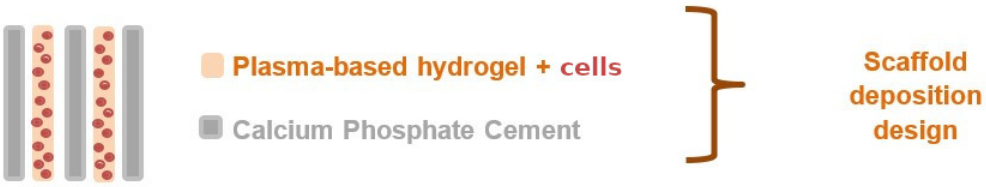

Figure 4.20: Biphasic deposition strategy with alternate strands. Cells are embedded in the soft and nutrient-rich hydrogel, while the CPC is deposited next to it to provide the mechanical and mineral properties required to be used as bone support.

The complete protocol can be found in the original article of biphasic printing [77] and the new paper derived from this work [114]. Also, more details are available on p.121.

Briefly (Figure 4.21), once the materials were prepared as mentioned above and after the completion of the bioprinting process, the constructs must be left in humidity at sterile conditions for 10 minutes for initial CPC setting.

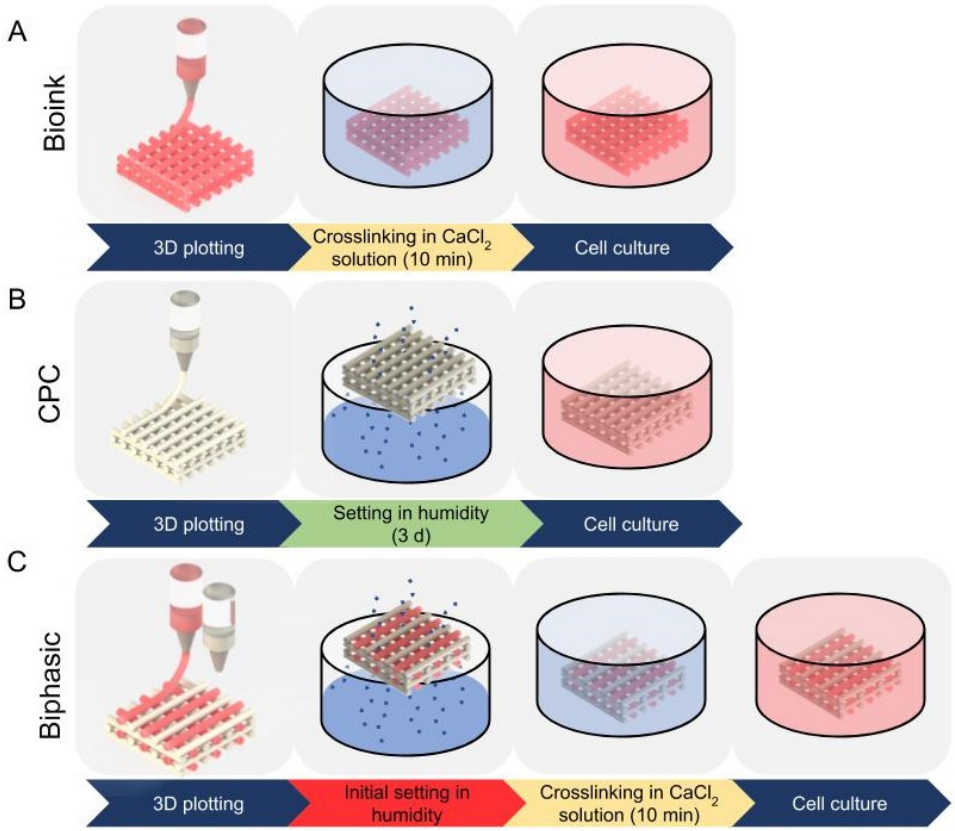

Figure 4.21: Summarized protocol of the post-printing process for the plasm bioink, the CPC-paste and the biphasic constructs. Reproduced with permission of the journal and the authors [77].

Humidity is better than a liquid bath because it avoids the formation of microcracks [115]. Then, the soft part (plasma based-hydrogel bioink) must be crosslinked with a solution of $CaCl_2$ (100 mM) for 10 min. Afterwards, $CaCl_2$ is removed and cell culture medium (DMEM) is added.

4.4.1 *Fabrication of open-porous, volumetric constructs in clinically relevant dimensions for bone regeneration*

The plasma-alg-mc bioink promoted MSC spreading within the hydrogel matrix, exhibiting a fibroblast-like phenotype, features that have been

shown beneficial for the differentiation to osteoblasts [116]. Therefore, the applicability of the plasma-alg-mc bioink for bone cells was investigated. Plottable CPC are promising materials for bone replacement, due to their physicochemical resemblance of the native bone mineral. Therefore, it was examined, whether plasma-alg-mc could be combined with CPC in a multichannel plotting process in order to come closer to bone-like tissue equivalents.

◀ *Biphasic deposition strategy*

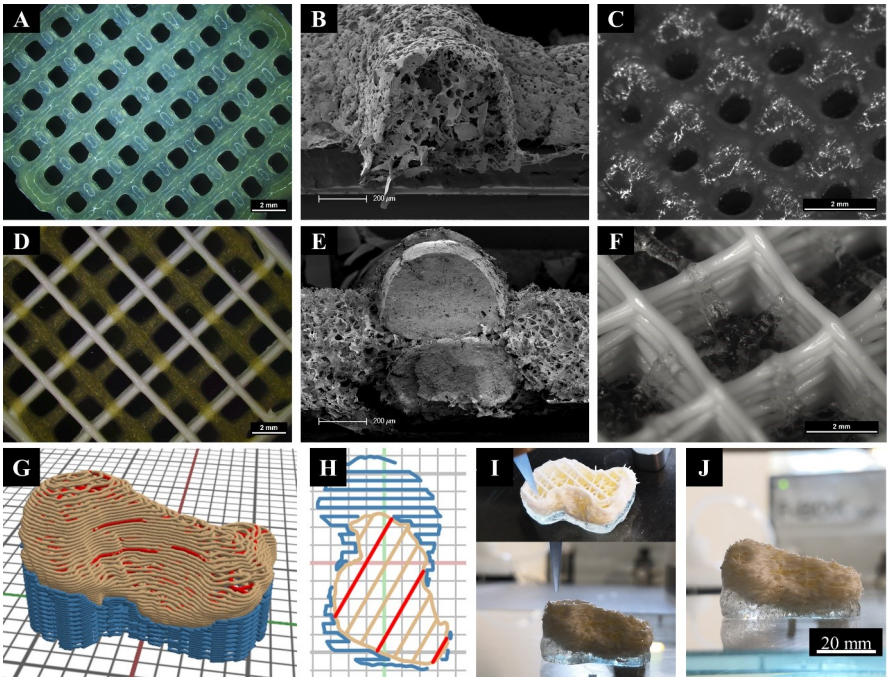

Figure 4.22: Stereo and scanning electron microscopical images of monophasic plasma-alg-mc (A-C) and biphasic plasma-alg-mc/cpc scaffolds (D-G). (A, D) Open porosity was achieved in vertical direction after plotting and cross-linking with 100 mM $CaCl_2$ solution. (B, E) Lateral view of the scaffolds. (C, F) Micrographs of volumetric constructs: (C) 8 layers of the monophasic blend, and (F) 20 layers alternating the same blend with CPC. (G) Full sliced 3D model of the scaphoid and (H) layer design of one layer; blue: sacrificial ink, white: CPC, red: plasma-alg-mc. (I, J) Plotting process of the biphasic scaphoid bone, the sacrificial ink appears transparent, CPC white and plasma-alg-mc yellowish.

Biphasic CPC/plasma-alg-mc scaffolds were successfully plotted with alternating layer deposition (0°/90°) (Figure 4.22 A-C). Structural

characterizations of the scaffolds were performed through stereo and scanning electron microscopy. Top views of the scaffolds after plotting, initial humidity setting for 20 min and crosslinking with 100 mM $CaCl_2$ solution for 10 min revealed open porosity and high shape fidelity of the biphasic structures in multiple layers.

The CPC strands contributed positively to the shape fidelity of every single plotted layer, and thereby for the entire plotted structure, as they did not fuse in z-direction (Figure 4.22 B). In the biphasic structures even horizontal pores between the layers could be achieved (Figure 4.22 C), which was not possible with the monophasic plasma-alg-mc scaffolds (Figure 4.12).

It was concluded, that biphasic structures consisting of CPC and plasma-alg-mc are beneficial to achieve volumetric constructs of clinically relevant size. To prove that, a scaphoid bone model was reconstructed from cone beam computed tomography data and plotted utilizing a sacrificial ink based on pure methylcellulose, as recently published [117]. The sacrificial ink was needed during fabrication to support overhanging structures and concave and convex surfaces of the scaphoid bone.

The biphasic scaphoid bone model could be plotted with high shape accuracy, exhibiting the typical peanut-like shape (Figure 4.22 D-G). The sacrificial ink was washed away without residues after post-processing (hardening/crosslinking) of the biphasic structure.

In addition, the combination of CPC and plasma-alg-mc allowed the fabrication of more complex layer arrangements (0°/72°/144°/216°/288°) and advanced pore geometries like a gyroid structure (Figure 4.23).

Macroporous structure of the plotted constructs was imaged by a stereo light microscope (Leica M205 C equipped with DFC295 camera, Germany). Freeze-dried samples were further analysed by scanning electron microscopy (SEM; Philips XL 30/ESEM, operated in SEM mode) at a voltage of 3 kV (spot size 3) with field emission gun (n=3).

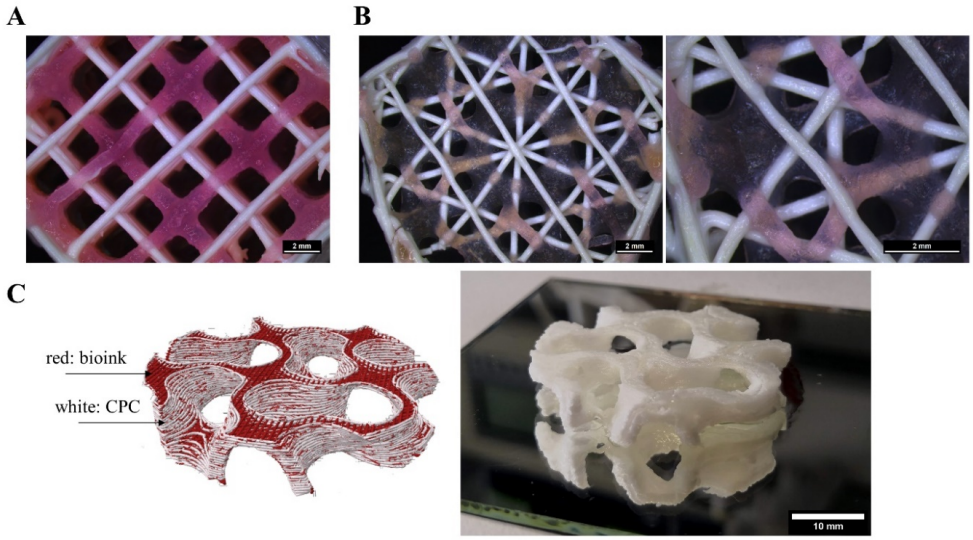

Figure 4.23: (A) Microscopic picture of a biphasic scaffold consisting of CPC/plasma-alg-mc, plotted in a 0°/90°. (B) A more complex layer orientation of 72°changed the pore morphology of the biphasic constructs. (C) Biphasic gyroid structure of CPC and plasma-alg-mc, which could be fabricated with high shape fidelity.

4.4.2 *Volumetric strand swelling and pore size*

Monophasic plasma-alg-mc and biphasic CPC/plasma-alg-mc constructs were plotted and volumetric strand swelling of the hydrogel ink as well as the pore size were investigated by measuring the strand width and the smallest distance between two adjacent strands at different time points. More details at p. 122.

It was observed that the strand width of plasma-alg-mc within biphasic scaffolds was higher compared to the strand width of monophasic plasma-alg-mc scaffolds over the whole time of investigation, indicating stronger swelling. Moreover, the average pore size decreased stronger for the biphasic construct (Figure 4.24 A).

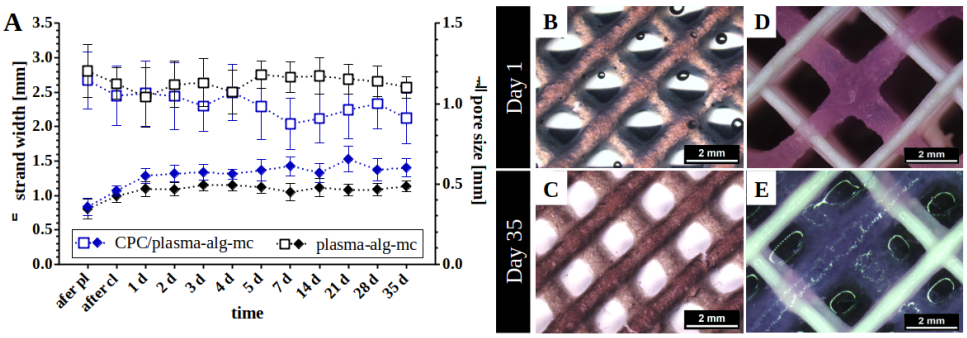

Figure 4.24: (A) Change of the strand width (♦) of plasma-alg-mc strands and change of the pore size (□) in either a monophasic (shown as black) or a biphasic (shown as blue) structure, where CPC strands were intercalated (n=5, mean±SD). (B-E) Stereo light microscopical pictures of the monophasic plasma-alg-mc (B,C) and the biphasic CPC/plasma-alg-mc (D,E) structures after 1 and 35 days of incubation in cell culture medium. Even after 35 days of incubation, open-porous structures were observed in both configurations.

In general terms, both groups showed the same swelling kinetics: the strand width increased significantly ($p<0.05$) within the first 3 days, then decreased slightly and afterwards showed an almost constant value.

In the 35 days studied, plasma-alg-mc strands in monophasic scaffolds showed an increase of approximately 1.4-fold of their original width, whereas those strands in biphasic structures increased their strand widths up to 1.7-fold.

The pore sizes after plotting were determined as 1.20±0.17 mm and 1.14±0.17 mm for plasma-alg-mc and CPC/plasma-alg-mc constructs, respectively. After 35 d, the average pore size decreased to 1.10±0.07 mm (plasma-alg-mc) and 0.91±1.57 mm (CPC/plasma-alg-mc), evidencing the observation of the increased strand swelling of the hydrogel in presence of CPC strands. Crucially for our approach, in both conditions an open porosity over the whole time of observation was achieved and the pore sizes were acceptable for bone-like constructs (Figure 4.24 C, E).

4.4.3 *Cell viability of MSC in the plasma-based bioink within biphasic, mineralized constructs*

◀ *Obj 6.*

Research question: *Biological assays to test viability and functionality*

Biphasic constructs consisting of cell-laden plasma-alg-mc and CPC were plotted and evaluated for post-plotting cell viability at day 1, giving evidence of cell damage caused by extrusion and by interaction of the cells with the two materials. To study the effect of plasma, a PBS-alg-mc bioink was used as control.

Representative confocal fluorescence microscopy image stacks are shown in Figure 4.25 A. The black and therefore optically opaque structures in the brightfield mark the CPC strands, which show no signal under the confocal microscope. In PBS-alg-mc, a clear drop of cell viability was observed at the CPC/bioink interface, as the number of living cells decreased distinctly when they are in direct contact of the bioink with the CPC in comparison to the cells surrounded only by the bioink, which are separated from the CPC by the macropores.

The calculated cell viabilities are presented in Figure 4.25 B. Monophasic PBS-alg-mc and plasma-alg-mc constructs revealed cell viabilities of 49.8±4.9% and 77.6±2.7%, respectively. Biphasic PBS-alg-mc scaffolds did not show a significantly different cell viability (denoted as biphasic global in Figure 4.25 B), repeatedly proving previous findings [77].

However, at the interface to CPC, denoted as biphasic CPC interface the cell viability was significantly decreased in comparison to monophasic constructs (37.8±14.5%, $p<0.05$). **In CPC/plasma-alg-mc constructs, no differences in the cell viability were observed**; the viability in biphasic scaffolds at the interface between CPC and plasma-alg-mc was determined as 79.2±5.6%.

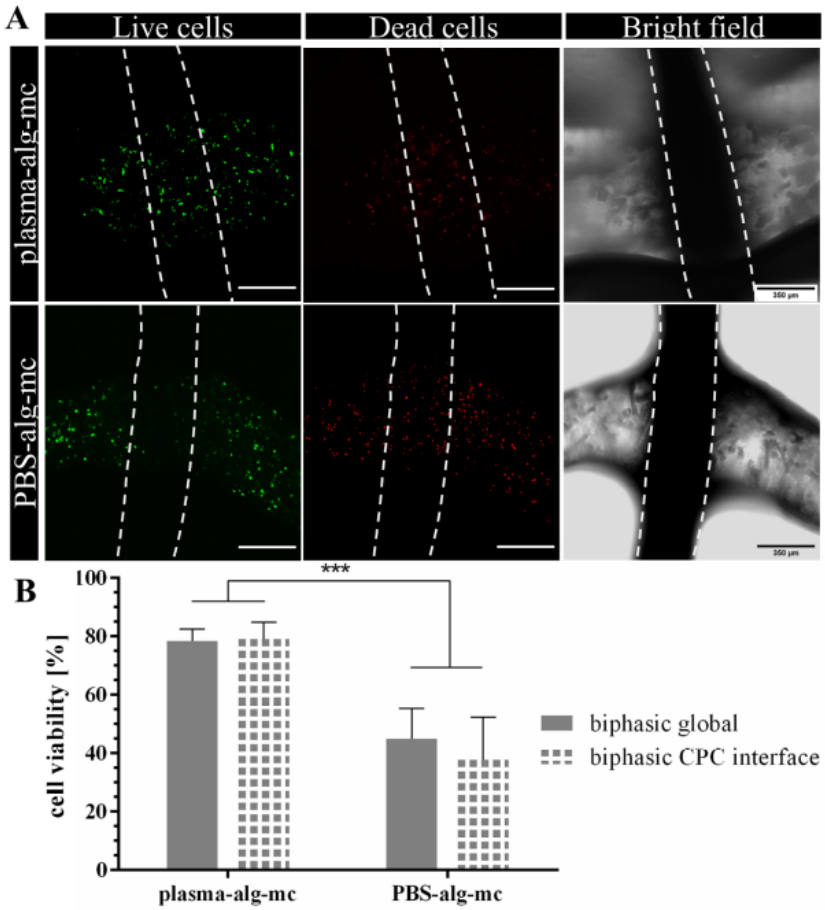

Figure 4.25: (A) Representative images of living (green) and dead (red) cells in plasma-alg-mc and PBS-alg-mc bioinks at the CPC-bioink crossing point (for the observation, the bioink was on top of the CPC). Dotted lines mark the acellular CPC strand. Scale bars: 350 µm. (B) Calculated cell viabilities of biphasic CPC/bioink constructs (denoted as biphasic global) and cell viabilities in biphasic constructs at the CPC/bioink interface. n=7, mean±SD, ***p<0.001.

4.4.4 *Cell migration and proliferation of MSC in long-time culture*

Obj 6. cont ►

Research question:
Tissue evolution and maturationin vitro

After bioplotting, a cell-laden CPC/plasma-alg-mc construct was imaged by optical coherence tomography (OCT) (by another member of the lab, David Kilian), whose reconstruction is shown in Figure 4.26 A. The OCT measurement confirmed that stable macropores were also achieved with cell-

laden plasma-alg-mc bioinks. Cell behaviour over a long-period of time in culture was investigated by evaluating live/dead staining (Figure 4.26 B).

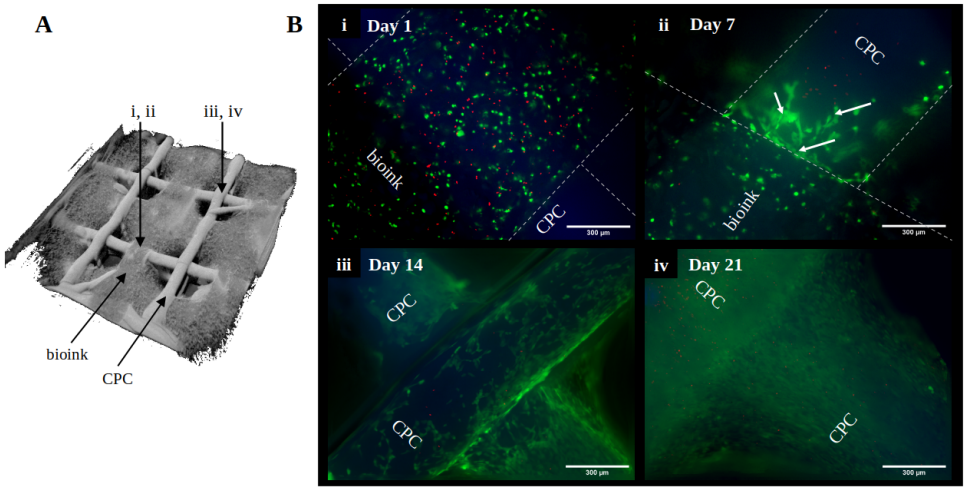

Figure 4.26: (A) 3D reconstruction of an optical coherence tomography analysis of a cell-laden biphasic construct consisting of CPC (white) and the cell-laden plasma-alg-mc bioink (opaque-porous). (B) Cell viability of bioplotted, biphasic constructs consisting of a cell-laden plasma-alg-mc bioink and CPC. Living cells: green, dead cells: red, CPC: blue autofluorescence. MSC remained encapsulated in the hydrogel (day 1, i). Later on, the MSC migrated to the CPC strands (day 7, ii) where they attached and proliferated to a great extend (day 14 and day 21, iii, iv), covering the whole CPC surface and bridging the macropores. Scale bars represent 300 µm.

Three different zones within the biphasic constructs were identified as areas of interest:

1. the interface of two bioink strands (bioink-bioink interface),
2. the interface of two CPC strands (CPC-CPC interface) and
3. the interface of the bioink and CPC (bioink-CPC interface).

Figure 4.26 B shows selected images of the CPC-bioink interface at day 1 and day 7 as well as the CPC-CPC interface at day 14 and 21. After 1 day of culture, live and dead cells were found within the plasma-alg-mc bioink

without significant changes on the cell viability at the bioink-bioink and bioink-CPC interface. There were no cells at the CPC-CPC interface. MSC had a roundish shape (Figure 4.26 B i).

Latest after 7 days, MSC migrated from the bioink to the CPC strands at the bioink-CPC interface, where they attached and elongated (Figure 4.26 B ii, white arrows). Cells in the vicinity of the bioink were found to be metabolically active, in addition, some dead cells were observed at regions of the CPC strands which were more distant from the bioink.

With ongoing culture, the cell density in the bioink, especially at the bioink-bioink interface was decreased. However, remaining cells showed an elongated and spread morphology. Subsequently, cell migration progressed until the CPC strands were further populated by MSC.

After 14 days, nearly all zones of the biphasic constructs were covered by cells originating from the bioink-CPC interface; only at the CPC-CPC interface some cell-free zones were observed (Figure 4.26 B iii).

After day 21, these areas appeared to be fully covered by a dense cell-network. Furthermore, MSC still proliferated and started bridging the macropores around the CPC-CPC interface (Figure 4.26 B iv).

This strong cell layer did not detach from the biphasic construct, but was stable for longer than a culture time of 35 days. At the CPC-CPC interface, a few dead cells were found after day 14 and 21, respectively. The number of MSC in the biphasic system was evaluated by measurement of the DNA content (Figure 4.27). After a slow increase of the cell number during the first 7 days, the cell number significantly increased until day 28.

Exemplarily, at day 1 the cell number per scaffold was determined as $0.32 \cdot 10^5 \pm 0.04 \cdot 10^5$ and at day 28 the cell number per scaffold increased to $6.71 \text{x} 10^5 \pm 1.91 \cdot 10^5$, which complies with a 20-fold higher cell number after 4 weeks of cell culture, most probably due to the proliferation of the MSC on the CPC strands.

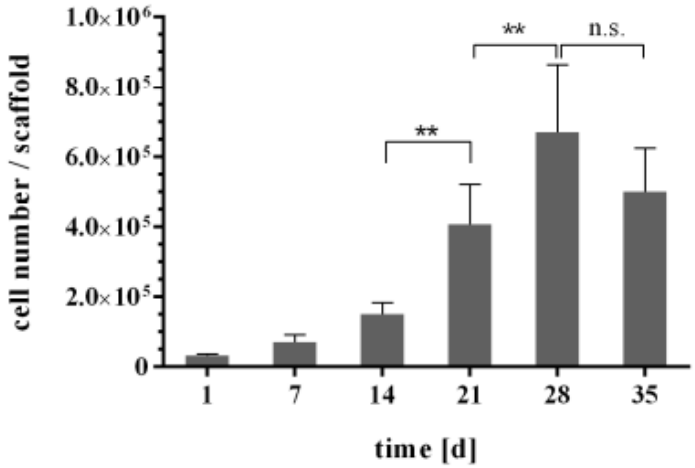

Figure 4.27: Cell number per scaffold in bioplotted biphasic CPC/plasma-alg-mc constructs, determined by measurements of the DNA content. MSC proliferated within the mineralized constructs until day 28, afterwards no significant change of the cell number was measured (n=5 for d 1 - d 28, n=3 for d 35, mean ± SD, **p<0.01, n.s. not significant).

After 28 days, no significant change of the cell number was determined.

4.4.5 *Further in vitro testing*

◄ *Obj 4. cont*

Research question: *Creation of size relevant tissues*

As continuation of the work here presented, but performed mainly by another PhD Student (Tilman Ahfeld) of TU Dresden, more studies were carried out with normal MSC to prove the osteogenic differentiation of primary osteoprogenitor cells into the biphasic constructs.

Also, bigger structures were plotted, with internal channels to obtain vascularized bone-like constructs by bioplotting of endothelial cells in a complex volumetric bone model, as can be seen at Figure 4.28 (up to 105 piled layers, 15 mm height, 17.5 mm of diameter, with holes of 5 mm). More details can be found in the paper that contains the work here presented [114].

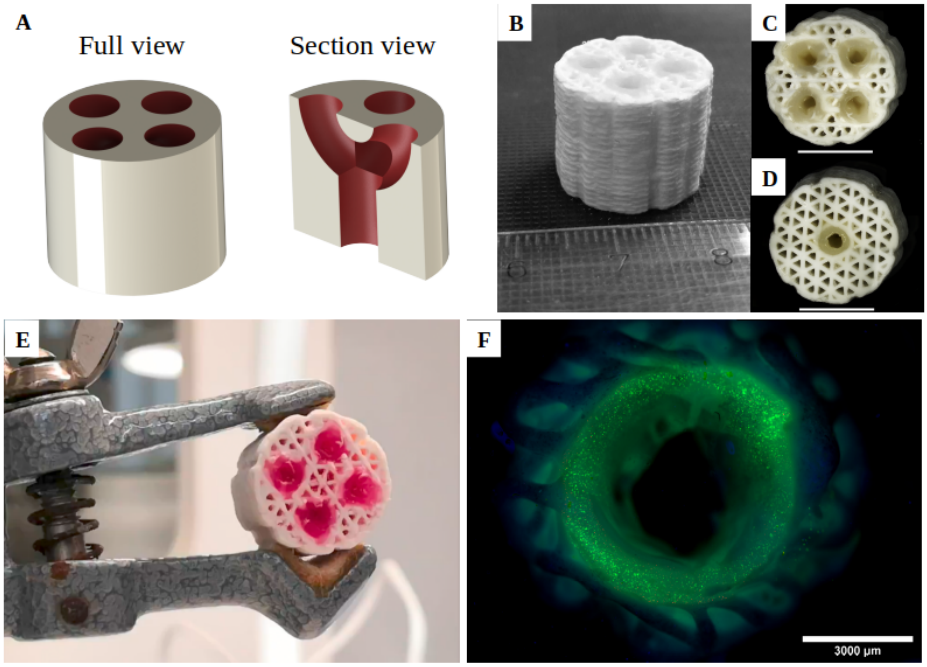

Figure 4.28: Development of a perfusable CPC/plasma-alg-mc construct. (A) Full & section view CAD model; white: CPC, red: the perfusable channel, made w/ plasma-alg-mc, which branches into four channels; (B-D) Images of the plotted biphasic construct with 105 layers. Scale bars (C & D): 10 mm. (E) The plotted scaffold after perfusion (phenol red). The hydrogel was stained evidencing perfusion; (F) Fluorescence microscopic image of a live/dead stained bioplotted lumen, day 1. Cells: coculture of endothelial HUVEC & MSC; G: living cells, R: dead cells, B: autofluorescent CPC. Scale bar (F): 3 mm.

4.4.6 *Biphasic constructs considerations*

In this work, a novel plasma-based bioink, which can be utilized for extrusion-based bioprinting in air as plotting environment was developed. Thanks to the nature of plasma, cells can easily spread and start to remodel the damaged tissue, following the natural process of wound healing. In addition, due to the presence of proteins and nutrients, cells can remain suspended in the bioplotter cartridge for many hours (tested up to 4h), and still remain viable and functional.

Porous 3D constructs with excellent shape fidelity could be fabricated independently from additional assistive equipment like a support bath or a crosslinking atmosphere - that broadens the applicability of this bioink in comparison to the plasma-based bioinks which have been developed before [49, 118, 119].

The great potential of the plasma-alg-mc bioink was tested for engineering of bioplotted bone grafts. The complex structure, need of vascular supply and opportunity to combine bone-like constructs with those mimicking other tissues (like cartilage - for the treatment of osteochondral defects) make bone an interesting target to use the methods of bioprinting [120].

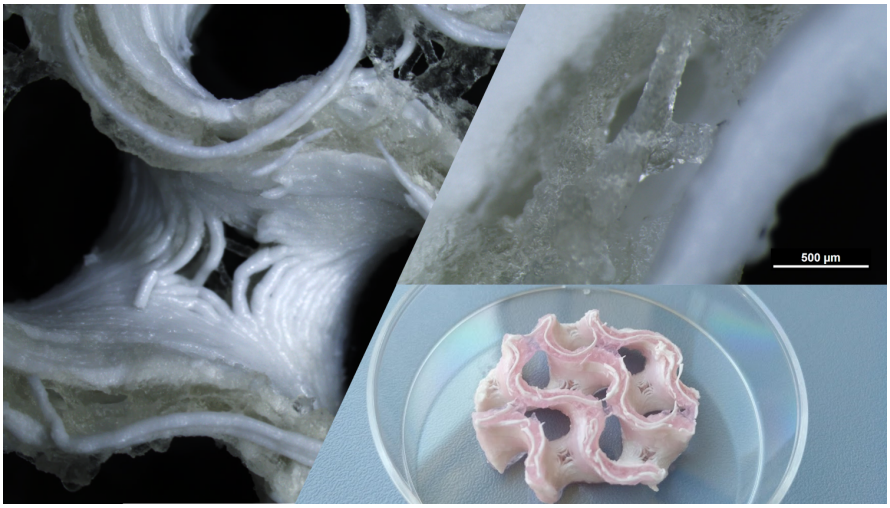

Figure 4.29: Biphasic constructs: external macropores and internal microstructures. Gyroid geometry, biphasic deposition.

The drop of cell viability was not observed for plasma-alg-mc, when compared with PBS-alg-mc [77]; living and dead cells were homogeneously distributed throughout the whole bioink strands without notable change at the CPC/bioink interface.

Both, the plasma-based bioink and the biphasic CPC/plasma-alg-mc system are promising candidates for the fabrication of tissue engineered (bone) grafts comprising a patient-specific bioink, a defect-adapted shape

and autologous cells for a fully patient-tailored tissue graft.

Another option to modulate the rigidity of bioplotted constructs is the alternating strand deposition of stiff materials and cell-laden bioinks [31]. For example, thermoplastic poly-ϵ-caprolactone (PCL)-bioink constructs were successfully matured from cartilaginous templates to bone tissue [121], enhanced the development of mineralized tissue by usage of gene activated bioinks [122] or were spatially ordered to osteon-like structures [123].

In this PhD thesis, the importance of the printing parameters when working with PCL was also studied, as it was found that the mechanical integrity of the construct and its internal structure can be highly affected.

5

DESIGN AND DEVELOPMENT OF THE PROOF OF CONCEPT WORKBENCH FOR SPACE CONDITIONS

◂ *Obj 4.*

Research question 2: *Is it feasible to translate this technology to altered gravity environments? [...]*

Some of the space flight environmental conditions that crew will face along their travel to other planets, such as microgravity or radiation, are not easy (or cheap) to recreate on the Earth. Neither the reduced gravity that they will encounter in the surface of those celestial bodies.

For microgravity, different approaches have been developed for research and industry. For example, the ZARM Drop Tower in Bremen, that allows samples or experiments to free fall from 120 m inside a capsule (drop mode) creating 4.72 s of microgravity. If instead of leaving it fall, the sample is catapulted from the bottom and allowed to fall back again (catapult mode), 9.3 s can be achieved. The drawback of this experiment, is that in the second mode the upward acceleration reached goes up to 35 G which can affect the materials inside. Afterwards, in both cases, the deceleration suffered is of approximately 50 G[1].

If more time is required, another option is through parabolic flights[2]. With this technique, microgravity can be obtained up to 20 s, with an acceleration/deceleration of 2 G. However, to study effects on cells, or biological tissue maturations, those times are still very brief.

1 www.zarm.uni-bremen.de/en/drop-tower/general-information.html

2 www.esa.int/Our_Activities/Human_and_Robotic_Exploration/Research/Parabolic_flights

To study cell differentiation and tissue ingrowth, the study conditions must be kept for at least 14-21 days. For that, an orbiting experiment aboard a satellite or even a more complex infrastructure would be requiered. Currently, the European Space Agency (ESA) offers different programmes to put projects on orbit.

For example, the "Orbit Your Thesis! (OYT)" programme gives master and PhD candidates the opportunity to fly a scientific experiment in microgravity conditions onboard the International Space Station (ISS). Successful applicants are given the opportunity to design, build and operate a fully autonomous experiment that will stay onboard the ISS for a period lasting up to 4 months in the "ICE Cubes" facility (Figure 5.1).

Figure 5.1: Ice Cubes in Columbus mock-up, 2017. Obtained from ESA Education website.

However, these approaches are limited for a few candidates, and the expenses that they involve are quite high. For that reason, a previous and cheaper step that allow us to demonstrate that our biomaterials were stable enough to be printed in altered gravity conditions is required. With this proof of concept (POC), initial results to apply for further test can be carried out.

◀ *Obj 4. cont.*

Two different approaches, further explained in the following sections, are proposed as a previous step:

Research question 2: *How can we demonstrate it on Earth? [...]*

1. Inversion of printed samples, to test the stability, viscosity and attachment between layers of the biomaterials once printed.
2. Inversion of a complete bioprinter to work with hanging biomaterials while been deposited. With this trial, the materials' viscosity can be tested to see if they can remain stable in a range of [-G, G] forces.

5.1 INVERTED SAMPLES

To check the stability of and gravity effects on the plasma-bioink and CPC-based constructs after being deposited, the bioplotted constructs were mounted upside down directly after printing and images were taken every 10 seconds for 5 minutes, using a time-lapse camera (figure 5.2). The samples were left afterwards to check the maximum time before detaching, but they dried out before that, showing a rather good coupling.

The taken images were analysed with Fiji [124], and the statistical analysis revealed that no significant deformation of the constructs was observed. Two different compositions were analyzed: the plasma-bioink and the ready-to-use CPC paste. This test revelaed that both materials are viscous enough to attach to the printing surface, and that the forces between the layers (material cohesion) would allow the use of this material under altered gravity conditions.

With this result, the next step was considered: bioprinting of those materials directly at inverted gravity direction, going up in the number of layers.

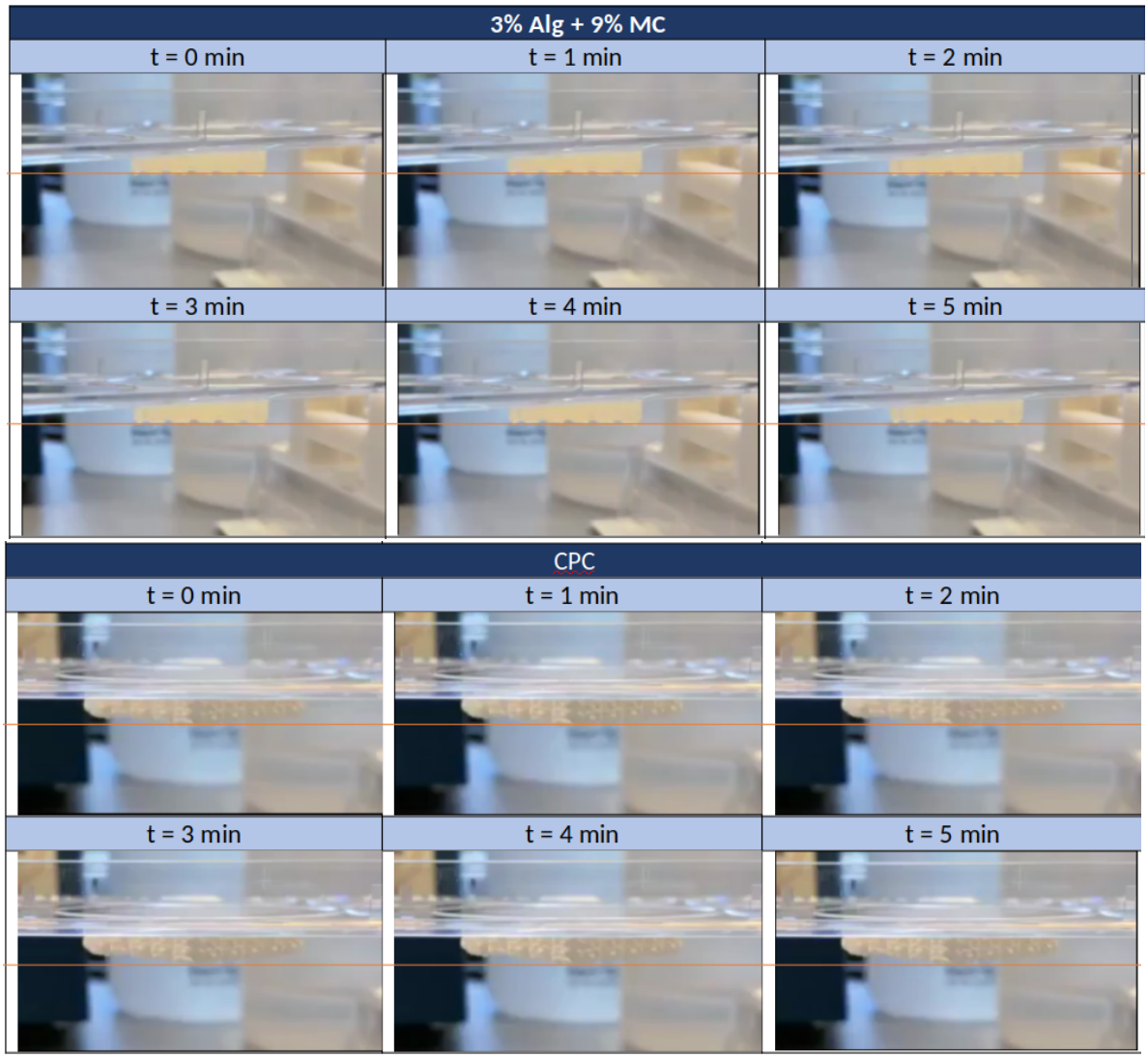

Figure 5.2: Plasma-based hydrogel and CPC samples inverted after printing to test stability and gravity effects.

5.2 INVERTED BIOPRINTER

◀ *Obj 5.*

Research question: *Design and manufacture and adaptation of a DIY extruder to create a POC workbench*

As shown in the state-of-the-art (Section 2.3), many technologies are already available for bioprinting. After studying the different technical aspects of each of them (complexity, resolution, adaptability to space requirements, size and characteristics of the demanded environment, reusability of pieces and price, summary at Table 2.1), micro-extrusion was chosen because of its relative simplicity, cost, easy translation to altered gravity conditions and the fact that for the selected types of tissue, very high resolution is not required.

Two microextrusion bioprinters where used for this study, a GeSiM BS3.1 (Figure 2.4) to create the biological constructs and an inverted in-house developed printer (based on a BQ Hephestos 1, Figure 5.3 A) to demonstrate the printability of the materials under inverted gravity conditions (-G).

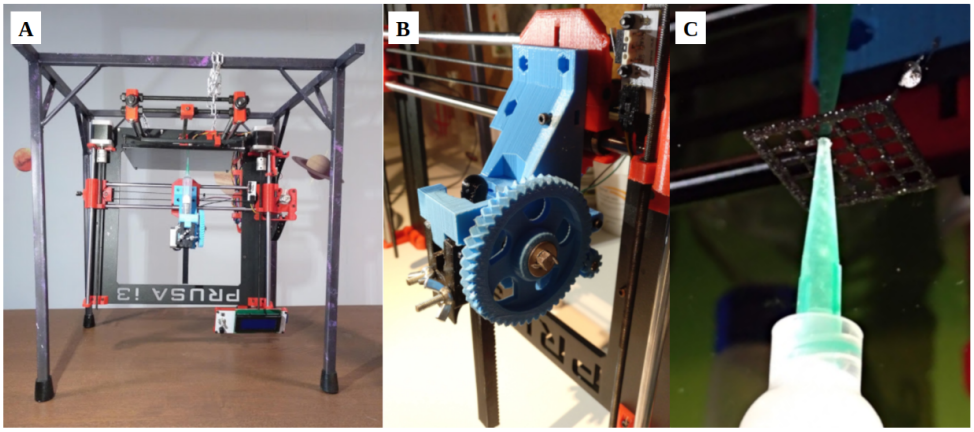

Figure 5.3: Inverted printing experiment. A) In-house developed bioprinter for altered gravity proof of concept, B) DIY printable extruder based on an open design (Harry's paste extruder on Thingiverse, by Harry Streuli), C) Printing a soft scaffold in inverted orientation, photo taken at the 4th layer.

It must be highlighted that this extreme configuration was used just to test the stability of the materials in that condition, so it can be assured that under reduced gravity (similar to the one present in space) it will not float

or detach. As it was introduced at the beginning of this chapter, to study the impact of altered gravity in the biological activity, more long-term test would be required.

The in-house developed bioprinter was based on a BQ Hephestos 1, similar to the Prusa i3 printer. Two main modifications were made to the machine:

1. The thermoplastic extruder was replaced by a DIY printed one, capable of work with pastes (Figure 5.3 B).
2. A structure was build to hang the printer upside-down, in order to obtain the opposite gravity forces while printing (Figure 5.3 A).

5.2.1 *DIY paste-extruder*

The project started with a previous developed version of a DIY syringe pump that allowed us to work with liquids withing a commercial DIY printer (Figure 5.4). It was a model fully developed by Nieves Cubo-Mateo [49], for the development of a new deposition system to create human dermo-epidermal skin equivalents [49]. Extruder parts available at GitHub.

Figure 5.4: First DIY extruder developed to pump low viscous liquids into a 3D Printer.

However, the developed paste presented a non-Newtonian fluid behaviour and was too viscous to be pumped along the silicon tubes. Therefore, a new system to be able to deposit the bioink was needed.

For that, an open-source paste extruder (Harry's paste extruder on Thingiverse, by Harry Streuli) was adapted to the project needs. All the information about this new version can be found at GitHub and at Openbioprinting.org. Briefly: it was modified to be more easily adapted to a prusa printer; an internal space was created to adapt 10 cc syringes and cartridges with a 'click'; and some mechanical elements (rack, pinion) were redesigned and improved for a better movement transmision.

A protocol to adapt the slicing software (to be able to work with pastes and liquids) and the most common firmware used at 3D Printers, was also developed. More information and drawings can also been consulted on p. 125.

5.2.2 *Inverted printing*

Once the DIY extruder was working, a steel support (Figure 5.3 A) was built to hang the printer upside-down, obtaining and inverted configuration.

In this position, materials will tend to drop if the cohesion between layers or if the viscosity of the material is not high enough. However, this opposite force can also be an advantage for the development of 3D constructs, as one of the most common problems that soft bioinks carry is the collapse of the material because of gravity. In this case, the construct is not built under compression because of this force, but under stretch.

For the POC demonstrators, cylinders of 20 mm in diameter were printed over a glass surface, with a needle tip of 410 µm. 50 layers of 267 µm in height were piled and the samples were left hanging to study the stability (Figure 5.5). They remain attached and without deformation for 20 minutes. Then they were detach and stabilized.

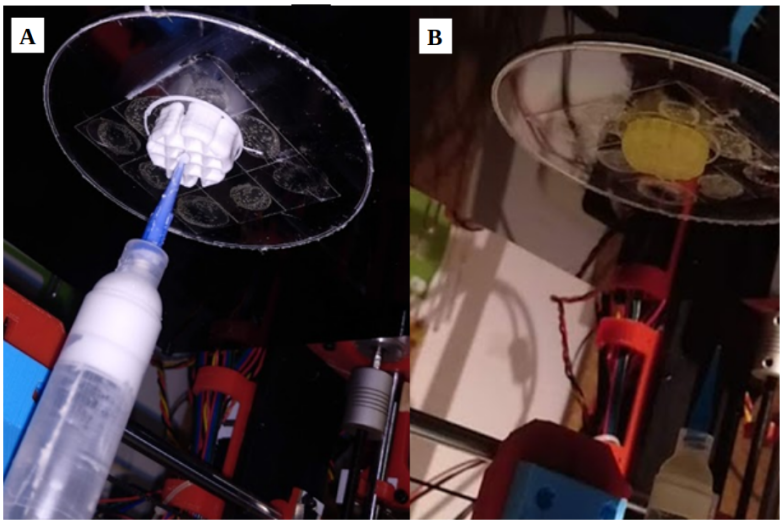

Figure 5.5: Inverted printing experiment. A) CPC-paste, 50 layers printing, 20 mm diameter cylinder; B) Plasma-based bioink, 30 layers printing, 20 mm diameter cylinder. In both cases, the tip employed had a diameter of 410 μm.

With this test, it was shown that the materials chosen for the study have a proper viscosity and cohesion to be used under altered gravity conditions [-G, G]. Also, that the selected technology (microextrusion bioprinting) has a good potential for its translation to space conditions.

⁕ RESEARCH PROCEDURES AND PROTOCOLS

P1 PLASMA-BASED BIONK DEVELOPMENT

P1.1 Plasma protein characterization

Because of the variable nature of plasma, plasma from 5 donors (derived from the local blood donation service, the Deutsches Rot Kreuz) was pooled to obtain a uniform mixture.

Afterwards, protein content as well as presence of growth factors of the pool was investigated in order to better estimate the biological performance of the plasma used in this study. For that, Proteome Profiler Arrays (Human Angiogenesis Array Kit and Human Cytokine Array, R& D Systems Inc., Minneapolis, MN, USA) according to the manufacturer's protocol.

To determine the solid content of the plasma pool (84.4 $mg \cdot mL^{-1}$), 3 mL of plasma were lyophilized and weighed. Additionally, the fibrinogen content was determined as 2.26 $mg \cdot mL^{-1}$ using the Clauss fibrinogen assay [79] by the Universitätsklinikum Carl Gustav Carus Dresden.

P1.2 Plasma based bioink preparation

Fresh frozen human plasma was provided by a local blood bank (Deutsches Rotes Kreuz - Blutspendedienst Nord-East). As plasma contains many coagulation factors that can vary strongly from one patient to another, the plasma of 5 donors was pooled for all the experiments to avoid variations along the study.

Alginic acid sodium salt from brown algae (M/G ratio 1:2) and methylcellulose (M0512, Sigma, USA, molecular weight of ≈ 88.000 Da, 4.000 cP·s) were purchased by Sigma-Aldrich (Merk). Alginate (alg) and methylcellulose (mc) powders were sterilized by autoclaving at 121°C for 20 min before used.

A plasma-alginate-methylcellulose (plasma-alg-mc) ink was prepared as follows:

1. 0.7 mg of tranexamic acid (Amchafibrin©, Rottapharm, Spain) was added per miligram of fibrinogen (fibrin content within plasma was 2.26 $mg.mL^{-1}$), to prevent early fibrinolysis, allowing printed constructs to be stable *in vitro* for a longer period of time.
2. Alginate was dissolved at a concentration of 30 $mg.mL^{-1}$ directly in the thawed plasma (RT).
3. Methylcellulose was added at a concentration of 90 $mg.mL^{-1}$.
4. The blend was homogenized by gentle manual stirring and methylcellulose was allowed to swell for 2 h for complete dissolution before printing or adding the cells.
5. When included, cells were added in a concentration of 5.10^6 cells suspended in 300 µL of cell media, per gram of paste.

P1.3 Rheological test: bioink assessment

Plasma, plasma-alg and plasma-alg-mc pastes were evaluated for rheological behavior (Ares-G2, TA Instruments, New Castle, Delaware, USA and Rheotest RN 4, Medingen, Germany). Shear thinning was tested at constantly increasing shear rates from 0-100 s^{-1} over 1200 s (increment 0.08 s^{-1}) using a plate-plate geometry (d = 60 mm for liquid plasma; d = 50 mm for plasma-alg and plasma-alg-mc) with a gap distance of 0.1 mm at 25°C.

After an initial amplitude sweep test to detect the linear viscoelastic region, oscillatory frequency sweep tests (f = 0.01 s^{-1} - 10 s^{-1}) were

performed on the plasma-alg-mc paste and storage modulus as well as loss modulus were obtained from the data.

Shear recovery tests of plasma-alg-mc were performed as follows: a low shear rate (5 s^{-1}) inducing shear stresses of the linear viscoelastic region (LVR), was applied for 200 s, afterwards a 100-fold higher shear rate inducing shear stresses outside the LVR of 500 s^{-1} was applied for 100 s.

The procedure was repeated three times and viscosity was measured during the entire experiment. Shear thinning experiments, frequency sweep tests and shear recovery tests were repeated three times.

P1.4 Cell isolation and expansion

Immortalized human mesenchymal stem cells expressing human telomerase reverse transcriptase (MSC) [125] were expanded in monolayer culture at 37°C and 5% CO2 in DMEM (Biochrom, Germany), containing 10% FCS (Corning), 100 U/mL penicillin, and 100 µg/mL streptomycin (PS) (Biochrom). Culture medium was changed twice a week.

Human preosteoblasts (hOB) were isolated from the femoral head of an osteoarthritic patient (female, 56 years) undergoing total hip replacement at the University Hospital Carl Gustav Carus Dresden (Germany) after informed consent (approval by the ethics commission of TU Dresden, EK 303082014) as previously published [126]. In short, spongious bone fragments (1-2 mm in diameter) were dissected, washed 4-5 times with Hank's balanced salt solution (HBSS, Thermofisher Scientific), and treated twice with collagenase II solution (1 mg · mL^{-1} collagenase II, 235 U·mg^{-1}, Biochrom, Berlin, Germany in Minimal Essential Medium, α-modification (α-MEM), 10% FCS, 2 mM L-glutamine, PS, 3 mM $CaCl_2$). The supernatant of the second collagenase treatment was harvested, cells were pelleted by centrifugation and expanded in α-MEM containing 15% FCS (Corning) and PS. Cells of the 4th passage were used for the experiments.

Human dental pulp stem cells (hDPSC) were isolated from human wisdom teeth as previously published [127]. The ethics commission of TU Dresden approved the application of hDPSC for *in vitro* experiments (EK 106042010). Cells were expanded to the 5th passage in monolayer culture at 37°C and 5% CO2 in DMEM (Biochrom), containing 20% FCS (Corning) and PS. Culture medium was changed twice a week.

Human Umbilical Vein Endothelial Cells (HUVEC) were purchased from Promocells (Heidelberg, Germany). Cell were expanded in Endothelial Cell Growth Medium (Promocell) to the 4th passage; the culture medium was changed twice a week.

P1.5 Bioplotting of MSC embedded at the plasma-based bioink

Human mesenchymal stem cells (MSC), immortalized by ectopic expression of human telomerase reverse transcriptase (hTERT) by lentiviral gene transfer [102], were used. MSC were encapsulated into the bioink at a concentration of $5{\cdot}10^6$ cells/mL of bioink of paste, subsequently plotted and crosslinked with 100 mM $CaCl_2$ for 10 min before incubation in DMEM.

As plasma-free control, a bioink with similar concentrations of alginate and methylcellulose but dissolved in PBS (PBS-alg-mc), was used, which was described before [102].

P1.6 Fabrication of cell-laden constructs

After trypzination from cell culture flasks, cells were centrifuged and resuspended in 100 µL cell culture medium per gram of the used bioink. The final cell concentrations were $5{\cdot}10^6$ cells/mL bioink for MSC, $2.5{\cdot}10^6$ cells/mL bioink for hOB, $4{\cdot}10^6$ cells/mL bioink for hDPSC and $6{\cdot}10^6$ cells/mL bioink for a HUVEC/MSC co-culture (ratio 1:1).

Afterwards, cell suspensions were mixed by hand into plasma-alg-mc and PBS-alg-mc, transferred into the plotter cartridges and afterwards deposited and post-processed as described before in a sterile environment. Bioplotted constructs containing MSC were cultured in DMEM supplemented with 10% FCS and P/S.

Constructs containing hOB and hDPSC were cultured in α-MEM with 15% FCS and PS for 7 days, afterwards osteogenic media (α-MEM with 10% FCS, PS, 10^{-7} M dexamethasone, 10 mM β-glycerophosphate and 0.05 mM ascorbic acid 2-phosphate, denoted as OS +) or basal media (α-MEM with 10% FCS and PS, denoted as OS -) were applied for 21 days. The bioplotted HUVEC/MSC coculture was cultured in Endothelial Cell Growth Medium.

P2 PCL printing and characterization

P2.1 PCL characterization

The PCL [$(C_6H_{10}O_2)_n$] used in this project was directly provided as a 1.75 ± 0.005 mm filament for standard 3D printers (3D4makers.com, Haarlem, Netherlands, Mw: 84500 ± 1000 Da, ρ=1.145 g/cm^3, 100% pure, yield stress for the raw material, 17.2 MPa, Young modulus, E = 470 MPa). Data provided by the manufacturer.

Further thermal gravimetric analysis (TGA) were performed in a TA-Q500 (TA Instruments, Hüllhorst, Germany). A temperature range of 54 - 600°C, with a heating rate of 10°/min and N_2 atmosphere was used.

Differential scanning calorimetry (DSC) was performed in a DSC 7 (Perkin Elmer, Waltham, MA, USA. A temperature range of -65 - 250°C and a heating rate of 10°/min and N_2 atmosphere was configured. The powder required for these characterizations was obtained by pulverizing filament pieces with a blade grinder in liquid nitrogen.

P2.2 PCL scaffold characterization

Images of the manufactured scaffolds were obtained with an optical microscope (Y-FL eclipse 400, Nikon, Tokyo, Japan). Pore morphology was determined by imaging cut samples using a XL30, scanning electron microscope (Phillips, Eindhoven, Netherlands), operating at 25 kV. Specimens were coated with Au-Pd using a Polaron SC7640 (Quorum Tech. LTD, Kent, UK) sputter coater. Fiji software (ImageJ v1.52h, U.S. National Institutes of Health, Bethesda, MD, USA)was used for image analysis [124].

For the compression analysis, a QTest 1/L (Elite- MTS Systems Corporation Cary, North CA, USA) universal test machine was used. The load cell was configured for 1.000 N, with a maximum deformation of 20% at a speed of 5 mm/min. In this case, specimens were printed following the EN ISO 640 standard, as cylinders of 20 mm in height and with a diameter of 10 mm. As explained before in Section 2.3, six different specimens were tested (and for each one, the number of samples were six, n = 6). For each one, the compressive modulus of the scaffold, as well as the maximum load applied before breaking, were calculated.

The viscoelastic properties and the complex modulus of the PCL filament were evaluated by dynamic mechanical thermal analysis (DMA) as a function of time/frequency and temperature using a DMA 861e (Mettler Toledo, Schwerzenbach, Switzerland). The dynamic heating scans were performed from -90 to 40°C at 2°C/min and 1, 3, 10 and 30 Hz. The static load strain and the dynamic load strain used in these experiments were 3 N (150%) and 2 N, respectively. For these analyses, the ISO 6721 protocol was followed for the printing of specimens: rectangles of 10x5 mm^2 with a thickness = 50 μm and one perimeter of shell).

GraphPad Prism 6 software (Graphpad Software, San Diego, CA, USA) was used for the statistical analysis. One-way analysis of variance (ANOVA) was performed with multiple comparisons to check for significant differences ($p < 0.05$).

P3 biphasic constructs

P 3.1 Biphasic constructs plotting

CPC was used as ready-to-use paste without further modification. Briefly, CPC paste (precursor powders: α-tricalcium phosphate, dicalcium phosphate anhydrous, calcium carbonate, precipitated hydroxyapatite and as catalyst potassium hydrogen phosphate; carrier liquid: Miglyol, Cremophor ELP and Amphisol A) was manufactured by INNOTERE GmbH (Radebeul, Germany) and sterilized by γ-irradiation (25 kGy).

Plasma-based bioink was prepared as stated on p. 115.

Then, Plasma-alg-mc and CPC were transferred into 10 mL cartridges (Nordson EFD, Oberhaching, Germany) and processed by a pneumatic-driven multichannel extrusion plotter (Bioscaffolder 3.1, GeSiM mbH, Radeburg, Germany). The inks were dispensed through dosing needles (Globaco, Rödermark, Germany); the plotting parameters are summarized in Table P.1.

Cubic-shaped (base area 16x16 mm^2 and 20x20 mm^2) monophasic and biphasic scaffolds were fabricated with a strand distance of 2 mm and layer-to-layer orientation of 90°. If not differently mentioned, scaffolds were plotted with 4 layers and needles of an inner diameter of 410 µm were used. Monophasic scaffolds were crosslinked for 10 min in a bath of 100 mM $CaCl_2$ solution.

Biphasic constructs were post-processed as described previously [77]. In brief, biphasic constructs were allowed to set in water-saturated atmosphere (humidity > 95%) at 37°C for 20 min, afterwards crosslinking solution (100 mM $CaCl_2$) was added to the scaffolds for 10 min and subsequently scaffolds were transferred to cell culture medium before they were used for further experiments.

Table P.1: Plotting parameters for the biphasic constructs

	Needle [µm]		Air pressure [kPa]	Plotting speed [mm $\cdot s^{-1}$]
CPC	410	260		
Plasma-alg-mc	250	120	65	10
	410	260	55	10
	610	360	50	10
PBS-alg-mc	410	260	85	9

P3.2 Volumetric strand swelling and pore size

Monophasic plasma-alg-mc and biphasic CPC/plasma-alg-mc constructs were plotted (base area 12x12 mm^2, 4 layers) and volumetric strand swelling of the hydrogel ink as well as the pore size were investigated by measuring the strand width and the smallest distance between two adjacent strands at different time points: before and after crosslinking, and at days 1, 2, 3, 5, 7, 14 and 21 of incubation in cell culture medium consisting of DMEM (Dulbecco's Modified Eagle's Medium, Gibco, Thermo Fisher), 10% fetal calf serum (FCS), 100 $U \cdot mL^{-1}$ penicillin and 100 $mg \cdot mL^{-}1$ streptomycin (Pen/Strep) (all from Biochrom, Berlin, Germany).

For measuring, photographs of different scaffolds (n=5) were taken by stereo light microscopy and strand widths were analyzed with Fiji [124].

P3.3 Cell viability and morphology

Cell viability was investigated by a live/dead assay using Calcein AM/ethidium homodimer-1 staining (LIVE/DEAD^{TM}Viability/ Cytotoxicity Kit, for mammalian cells, Thermofisher Scientific) following the manufacturer's protocol. Confocal laser scanning microscopy (cLSM,

Leica TCS SP5, Leica Microsystems, Wetzlar, Germany) was used to determine quantitative cell viability of MSC at day 1 of plasma-alg-mc, PBS-alg-mc and its biphasic equivalents (n=3).

Cell viability was assessed by semi-automatic counting of living cells and dead cells with averaged thresholds derived by all image stacks (n=7 per group). The viability was determined as the ratio of living cells divided by the total cell number (which equals the sum of living and dead cells).

At later time points, fluorescence microscopy (Keyence 9000 Fluorescent Light Microscope) was used to investigate cell morphology. In differentiation experiments, live/dead staining was performed to control cell morphology, but only one scaffold per group and time point was assessed due to the limited available number of primary cells.

P3.4 Quantification of cell number and ALP activity

At distinct time points, plotted constructs containing MSC, hOB or hDPSC were washed with HBSS (Fisher Scientific) and frozen at -80°C until biochemical analysis. After thawing, samples were incubated with 2 mL lysis buffer (1% Triton X-100 in PBS) for 3 h on ice. DNA determination was performed using Quantifluor^{TM}ds DNA quantification reagent (Promega, WI, USA) according to manufacturer's instructions.

A calibration line was constructed from cells with different concentrations, which were frozen and lysed in the same way. 10 µL of cell lysates were transferred in triplicates into a 96 well plate and 190 µL of the Quantifluor^{TM}working solution were added to each sample. The plate was protected from light and incubated for 5 min at room temperature. Fluorescence was read with a multifunction microplate reader (Infinite 200 PRO, Tecan, Switzerland) at an excitation and emission wavelength of 485 nm and 535 nm, respectively.

ALP activity was quantified by incubating 20 µl of each lysate with 80 µl substrate solution (1 $mg \cdot mL^{-1}$ 4-nitrophenylphosphate in 0.1 M diethanolamine, 0.1% Triton X-100, 1 mM $MgCl_2$, pH 9.8 - all from Sigma) for 30 min at 37°C. After stopping the enzymatic reaction with 1 M NaOH, absorbance at 405 nm was determined with the microplate reader.

A calibration line was established using different concentrations of 4-nitrophenol. ALP activity was related to cell number from the same lysate to obtain specific ALP activity.

P4 DIY BIOPRINTER: ASSEMBLY AND CALIBRATION

All the information summarized in this chapter, is also available online under C.C. S-A. License, at Openbioprinting.org.

P4.1 Bill of Materials (BOM)

- Cartesian platform - Hephestos 1 (Prusa i3 BQ)[3]
- 6 Printable pieces for the extruder (3D STL can be seen at Table P.2 and 2D drawings (dwg.) at p. 191):
  - Base_support *[Dwg. 1, Element 1].*
  - Spring_press *[Dwg. 10, Element 8].*
  - Internal_gear *[Dwg. 7, Element 6].*
  - Plunge *[Dwg. 8, Element 7].*
  - Small_gear *[Dwg. 5, Element 5].*
  - Big_gear *[Dwg. 4, Element 4].*
- 1 x NEMA 17 step motor, 1.8°*[Dwg. 11, Element 9].*
- Spacer (or 6 x Flat washer, galvanized steel M-8. DIN 125-B) *[Dwg. 3, Element 3].*
- 1 x Milled screw M-8 x 60 mm DIN 933 *[Dwg. 2, Element 2].*
- Normalized elements:
  - 2 x Threaded rod, galvanized steel. M-4 x 60. DIN-976 *[Dwg. 12, Element 10].*
  - 2 x Wing nut, galvanized steel. M-4. DIN-315 *[Dwg. 12, Element 11].*
  - 2 x Hex nut, galvanized steel. M-4. DIN-934 *[Dwg. 12, Element 12].*

3 More info, schemes and downloads at: https://reprap.org/wiki/Prusa_i3_Hephestos/es

- 2 x Hex nut, galvanized steel. M-3. DIN-934 *[Dwg. 12, Element 13].*
- 2 x Cylindrical Head Allen Screw, galvanized steel. M-3 x 15. DIN-912 *[Dwg. 12, Element 14].*
- 2 x Wide flange whaser, galvanized Steel. M-3. DIN-9021 *[Dwg. 12, Element 15].*
- 1 x Set screw, bluing Steel M-3 x 8. DIN-916 *[Dwg. 12, Element 16].*
- 2x Form B Flat washer, galvanized steel M-8. DIN-125-B *[Dwg. 12, Element 17].*
- 2 x Compression spring, 20 x 5 mm, 1,67 N/mm. DIN-2095 *[Dwg. 13, Element 18].*
- 1 x Cylindrical slotted head screw, galv. Steel M3 x 30. DIN-84 *[Dwg. 13, Element 19].*
- 1 x Threaded rod, galvanized steel. M-4 x 18. DIN-976 *[Dwg. 13, Element 20].*
- 1 x Self-Locking nut, galvanized Steel. M8. DIN-985 *[Dwg. 13, Element 21].*
- 1 x Rigid balls bearing, 624Z. diam. 4 x diam. 13, thickness 5mm. DIN-625-1 *[Dwg. 13, Element 22].*
- 2 x Rigid balls bearing, 608Z. diam. 8 x diam. 22, thickness 7mm. DIN-625-1 *[Dwg. 13, Element 23].*

A summary of the printable pieces can be found below, at table P.2. Some of them have been used as obtained from Thingiverse (5, 6) and the others have been adapted and redesigned for a better mechanical fit. In the name, a reference to the drawings (Dwg.) where they appear is included, along the element number (E.).

n	Und.	Name	Piece	Description
1	1	*Base support (Drw.1, E.1)*	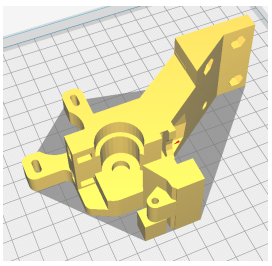	Support to attach all the extruder parts to the x-carriage
2	1	*Spring press (Drw.10, E.8)*	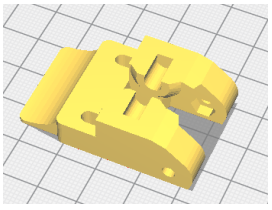	To provide an elastic force that keeps the gear/plunge working
3	1	*Internal gear (pinion) (Drw.7, E.6)*	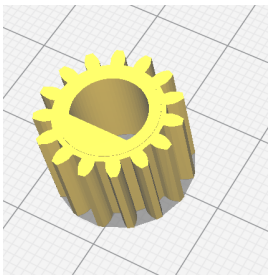	Internal gear to convert rotation into lineal movement with a pinion/rack mechanism (Drw.9).
4	1	*Plunge (rack) (Drw.8, E.7)*	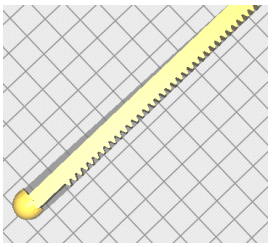	Rack (linear gear) of the mechanism that pushes the plunge of the syringe.

5	**1**	*Small drive gear (small herringbone) (Drw.5, E.5)*	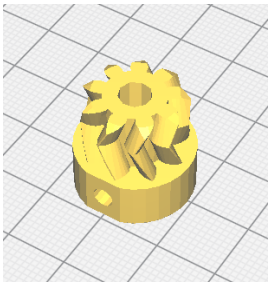	Gear connected to the step motor to transmit the movement
6	**1**	*Big drive gear (big herringbone) (Drw.4, E.4)*	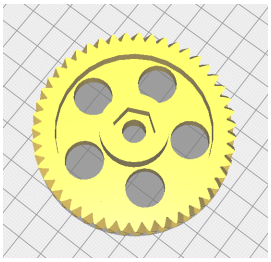	Reduction gear to increase the resolution and torque.

Table P.2: Identification of the printable pieces. Some of them have been used as obtained from Thingiverse (5, 6) and the others have been adapted and redesigned for a better mechanical fit.

P4.2 Assembly

The construction and assembly of the extruder is explained in the next pages, with subset drawings at Annex C.3. Also, an interactive 3D model of the complete assemblied extruder can be consulted online: https://a360.co/2EwcIV1.

P4.3 Calibration and software adaptation

To be able to work with the new extruder in any printer, some basic data from the mechanical transmission is necessary to obtain the *steps per unit*. This is a parameter present in all the axis or a normal 3D printer that works with stepper motors. It represents how much must rotate the stepper motor to obtain a movement of 1 mm at the end of the transmision. For example, when the x, y or z-axis moves 1 mm. This number can be calculated following the movement of the mechanical parts conected to the motor.

In our case, the motor (which rotates 1.8°per step) moves solidary with a small herringbone (double helical) gear [Piece 5]. Then a reduction system transforms this movement into a smaller rotation, but with higher torque. Solidary to this big herringbone gear [Piece 6], is a pinion [Piece 3] that translates the rotational movement to a linear one, thanks to a pinion-rack system. This rack [Piece 4] will act as the plunge that will press the syringe. Therefore, this is the final element of the transmission, the one that should move 1 mm.

The calculations requiered to obtain the number of steps that the motor must rotate to achieve this movement (steps_per_unit) are reflected in Figure P.1.

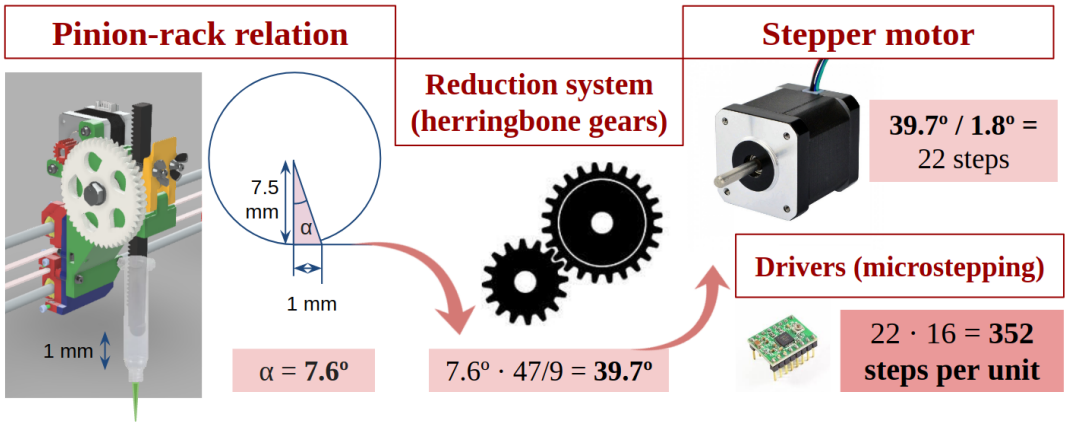

Figure P.1: Transmision movement scheme to calculate the **'steps per unit'** for the extruder motor. It may change for other printers microstepping.

P4.4 Firmware adaptation (MARLIN)

Marlin is composed by many files and libraries. In this case, a version of Marlin adapted to the desired printer model was obtained and some modifications were performed at 'Configuration.h'.

1. **# define TEMP_SENSOR_0 to 998:** this will tell the printer that the current temperature of the extruder is 25 °C always. This is necessary to print, as the extruder heating is not used, neither the temperature sensor of the extruder.
2. **# define EXTRUDE_MINTEMP to 20:** to remove the limitation of printing only over 170 °C, that is normally preinstalled in the printers.
3. **# define INVERT_E0_DIR to false:** *Only when necessary*, if the extruder is moving in the opposite direction.
4. **# define Z_RAISE_BEFORE_HOMING to n**: tto avoid collision, if transwells or any other recipient is used for bioprinting. This can also be changed at 'Start G-Code' inside the slicing software.
5. **# define DEFAULT_AXIS_STEPS_PER_UNIT (x,y,z, E):** where (x,y,z) is given by default depending on the printer model and E is changed

to 352[4] to set up the correct volume deposition. This number is given by the movement translation from the rotating advance of the stepper motor to the linear movement of the plundge that press the syringe with the paste, as explained in Figure P.1.

P4.5 Slicing program (Cura, Ultimaker)

This section will describe the configuration requiered in the slicing software (Cura, Ultimaker) to generate the trajectories (.gcodes) and deposit the correct volume of paste.

In the first place, we need to access the *printer settings* menu and change the configuration of the 'compatible filament diameter' to 18 mm, which is normally the diameter of the 10 cc cartridge / syringe.

The, at *Filament* menu, we introduce again this number (18 mm) where the size of the filament plastic used is normally configured. We need to change also the temperature required for the thermoplastic melting to the 25°C, and configure the temperature of the hot base if required.

In the printing menu configuration we need to check also some submenus:

- **Filament diameter**: The cartridge diameter, which along with the mm extruded give us the volume of material that enters in the system. In our case, the Nordson cartridges are set to 18 mm.
- **Bed temperature:** 37 °C, if cells are present.
- **Layer height:** 65% of the noozle/needle tip diameter.
- **Retraction:** Disabled, to avoid the introduction of air inside the cartridges

4 This number can change if other microstepping relation is used by the printer electronics board.

Part IV

DISCUSSION AND CONCLUSIONS

- **Chapter 6.** Answers to research hypothesis and questions
- **Chapter 7.** Conclusions

In this last chapter, the research questions enumerated at the beggining of the document (Section 1.2) will be quickly discussed and answered, as a summary of the conclusions and findings exposed along the document.

Also, a brief synopsis regarding the achievement of the desired specific objectives is included.

Finally, a list of devices, knowledge and valuable products generated as outcomes of the thesis is also listed.

6

ANSWERS TO RESEARCH HYPOTHESES AND QUESTIONS

The aim of this PhD Thesis was to test some **research hypotheses** based on the following questions:

- Which are the main clinical scenarios that crew will face on the Moon, Mars or in a low Earth orbit (LEO) mission - as at the ISS or the Deep Space Gateway - and how bioprinting can be a technology of interest for such missions? (Section 6.1)
- Which are the materials that fit better to the technical requirements obtained? Can we develop a bioink for the bioprinter based on them? (Section 6.2)
- Is it feasible to translate this technology (3D bioprinting) to altered gravity environments? How can we demonstrate it on Earth, with a first, low-cost, approach? (Section 6.3)

In the next sections, answers to each one of these questions are listed, obtained with the knowledge and information that was found along the work here presented.

Finally, a short conclusion will be presented trying to summarize the main findings.

6.1 SPACE EXPLORATION: CLINICAL SCENARIOS

First of all, it was necessary to analyse the main possible clinical scenarios that the crew will face in a long-term expedition, as a manned flight to Mars. With this data, it was considered that 3D printing and bioprinting (with microextrusion, the selected and more mature technology) may be of use in those cases. Both technologies improve the autonomy of the crew in any mission, as provide with tools and tissues that can be manufactured on demand.

After this deep study, looking close to real experimental data obtained from previous space exploration missions and having in mind the new challenges and technical requirements that a long-term missions will entail, the following conclusions were obtained:

- The tissues most exposed to damage (by accidents, radiation or altered gravity effects) and those that can be of interest for the first experiments (because of the maturity of the required technology and environment) are skin, cartilage and bone.
- 3D printing can be of use for the fabrication of tailored casts, prosthesss and recyclable surgery tools.
- 3D bioprinting can be used for the development of tissue constructs that can be matured *in vitro* or *in vivo* for the replacement of partial damaged tissues or even complete organs, once the technology is ready.

6.2 DEVELOPMENT OF NEW (BIO)MATERIALS FOR ISOLATED SYSTEMS

Up to now, the efforts and work spent into space exploration research, have given back many unexpected benefits to the humans on Earth. For example, the development of water purification stations that can be used onboard the ISS can be translated to isolated areas, as those in Africa [1].

Space exploration presents many challenges and technical requirements due to the the fact that the crew needs to be as autonomous as possible, and ideally live in a closed ecosystem where everything can be recycled. This idea can be also translated to the Earth, as the strategies and technologies developed for such environments can also be of used in isolated regions or places with no easy access to basic resources, as water or electricity.

In addition, the concept of closed systems (similar to 'circular economy') is something that can be heard more and more everyday, as humans need to increase the sustainability of our processes if we want to continue living on this planet without damaging it more and more.

In the case of this study, it was decided to use materials that can be easily obtained in missions where humans are present:

- Plasma, obtained easily from blood. It can be extracted regularly and pooled from different persons.
- Biomaterials obtained from plants and algae (cellulose, alginate), that can be grown and harvested in a controlled environment.
- Mineral components, that can be derived from bone rest of other species (as the calcium carbonate from shells).

The use of low cost (DIY) technologies that can be replicated in other parts of the world, and that are free and shared online (open source) by a huge community, will make the translation and the spread of this research easier.

1 Data obtained from NASA website. Accessed on 15/11/2019 https://www.nasa.gov/mission_pages/station/research/benefits/water_purification.html

6.3 TRANSLATION OF 3D BIO/PRINTING TECHNOLOGY FROM THE EARTH TO SPACE CONDITIONS. DEMONSTRATION.

Given the limited availability of medical equipment and supplies that astronauts must face outside Earth, it has been previously highlighted that the ability to print their own personalized tools and medical devices (as tailored casts) through 3D printing represents a great advantage.

Going a little bit further and thinking about the possibility of obtaining bioprinted living tissues to replace those that have been injured, or even complete organs in the future, this can mean an important breakthrough for space extraterrestrial settlements and mankind.

BP is used as a precise technology that allows scientist to create complex 3D cultures and tissue equivalents. In contrast with the classic methods employed on TE, different cell types can be deposited in specific regions of the engineered constructs. In addition, it maybe offers a solution for vascular supply in future, as internal channels can be added while the tissue is being built.

As BP works in a semi-automatic manner, it would allow non-specialized crew to create different types of tissues, without the need of full knowledge about it, with very few instructions and the help of the software.

Another advantage of having a bioprinter is that once this machine is available in space, it would be able to generate new different tissues as they are investigated on Earth, as the design can be modular, updated with new features and adjustable to the needs of the crew in each moment. This can be better understood, if the bioprinter is thought of as a kitchen robot, where different recipes can be pre-programmed and the final result will depend on the materials and tools previously introduced. Indeed, the same machine can be adjusted to work with thermoplastics (normal 3DP) or with cells and pastes, simplifying and reducing the necessary hardware - and therefore space and weight on board. As they can be installed in closed,

sterile chambers, the risk of liquid leakage or contamination can be decreased.

Even all the treatments can be translated to Space and other planets if a proper environment is set up for surgery - a facility with the required gravity or liquid-management system.

Translation of bioprinting to application in space is not only related to the printing process itself, but also to questions like applicable cell sources, systems for cell proliferation, suitable biomaterials, devices for maturation of the constructs post printing and systems which allow surgical interventions which is especially challenging under microgravity conditions. Finally, as much of the materials used for the whole process as possible need to be recycled as the loading capacity in space flight is very limited, especially when it comes to long-term missions and those to distant destinations (Figure 6.1).

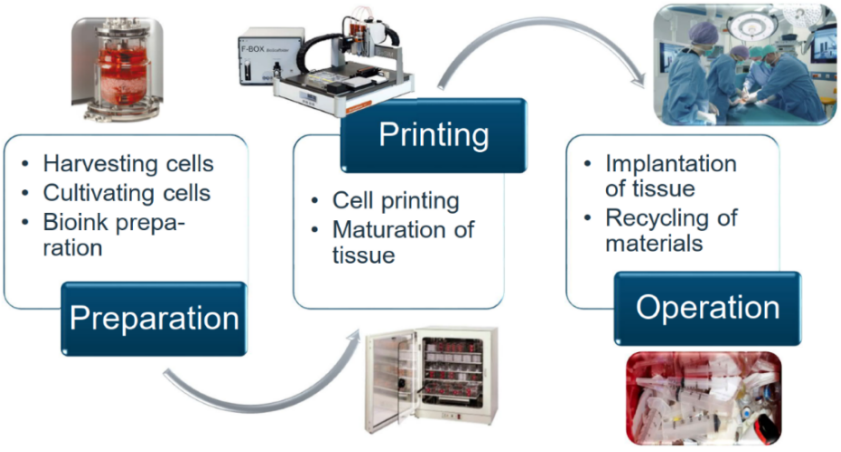

Figure 6.1: Schematic showing the different work steps for medical application of bioprinting in space. Image previously submited by OHB 2019 to ESA (contract No. 4000123640/18/NL/BJ/gp). Reused with permision of OHB System AG, 2020.

Whereas for most mesenchymal tissues (bone, cartilage, tendon etc.) autologous mesenchymal stem cells, isolated from the patient's bone marrow or fat tissue can be suitable cell sources, other cell types might be

derived from induced pluripotent stem (iPS) cells. Systems for cell proliferation are available but generation of high cell numbers as they would be needed to fabricate tissue-like constructs of clinically relevant dimensions is still challenging, takes long time and needs large volumes of cell culture media and supplements which will be difficult to provide during space exploration missions. Every research in this field, therefore, has to take these limitations into account.

In the experiments here presented, it has been demonstrated that personalised bioinks (hydrogels suitable for suspension and bioprinting of live cells) can be prepared easily from human blood plasma and renewable biopolymers like alginate and methylcellulose. In case of a medical application the plasma could be obtained from the patient her/himself which also would be applicable in space. It can be isolated through mechanical separation (centrifugation) from blood.

It has also been demonstrated that such bioinks and support materials, like a self-setting calcium phosphate bone cement (CPC) suitable for extrusion (bio)printing, are so adhesive that they can even be printed upside-down and therefore, against Earth's gravity. The photos shown in Figure 6.2. demonstrate the setup and printing of a biopolymer hydrogel as well as the CPC.

Although PCL was not used for the final approach, it is still considered a good alternative to be combined with bioinks under physiological conditions or having in consideration special morphologies or printing strategies C.2.

Along that study it was also discovered that there are several printing parameters, not usually reported, that may affect the performance of 3D-printed scaffolds. Other than the porous design, these parameters include slow cooling rate, the use or not of alternate layers, the alignment of the printing starting point and the infill with a complementary gel.

The cooling rate is an important parameter for the final characteristics

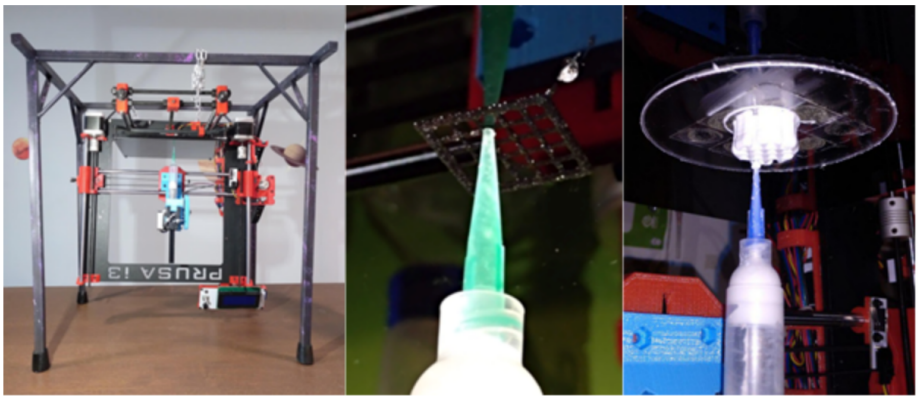

Figure 6.2: Extrusion printing upside-down, i.e. against Earth's gravity: Prusa i3 printer with extrusion printhead mounted upside-down (left), printing of 5 layers of a biopolymer-based hydrogel (suitable as bioink for bioprinting; centre) and printing 50 layers of a pasty CPC.

of the scaffold. Forcing cooling down leads to higher internal and external shape fidelity in scaffolds made with polymers whose T_g is below room temperature, as in PCL. The cooling rate, or even printing speed, can be modified to obtain more chaotic micropatterns including nanofibers without the need of using further technologies.

The use of alternated layers involves the generation of more anisotropic structures, as the z-axis pore is limited to the layer height, while the x,y-pore size can be tailored to specific needs. The defects created because of the alignment, or the lack of it, in the new layer starting point, significantly affects the mechanical behaviour of the scaffolds.

7

CONCLUSIONS

► The international space agencies have begun to investigate the requirements for both a human settlement on the Moon and manned missions to Mars.

In this work, the main possible clinical scenarios that the crew will face in such a long-term expedition, as a manned flight to Mars, has been analyzed. With this data, we considered that 3D printing and bioprinting (with microextrusion, the selected and more mature technology) may be of use in those cases.

3D printing can be of use for the fabrication of tailored casts, prostheses and recyclable surgery tools, and 3D bioprinting can be used for the development of tissue constructs that can be matured *in vitro* or *in vivo* for the replacement of damaged tissues or even complete organs, if the technology would make this possible once. The tissues which might become injured most likely, and those that are of interest for the first experiments (because of the maturity of the required technology and environment), are skin, cartilage and bone.

► The development of 3D printing in this field brings unique challenges, which must be accounted for in the design of experiments. The common printing process parameters must be considered as important factors in the design and quality of final 3D-printed products

There are several printing parameters, not usually reported, that may affect the performance of 3D-printed scaffolds. Other than the porous design, these parameters include cooling rate, the use or not of alternate

layers or the alignment of the printing starting point. The cooling rate is an important parameter for the final characteristics of the scaffold. Forcing cooling down leads to higher internal and external shape fidelity in scaffolds made with polymers whose T_g is under room temperature, as in PCL. The cooling rate, or even printing speed, can be modified to obtain more chaotic micropatterns including nanofibers without the need of using further technologies. The use of alternated layers involves the generation of more anisotropic structures, as the z-axis pore is limited to the layer height, while the x,y-pore size can be tailored to specific needs. The defects created because of the alignment, or the lack of it, in the new layer starting point, significantly affects the mechanical behaviour of the scaffolds.

▶ For bioprinting, a novel bioink was developed, which combines the favorable biological properties of human plasma, which can potentially be derived as autologous material from the patient to be treated, with the excellent plotting properties and high shape fidelity of alginate-methylcellulose blends. It can be bioplotted with good shape fidelity and promotes high postplotting cell viability and cell attachment resulting in the formation of intercellular interactions. The plasma-based bioink was successfully combined with a hydroxyapatite-forming calcium phosphate cement which resembles the native mineral of bone. The results showed that the plasma-based bioink and CPC form a synergistic system supporting adhesion, proliferation, and osteogenic differentiation of bone cells. Both, the plasma-based bioink and the biphasic CPC/plasma-alg-mc system are promising candidates for the fabrication of tissue engineered (bone) grafts comprising a patient-specific bioink, a defect-adapted shape and autologous cells for a fully patient-tailored tissue graft.

▶ An in-house developed bioprinter was designed and manufactured. It is based on a BQ Hephestos 1 (Prusa i3) and it was designed and built as a workbench, to demonstrate that our biomaterials were stable enough to be printed in altered gravity conditions. Two main modifications were made to the machine: the thermoplastic extruder was replaced by a DIY printed

one, capable of working with pastes, and a scaffold was built to mount the printer upside-down, in order to obtain the opposite gravity forces while printing.

Thanks to this bioprinter, it has been demonstrated that the developed bioinks and support materials, like the self-setting calcium phosphate bone cement or the thermoplastics like polycaprolactone, are suitable for extrusion (bio)printing, and they are so adhesive that they can even be printed upside-down and therefore, against Earth's gravity.

BIBLIOGRAPHY

[1] Alberto Valero-Gomez, Mario Almagro-Cádiz, Nieves Cubo Mateo, Juan Gonzalez-Gomez, Alberto Valero-Gómez, Nieves Cubo-Mateo, and Juan González-Gómez. A new Paradigm for Open Robotics Research with the C++ Object Oriented Mechanics Library Locomotion gaits View project Design, construction and testing of a 3D Bioprinter able to produce functional human skin. View project A new Paradigm for Open Robotics Research with the C++ Object Oriented Mechanics Library. Technical report, 2012.

[2] Ian Gibson, David Rosen, and Brent Stucker. *Additive manufacturing technologies: 3D printing, rapid prototyping, and direct digital manufacturing, second edition*. 2015.

[3] Jos Malda, Jetze Visser, Ferry P. Melchels, Tomasz Jüngst, Wim E. Hennink, Wouter J.A. Dhert, Jürgen Groll, and Dietmar W. Hutmacher. 25th anniversary article: Engineering hydrogels for biofabrication. *Advanced Materials*, 25(36):5011–5028, 2013.

[4] Vladimir Mironov, Richard P. Visconti, Vladimir Kasyanov, Gabor Forgacs, Christopher J. Drake, and Roger R. Markwald. Organ printing: Tissue spheroids as building blocks. *Biomaterials*, 30(12):2164–2174, 2009.

[5] Hyun Wook Kang, Sang Jin Lee, In Kap Ko, Carlos Kengla, James J. Yoo, and Anthony Atala. A 3D bioprinting system to produce human-scale tissue constructs with structural integrity. *Nature Biotechnology*, 34(3):312–319, 2016.

[6] Elliot S. Bishop, Sami Mostafa, Mikhail Pakvasa, Hue H. Luu,

Michael J. Lee, Jennifer Moriatis Wolf, Guillermo A. Ameer, Tong Chuan He, and Russell R. Reid. 3-D bioprinting technologies in tissue engineering and regenerative medicine: Current and future trends. *Genes and Diseases*, 4(4):185–195, 2017.

[7] Jörg Lehmann, Ronny M. Schulz, and Ralf Sanzenbacher. Strategische Betrachtungen zur Konzeption und Wahl von Tiermodellen bei nicht-klinischen Prüfungen von zellbasierten Therapeutika. *Bundesgesundheitsblatt - Gesundheitsforschung - Gesundheitsschutz*, 58(11-12):1215–1224, nov 2015.

[8] S. S. Panesar and K. Ashkan. Surgery in space. *British Journal of Surgery*, 105(10):1234–1243, sep 2018.

[9] Sunil C. Joshi and Abdullah A. Sheikh. 3D printing in aerospace and its long-term sustainability. *Virtual and Physical Prototyping*, 10(4):175–185, 2015.

[10] Jaesung Park, Yang Liu, Kenneth D. Kihm, and Lawrence A. Taylor. Characterization of lunar dust for toxicological studies. I: Particle size distribution. *Journal of Aerospace Engineering*, 21(4):266–271, 2008.

[11] W. W. Mendell and R. P. Heydorn. Lunar precursor missions for human exploration of Mars - III: Studies of system reliability and maintenance. In *Acta Astronautica*, volume 55, pages 773–780, 2004.

[12] Chee Kai Chua and Kah Fai Leong. *3D Printing and additive manufacturing: Principles and applications (with companion media pack) - fourth edition of rapid prototyping*. 4th edition, 2014.

[13] Nicolas Martelli, Carole Serrano, Hélène Van Den Brink, Judith Pineau, Patrice Prognon, Isabelle Borget, and Salma El Batti. Advantages and disadvantages of 3-dimensional printing in surgery: A systematic review. *Surgery (United States)*, 159(6):1485–1500, 2016.

[14] Erin A. Gillaspie, Jane S. Matsumoto, Natalie E. Morris, Robert J. Downey, K. Robert Shen, Mark S. Allen, and Shanda H. Blackmon.

From 3-Dimensional Printing to 5-Dimensional Printing: Enhancing Thoracic Surgical Planning and Resection of Complex Tumors. *Annals of Thoracic Surgery*, 101(5):1958–1962, 2016.

[15] Laith Alrubaiy and Kathem K. Al-Rubaiy. Skin substitutes: A brief review of types and clinical applications, jan 2009.

[16] François Berthiaume, Timothy J. Maguire, and Martin L. Yarmush. Tissue engineering and regenerative medicine: History, progress, and challenges. *Annual Review of Chemical and Biomolecular Engineering*, 2(1):403–430, 2011.

[17] W. C. Hymer, T. Salada, L. Avery, and R. E. Grindeland. Experimental modification of rat pituitary prolactin cell function during and after spaceflight. *Journal of Applied Physiology*, 80(3):971–980, 1996.

[18] L. Dintenfass, P. Osman, B. Maguire, and H. Jedrzejczyk. Experiment on aggregation of red cells under microgravity on STS 51-C. *Advances in Space Research*, 6(5):81–84, 1986.

[19] L. E. Freed, N. Pellis, N. Searby, J. de Luis, C. Preda, J. Bordonaro, and G. Vunjak-Novakovic. Microgravity cultivation of cells and tissues., 1999.

[20] Abdalla Eltom, Gaoyan Zhong, and Ameen Muhammad. Scaffold Techniques and Designs in Tissue Engineering Functions and Purposes: A Review, 2019.

[21] G. Horneck, R. Facius, M. Reichert, P. Rettberg, W. Seboldt, D. Manzey, B. Comet, A. Maillet, H. Preiss, L. Schauer, C. G. Dussap, L. Poughon, A. Belyavin, G. Reitz, C. Baumstark-Khan, and R. Gerzer. Humex, a study on the survivability and adaptation of humans to long-duration exploratory missions, part I: Lunar missions. *Advances in Space Research*, 31(11):2389–2401, 2003.

[22] Jeffrey Kahn, Catharyn T. Liverman, Margaret A. McCoy, Committee on Ethics Principles Spaceflights, Guidelines for Health Standards for

Long Duration, Exploration, Board on Health Sciences Policy, and Institute of Medicine. NASA Risk Management and Health Standards. jun 2014.

[23] K A Binsted and J B Hunter. HI-SEAS (Hawaii Space Exploration Analog and Simulation, hi-seas.org) as an opportunity for long-duration instrument/protocol testing and verification. Technical report, Cornell University, Manoa, Hawaii, 2013.

[24] Thomas Boland, Vladimir Mironov, Anna Gutowska, Elisabeth A. Roth, and Roger R. Markwald. Cell and organ printing 2: Fusion of cell aggregates in three-dimensional gels. *Anatomical Record - Part A Discoveries in Molecular, Cellular, and Evolutionary Biology*, 272(2):497–502, 2003.

[25] Natalja E. Fedorovich, Jacqueline Alblas, Joost R. De Wijn, Wim E. Hennink, A. B.J. Verbout, and Wouter J.A. Dhert. Hydrogels as extracellular matrices for skeletal tissue engineering: State-of-the-art and novel application in organ printing. *Tissue Engineering*, 13(8):1905–1925, 2007.

[26] Hemanth Gudapati, Madhuri Dey, and Ibrahim Ozbolat. A comprehensive review on droplet-based bioprinting: Past, present and future. *Biomaterials*, 102:20–42, sep 2016.

[27] Ibrahim T. Ozbolat and Monika Hospodiuk. Current advances and future perspectives in extrusion-based bioprinting. *Biomaterials*, 76:321–343, 2016.

[28] Pu Chen, Pu Chen, Haodi Wu, Soah Lee, Arun Sharma, Daniel A. Hu, Sneha Venkatraman, Adarsh Venkataraman Ganesan, Osman Berk Usta, Martin Yarmush, Fan Yang, Joseph C. Wu, Utkan Demirci, and Sean M. Wu. Bioacoustic-enabled patterning of human iPSC-derived cardiomyocytes into 3D cardiac tissue. *Biomaterials*, 131:47–57, 2017.

[29] Aurore Van de Walle, Claire Wilhelm, and Nathalie Luciani. 3D

magnetic stem cell aggregation and bioreactor maturation for cartilage regeneration. *Journal of Visualized Experiments*, 2017(122), apr 2017.

[30] Erin Lavik, Steve Bernstein, Adam Day, and Bryan Ibarra. Patent 20190187128, screen printing tissue models, June 2019.

[31] W. Schuurman, V. Khristov, M. W. Pot, P. R. Van Weeren, W. J.A. Dhert, and J. Malda. Bioprinting of hybrid tissue constructs with tailorable mechanical properties. *Biofabrication*, 3(2), 2011.

[32] Ferry P.W. Melchels, Maarten M. Blokzijl, Riccardo Levato, Quentin C. Peiffer, Myléne De Ruijter, Wim E. Hennink, Tina Vermonden, and Jos Malda. Hydrogel-based reinforcement of 3D bioprinted constructs. *Biofabrication*, 8(3), 2016.

[33] David Kilian, Tilman Ahlfeld, Ashwini Rahul Akkineni, Anja Lode, and Michael Gelinsky. Three-dimensional bioprinting of volumetric tissues and organs. *MRS Bulletin*, 42(8):585–592, aug 2017.

[34] Tuan D. Ngo, Alireza Kashani, Gabriele Imbalzano, Kate T.Q. Nguyen, and David Hui. Additive manufacturing (3D printing): A review of materials, methods, applications and challenges, jun 2018.

[35] Mohammadmahdi Mobaraki, Maryam Ghaffari, Abolfazl Yazdanpanah, Yangyang Luo, and D K Mills. Bioinks and Bioprinting: a Focused Review Social Impact of Bionanotechnology and 3D Printing View project 3D Printing for Radiology/Interventional Radiology View project Bioinks and bioprinting: A focused review. 2020.

[36] Carlos F. Guimarães, Luca Gasperini, Alexandra P. Marques, and Rui L. Reis. The stiffness of living tissues and its implications for tissue engineering, may 2020.

[37] Juan He, Xiaoyu Zhang, Xinyi Xia, Ming Han, Fei Li, Chunfeng Li, Yunguang Li, and Dong Gao. Organoid technology for tissue engineering. *Journal of Molecular Cell Biology*, (00):1–11, 2020.

[38] Shen Ji and Murat Guvendiren. Recent Advances in Bioink Design for 3D Bioprinting of Tissues and Organs, apr 2017.

[39] Pallab Datta, Ananya Barui, Yang Wu, Veli Ozbolat, Kazim K. Moncal, and Ibrahim T. Ozbolat. Essential steps in bioprinting: From pre- to post-bioprinting, sep 2018.

[40] Clarissa Tomasina, Tristan Bodet, Carlos Mota, Lorenzo Moroni, and Sandra Camarero-Espinosa. Bioprinting Vasculature: Materials, Cells and Emergent Techniques. *Materials*, 12(17):2701, aug 2019.

[41] National Research Council. *Recapturing a Future for Space Exploration: Life and Physical Sciences Research for a New Era*. The National Academies Press, Washington, DC, 2012.

[42] Katja Hölzl, Shengmao Lin, Liesbeth Tytgat, Sandra Van Vlierberghe, Linxia Gu, and Aleksandr Ovsianikov. Bioink properties before, during and after 3D bioprinting. *Biofabrication*, 8(3):032002, 2016.

[43] Paul Hourd, Nicholas Medcalf, Joel Segal, and David J. Williams. A 3D bioprinting exemplar of the consequences of the regulatory requirements on customized processes. *Regenerative Medicine*, 10(7):863–883, oct 2015.

[44] P. Li. 3D bioprinting: Regulation, innovation, and patents. In *3D Bioprinting for Reconstructive Surgery: Techniques and Applications*, pages 217–231. Elsevier Inc., jan 2018.

[45] Wei Sun, Binil Starly, Andrew C. Daly, Jason A. Burdick, Jürgen Groll, Gregor Skeldon, Wenmiao Shu, Yasuyuki Sakai, Marie Shinohara, Masaki Nishikawa, Jinah Jang, Dong Woo Cho, Minghao Nie, Shoji Takeuchi, Serge Ostrovidov, Ali Khademhosseini, Roger D. Kamm, Vladimir Mironov, Lorenzo Moroni, and Ibrahim T. Ozbolat. The bioprinting roadmap. *Biofabrication*, 12(2):022002, 2020.

[46] Vladislav A. Parfenov, Vladimir A. Mironov, Elizaveta V. Koudan, Elizaveta K. Nezhurina, Pavel A. Karalkin, Frederico Das Pereira,

Stanislav V. Petrov, Alisa A. Krokhmal, Timur Aydemir, Igor V. Vakhrushev, Yury V. Zobkov, Igor V. Smirnov, Alexander Yu Fedotov, Utkan Demirci, Yusef D. Khesuani, and Vladimir S. Komlev. Fabrication of calcium phosphate 3D scaffolds for bone repair using magnetic levitational assembly. *Scientific Reports*, 10(1):4013, dec 2020.

[47] G. Horneck, R. Facius, M. Reichert, P. Rettberg, W. Seboldt, D. Manzey, B. Comet, A. Maillet, H. Preiss, L. Schauer, C. G. Dussap, L. Poughon, A. Belyavin, G. Reitz, C. Baumstark-Khan, and R. Gerzer. HUMEX, a study on the survivability and adaptation of humans to long-duration exploratory missions, part II: Missions to Mars. *Advances in Space Research*, 38(4):752–759, 2006.

[48] Martin Braddock. Tissue Engineering and Human Regenerative Therapies in Space: Benefits for Earth and Opportunities for Long Term Extra-Terrestrial Exploration. *Innovations Tissue Eng Regen Med.*, 1(3):5, 2019.

[49] Nieves Cubo, Marta Garcia, Juan F. Del Cañizo, Diego Velasco, and Jose L. Jorcano. 3D bioprinting of functional human skin: Production and in vivo analysis. *Biofabrication*, 9(1), 2017.

[50] Jürgen; Lademann and Joachim Fluhr. This Issue at a Glance: Skin Reactions of Astronauts in Space and Microstructures of Topically Applied Formulations. *Skin Pharmacology and Physiology*, 21(5):245–245, 2008.

[51] H. Tronnier, M. Wiebusch, and U. Heinrich. Change in skin physiological parameters in space - Report on and results of the first study on man. *Skin Pharmacology and Physiology*, 21(5):283–292, sep 2008.

[52] Karsten König, Martin Weinigel, Anna Pietruszka, Rainer Bückle, Nicole Gerlach, and Ulrike Heinrich. Multiphoton tomography of astronauts. In Ammasi Periasamy, Peter T. C. So, and Karsten König,

editors, *Multiphoton Microscopy in the Biomedical Sciences XV*, volume 9329, page 93290Q. SPIE, mar 2015.

[53] Nicole Braun, Sabrina Binder, Hanna Grosch, Carmen Theek, Jasmina Ülker, Hagen Tronnier, and Ulrike Heinrich. Current Data on Effects of Long-Term Missions on the International Space Station on Skin Physiological Parameters. *Skin Pharmacology and Physiology*, 32(1):43–51, dec 2019.

[54] Thibaut Neutelings, Betty V. Nusgens, Yi Liu, Sara Tavella, Alessandra Ruggiu, Ranieri Cancedda, Maude Gabriel, Alain Colige, and Charles Lambert. Skin physiology in microgravity: A 3-month stay aboard ISS induces dermal atrophy and affects cutaneous muscle and hair follicles cycling in mice. *npj Microgravity*, 1:15002, 2015.

[55] Thomas Lang, Jack J.W.A. Van Loon, Susan Bloomfield, Laurence Vico, Angele Chopard, Joern Rittweger, Antonios Kyparos, Dieter Blottner, Ilkka Vuori, Rupert Gerzer, and Peter R. Cavanagh. Towards human exploration of space: The THESEUS review series on muscle and bone research priorities. *npj Microgravity*, 3(1), 2017.

[56] V. Schneider, V. Oganov, A. LeBlanc, A. Rakmonov, L. Taggart, A. Bakulin, C. Huntoon, A. Grigoriev, and L. Varonin. Bone and body mass changes during space flight. *Acta Astronautica*, 36(8-12):463–466, 1995.

[57] A LeBlanc, V Schneider, L Shackelford, S West, V Oganov, A Bakulin, and L Voronin. Bone mineral and lean tissue loss after long duration space flight. Technical Report 2, 2000.

[58] T. P. Stein. Weight, muscle and bone loss during space flight: Another perspective. *European Journal of Applied Physiology*, 113(9):2171–2181, sep 2013.

[59] Sara Tavella, Alessandra Ruggiu, Alessandra Giuliani, Francesco Brun, Barbara Canciani, Adrian Manescu, Katia Marozzi, Michele Cilli,

Delfina Costa, Yi Liu, Federica Piccardi, Roberta Tasso, Giuliana Tromba, Franco Rustichelli, and Ranieri Cancedda. Bone turnover in wild type and pleiotrophin-transgenic mice housed for three months in the international space station (ISS). *PLoS ONE*, 7(3), 2012.

[60] Daniel L. Belavy, Michael Adams, Helena Brisby, Barbara Cagnie, Lieven Danneels, Jeremy Fairbank, Alan R. Hargens, Stefan Judex, Richard A. Scheuring, Roope Sovelius, Jill Urban, Jaap H. van Dieën, and Hans Joachim Wilke. Disc herniations in astronauts: What causes them, and what does it tell us about herniation on earth?, jan 2016.

[61] J. Meseguer, A. Sanz-Andrés, I. Pérez-Grande, S. Pindado, S. Franchini, and G. Alonso. Surface tension and microgravity. *European Journal of Physics*, 35(5):55010, jul 2014.

[62] Marc M. Cohen, Michael T. Flynn, and Renee L. Matossian. Water Walls Architecture: Massively Redundant and Highly Reliable Life Support for Long Duration Exploration Missions. Technical report, 2012.

[63] Brian. Clegg. *Final frontier: the pioneering science and technology of exploring the universe*, volume 52. St. Martin's Press;, New York, first edit edition, aug 2015.

[64] Mark R. Campbell. A review of surgical care in space, 2002.

[65] Chris Kenning. Researchers Test Zero-Gravity Surgery Device, 2012.

[66] Lyndon Ihrke, Chris A.; Linn, Douglas Martin; Bridgwater. United States Patent: 8276958, 2008.

[67] Livia Roseti, Valentina Parisi, Mauro Petretta, Carola Cavallo, Giovanna Desando, Isabella Bartolotti, and Brunella Grigolo. Scaffolds for Bone Tissue Engineering: State of the art and new perspectives. *Materials Science and Engineering C*, 78:1246–1262, sep 2017.

[68] Jan Henkel, Maria A. Woodruff, Devakara R. Epari, Roland Steck,

Vaida Glatt, Ian C. DIckinson, Peter F.M. Choong, Michael A. Schuetz, and DIetmar W. Hutmacher. Bone Regeneration Based on Tissue Engineering Conceptions-A 21st Century Perspective, sep 2013.

[69] Satyavrata Samavedi, Abby R. Whittington, and Aaron S. Goldstein. Calcium phosphate ceramics in bone tissue engineering: A review of properties and their influence on cell behavior, sep 2013.

[70] Sergey V. Dorozhkin. Calcium orthophosphates as bioceramics: State of the art, nov 2010.

[71] Wouter Habraken, Pamela Habibovic, Matthias Epple, and Marc Bohner. Calcium phosphates in biomedical applications: Materials for the future?, mar 2016.

[72] Matti Kesti, Christian Eberhardt, Guglielmo Pagliccia, David Kenkel, Daniel Grande, Andreas Boss, and Marcy Zenobi-Wong. Bioprinting Complex Cartilaginous Structures with Clinically Compliant Biomaterials. *Advanced Functional Materials*, 25(48):7406–7417, dec 2015.

[73] David B. Kolesky, Kimberly A. Homan, Mark A. Skylar-Scott, and Jennifer A. Lewis. Three-dimensional bioprinting of thick vascularized tissues. *Proceedings of the National Academy of Sciences of the United States of America*, 113(12):3179–3184, mar 2016.

[74] Feng Zhu, Chu Qin, Lin Tao, Xin Liu, Zhe Shi, Xiaohua Ma, Jia Jia, Ying Tan, Cheng Cui, Jinshun Lin, Chunyan Tan, Yuyang Jiang, and Yuzong Chen. Clustered patterns of species origins of nature-derived drugs and clues for future bioprospecting. *Proceedings of the National Academy of Sciences of the United States of America*, 108(31):12943–12948, aug 2011.

[75] Giancarlo Lancini and Arnold L. Demain. Bacterial pharmaceutical products. In *The Prokaryotes: Applied Bacteriology and Biotechnology*, volume 9783642313, pages 257–280. Springer-Verlag Berlin Heidelberg,

jan 2013.

[76] Tilman Ahlfeld, Ashwini Rahul Akkineni, Yvonne Förster, Tino Köhler, Sven Knaack, Michael Gelinsky, and Anja Lode. Design and Fabrication of Complex Scaffolds for Bone Defect Healing: Combined 3D Plotting of a Calcium Phosphate Cement and a Growth Factor-Loaded Hydrogel. *Annals of Biomedical Engineering*, 45(1):224–236, jan 2017.

[77] Tilman Ahlfeld, Falko Doberenz, David Kilian, Corina Vater, Paula Korn, Günter Lauer, Anja Lode, and Michael Gelinsky. Bioprinting of mineralized constructs utilizing multichannel plotting of a self-setting calcium phosphate cement and a cell-laden bioink. *Biofabrication*, 10(4), 2018.

[78] Erik Trampe, Klaus Koren, Ashwini Rahul Akkineni, Christian Senwitz, Felix Krujatz, Anja Lode, Michael Gelinsky, and Michael Kühl. Functionalized Bioink with Optical Sensor Nanoparticles for O2 Imaging in 3D-Bioprinted Constructs. *Advanced Functional Materials*, 28(45):1804411, nov 2018.

[79] A. Clauss. Gerinnungsphysiologische Schnellmethode zur Bestimmung des Fibrinogens. *Acta Haematologica*, 17(4):237–246, 1957.

[80] Jinghao Sheng and Zhengping Xu. Three decades of research on angiogenin: A review and perspective, may 2016.

[81] J. C. Rau, L. M. Beaulieu, J. A. Huntington, and Frank C. Church. Serpins in thrombosis, hemostasis and fibrinolysis, 2007.

[82] Jagriti Upadhyay, Olivia M. Farr, and Christos S. Mantzoros. The role of leptin in regulating bone metabolism, jan 2015.

[83] Ana María Lauricella. Variabilidad de las redes de fibrina. *Acta Bioquimica Clinica Latinoamericana*, 41(1):7–19, 2007.

[84] Ariella Shikanov, Min Xu, Teresa K. Woodruff, and Lonnie D. Shea. Interpenetrating fibrin-alginate matrices for in vitro ovarian follicle development. *Biomaterials*, 30(29):5476–5485, oct 2009.

[85] Stephanie A. Smith, Richard J. Travers, and James H. Morrissey. How it all starts: Initiation of the clotting cascade. *Critical Reviews in Biochemistry and Molecular Biology*, 50(4):326–336, 2015.

[86] T. Ahlfeld, V. Guduric, S. Duin, A. R. Akkineni, K. Schütz, D. Kilian, J. Emmermacher, N. Cubo-Mateo, S. Dani, M. v. Witzleben, J. Spangenberg, R. Abdelgaber, R. F. Richter, A. Lode, and M. Gelinsky. Methylcellulose - a versatile printing material that enables biofabrication of tissue equivalents with high shape fidelity. *Biomaterials Science*, 2020.

[87] Aurora C. Hernández-González, Lucía Téllez-Jurado, and Luis M. Rodríguez-Lorenzo. Alginate hydrogels for bone tissue engineering, from injectables to bioprinting: A review. *Carbohydrate Polymers*, 229, feb 2020.

[88] M P Filippov and Br Kohn. Determination of composition of alginates by infrared spectroscopic method. Technical report.

[89] Aurora C. Hernández-Gonzáleza, Lucía Téllez-Juradoa, and Luis M. Rodríguez-Lorenzob. SYNTHESIS OF IN-SITU SILICA-ALGINATE HYBRID HYDROGELS BY A SOL-GEL ROUTE. *Carbohydrate Polymers*, page 116877, aug 2020.

[90] Ella Hodder, Sarah Duin, David Kilian, Tilman Ahlfeld, Julia Seidel, Carsten Nachtigall, Peter Bush, Derek Covill, Michael Gelinsky, and Anja Lode. Investigating the effect of sterilisation methods on the physical properties and cytocompatibility of methyl cellulose used in combination with alginate for 3D-bioplotting of chondrocytes. *Journal of Materials Science: Materials in Medicine*, 30(1):1–16, jan 2019.

[91] Jia Jia, Dylan J. Richards, Samuel Pollard, Yu Tan, Joshua Rodriguez,

Richard P. Visconti, Thomas C. Trusk, Michael J. Yost, Hai Yao, Roger R. Markwald, and Ying Mei. Engineering alginate as bioink for bioprinting. *Acta Biomaterialia*, 10(10):4323–4331, oct 2014.

[92] Murat Guvendiren, Joseph Molde, Rosane M.D. Soares, and Joachim Kohn. Designing Biomaterials for 3D Printing. *ACS Biomaterials Science and Engineering*, 2(10):1679–1693, 2016.

[93] Tiziana Fuoco, Astrid Ahlinder, Shubham Jain, Kamal Mustafa, and Anna Finne-Wistrand. Poly(ϵ-caprolactone-co-p-dioxanone): A Degradable and Printable Copolymer for Pliable 3D Scaffolds Fabrication toward Adipose Tissue Regeneration. *Biomacromolecules*, 21(1):188–198, 2020.

[94] Ben P. Hung, Bilal A. Naved, Ethan L. Nyberg, Miguel Dias, Christina A. Holmes, Jennifer H. Elisseeff, Amir H. Dorafshar, and Warren L. Grayson. Three-Dimensional Printing of Bone Extracellular Matrix for Craniofacial Regeneration. *ACS Biomaterials Science and Engineering*, 2(10):1806–1816, apr 2016.

[95] Zohreh Izadifar, Tuanjie Chang, William Kulyk, Xiongbiao Chen, and B. Frank Eames. Analyzing biological performance of 3D-printed, cell-impregnated hybrid constructs for cartilage tissue engineering. *Tissue Engineering - Part C: Methods*, 22(3):173–188, 2016.

[96] Joydip Kundu, Jin Hyung Shim, Jinah Jang, Sung Won Kim, and Dong Woo Cho. An additive manufacturing-based PCL-alginate-chondrocyte bioprinted scaffold for cartilage tissue engineering. *Journal of Tissue Engineering and Regenerative Medicine*, 9(11):1286–1297, 2015.

[97] Jin Hyung Shim, Ki Mo Jang, Sei Kwang Hahn, Ju Young Park, Hyuntae Jung, Kyunghoon Oh, Kyeng Min Park, Junseok Yeom, Sun Hwa Park, Sung Won Kim, Joon Ho Wang, Kimoon Kim, and Dong Woo Cho. Three-dimensional bioprinting of

multilayered constructs containing human mesenchymal stromal cells for osteochondral tissue regeneration in the rabbit knee joint. *Biofabrication*, 8(1), 2016.

[98] I. Chien Liao, Franklin T. Moutos, Bradley T. Estes, Xuanhe Zhao, and Farshid Guilak. Composite three-dimensional woven scaffolds with interpenetrating network hydrogels to create functional synthetic articular cartilage. *Advanced Functional Materials*, 23(47):5833–5839, dec 2013.

[99] Nieves Cubo-Mateo and Luis M. Rodríguez-Lorenzo. Design of thermoplastic 3D-Printed scaffolds for bone tissue engineering: Influence of parameters of "hidden" importance in the physical properties of scaffolds. *Polymers*, 12(7):1–14, jul 2020.

[100] R. Rosales Ibáñez, N. Cubo-Mateo, L.M. Rodríguez-Lorenzo, Rodríguez Navarrete, A., and M.L. Flores Sánchez. Potential Benefits from 3D Printing and Dental Pulp Stem Cells in Cleft Palate Treatments: An In Vivo Model Study. *Biomedical Journal of Scientific & Technical Research*, 16(2), 2019.

[101] A. Lode, C. Heiss, G. Knapp, J. Thomas, B. Nies, M. Gelinsky, and M. Schumacher. Strontium-modified premixed calcium phosphate cements for the therapy of osteoporotic bone defects. *Acta Biomaterialia*, 65:475–485, jan 2018.

[102] Kathleen Schütz, Anna Maria Placht, Birgit Paul, Sophie Brüggemeier, Michael Gelinsky, and Anja Lode. Three-dimensional plotting of a cell-laden alginate/methylcellulose blend: towards biofabrication of tissue engineering constructs with clinically relevant dimensions. *Journal of Tissue Engineering and Regenerative Medicine*, 11(5):1574–1587, may 2017.

[103] Naomi Paxton, Willi Smolan, Thomas Böck, Ferry Melchels, Jürgen Groll, and Tomasz Jungst. Proposal to assess printability of bioinks for

extrusion-based bioprinting and evaluation of rheological properties governing bioprintability. *Biofabrication*, 9(4), nov 2017.

[104] Myoung Hwan Kim, Yong Wook Lee, Won-Kyo Jung, Junghwan Oh, and Seung Yun Nam. Enhanced rheological behaviors of alginate hydrogels with carrageenan for extrusion-based bioprinting. *Journal of the Mechanical Behavior of Biomedical Materials*, 98:187–194, oct 2019.

[105] A. Cipitria, A. Skelton, T. R. Dargaville, P. D. Dalton, and D. W. Hutmacher. Design, fabrication and characterization of PCL electrospun scaffolds - A review, 2011.

[106] Bong Hyuk Choi, Yun Kee Jo, Cong Zhou, Hyon Seok Jang, Jin Soo Ahn, Sang Ho Jun, and Hyung Joon Cha. Sticky bone-specific artificial extracellular matrix for stem cell-mediated rapid craniofacial bone therapy. *Applied Materials Today*, 18:100531, mar 2020.

[107] Koichiro Uto, Sharmy S. Mano, Takao Aoyagi, and Mitsuhiro Ebara. Substrate Fluidity Regulates Cell Adhesion and Morphology on Poly(ϵ-caprolactone)-Based Materials. *ACS Biomaterials Science and Engineering*, 2(3):446–453, 2016.

[108] L. Moroni, J. R. De Wijn, and C. A. Van Blitterswijk. 3D fiber-deposited scaffolds for tissue engineering: Influence of pores geometry and architecture on dynamic mechanical properties. *Biomaterials*, 27(7):974–985, 2006.

[109] Deepak Gupta, Atul Kumar Singh, Neelakshi Kar, Ashwin Dravid, and Jayesh Bellare. Modelling and optimization of NaOH-etched 3-D printed PCL for enhanced cellular attachment and growth with minimal loss of mechanical strength. *Materials Science and Engineering C*, 98:602–611, may 2019.

[110] L. M. Rodríguez-Lorenzo, A. J. Salinas, M. Vallet-Regí, and J. San Román. Composite biomaterials based on ceramic polymers. I. Reinforced systems based on Al2O3/PMMA/PLLA. *Journal of*

Biomedical Materials Research, 30(4):515–522, apr 1996.

[111] Kosar Samadi, Michelle Francisco, Swati Hegde, Carlos A. Diaz, Thomas A. Trabold, Elizabeth M. Dell, and Christopher L. Lewis. Mechanical, rheological and anaerobic biodegradation behavior of a Poly(lactic acid) blend containing a Poly(lactic acid)-co-poly(glycolic acid) copolymer. *Polymer Degradation and Stability*, 170:109018, dec 2019.

[112] Fahimeh Shahabipour, Nureddin Ashammakhi, Reza K. Oskuee, Shahin Bonakdar, Tyler Hoffman, Mohammad A. Shokrgozar, and Ali Khademhosseini. Key components of engineering vascularized 3-dimensional bioprinted bone constructs, feb 2020.

[113] Joshua P. Temple, Daphne L. Hutton, Ben P. Hung, Pinar Yilgor Huri, Colin A. Cook, Renu Kondragunta, Xiaofeng Jia, and Warren L. Grayson. Engineering anatomically shaped vascularized bone grafts with hASCs and 3D-printed PCL scaffolds. *Journal of Biomedical Materials Research Part A*, 102(12):n/a–n/a, feb 2014.

[114] Tilman Ahlfeld, Nieves Cubo-Mateo, Silvia Cometta, Vera Guduric, Corina Vater, Anne Bernhardt, A. Rahul Akkineni, Anja Lode, and Michael Gelinsky. A Novel Plasma-Based Bioink Stimulates Cell Proliferation and Differentiation in Bioprinted, Mineralized Constructs. *ACS Applied Materials and Interfaces*, 12(11):12557–12572, mar 2020.

[115] Ashwini Rahul Akkineni, Tilman Ahlfeld, Anja Lode, and Michael Gelinsky. A versatile method for combining different biopolymers in a core/shell fashion by 3D plotting to achieve mechanically robust constructs. *Biofabrication*, 8(4):045001, 2016.

[116] Lanying Sun, Daniel Pereira, Qibao Wang, David Baião Barata, Roman Truckenmüller, Zhaoyuan Li, Xin Xu, and Pamela Habibovic. Controlling Growth and Osteogenic Differentiation of Osteoblasts on

Microgrooved Polystyrene Surfaces. *PLOS ONE*, 11(8):e0161466, aug 2016.

[117] Tilman Ahlfeld, Tino Köhler, Charis Czichy, Anja Lode, and Michael Gelinsky. A Methylcellulose Hydrogel as Support for 3D Plotting of Complex Shaped Calcium Phosphate Scaffolds. *Gels*, 4(3):68, aug 2018.

[118] Negar Faramarzi, Iman K. Yazdi, Mahboubeh Nabavinia, Andrea Gemma, Adele Fanelli, Andrea Caizzone, Leon M. Ptaszek, Indranil Sinha, Ali Khademhosseini, Jeremy N. Ruskin, and Ali Tamayol. Patient-Specific Bioinks for 3D Bioprinting of Tissue Engineering Scaffolds. *Advanced Healthcare Materials*, 7(11), jun 2018.

[119] Bárbara B. Mendes, Manuel Gómez-Florit, Alex G. Hamilton, Michael S. Detamore, Rui M.A. Domingues, Rui L. Reis, and Manuela E. Gomes. Human platelet lysate-based nanocomposite bioink for bioprinting hierarchical fibrillar structures. *Biofabrication*, 12(1), 2020.

[120] Swati Midha, Manu Dalela, Deborah Sybil, Prabir Patra, and Sujata Mohanty. Advances in three-dimensional bioprinting of bone: Progress and challenges. *Journal of Tissue Engineering and Regenerative Medicine*, 13(6):term.2847, apr 2019.

[121] Andrew C. Daly, Gráinne M. Cunniffe, Binulal N. Sathy, Oju Jeon, Eben Alsberg, and Daniel J. Kelly. 3D Bioprinting of Developmentally Inspired Templates for Whole Bone Organ Engineering. *Advanced Healthcare Materials*, 5(18):2353–2362, sep 2016.

[122] Gráinne M. Cunniffe, Tomas Gonzalez-Fernandez, Andrew Daly, Binulal N. Sathy, Oju Jeon, Eben Alsberg, and Daniel J. Kelly. * Three-Dimensional Bioprinting of Polycaprolactone Reinforced Gene Activated Bioinks for Bone Tissue Engineering. *Tissue engineering. Part A*, 23(17-18):891–900, sep 2017.

[123] Charlotte Piard, Hannah Baker, Timur Kamalitdinov, and John Fisher.

Bioprinted osteon-like scaffolds enhance in vivo neovascularization. *Biofabrication*, 11(2), 2019.

[124] Johannes Schindelin, Curtis T. Rueden, Mark C. Hiner, and Kevin W. Eliceiri. The ImageJ ecosystem: An open platform for biomedical image analysis, 2015.

[125] Wolfgang Böker, Zhanhai Yin, Inga Drosse, Florian Haasters, Oliver Rossmann, Matthias Wierer, Cvetan Popov, Melanie Locher, Wolf Mutschler, Denitsa Docheva, and Matthias Schieker. Introducing a single-cell-derived human mesenchymal stem cell line expressing hTERT after lentiviral gene transfer. *Journal of Cellular and Molecular Medicine*, 12(4):1347–1359, aug 2008.

[126] Anne Bernhardt, Sophie Wolf, Emilia Weiser, Corina Vater, and Michael Gelinsky. An improved method to isolate primary human osteocytes from bone. *Biomedizinische Technik*, 65(1):107–111, feb 2020.

[127] Jörg Neunzehn, Marie Theres Weber, Gretel Wittenburg, Günter Lauer, Christian Hannig, and Hans Peter Wiesmann. Dentin-like tissue formation and biomineralization by multicellular human pulp cell spheres in vitro. *Head and Face Medicine*, 10(1):25, jun 2014.

[128] Nieves Cubo Mateo, Sandra Podhajsky, Daniela Knickmann, Klaus Slenzka, Tommaso Ghidini, and Michael Gelinsky. Can 3d bioprinting be a key for exploratory missions and human settlements on the moon and mars? *Biofabrication*, 2020.

Part V

APPENDIX

A

OTHER OUTCOMES FROM THE THESIS

The development of this Thesis took **4 years (2016-2020)**, **3 different funding sources**, produced **4 articles** in Scientific Journals, **1 review**, **1 article** in a journal to spread science, **2 posters** in scientific conferences, and many workshops. It also included an **abroad stay of 3 months** in Germany, at Michael Gelinsky's Lab (TFO-TUD, Dresden).

A.1 PUBLICATIONS AND CONFERENCES

◀ *PAPERS*

- **Publication in peer reviewed journal:** Cubo-Mateo, N., Podhajsky, S., Knickmann, D., Slenzka, K., Ghidini, T., Gelinsky, M. (2020). "Can 3D bioprinting be a key for exploratory missions and human settlements on the Moon and Mars?" Biofabrication (In press). DOI: 10.1088/1758-5090/abb53a [128].
- **Publication in peer reviewed journal:** Cubo-Mateo, N., & Rodríguez-Lorenzo, L. M. (2020). "Design of Thermoplastic 3D-Printed Scaffolds for Bone Tissue Engineering: Influence of Parameters of "Hidden" Importance in the Physical Properties of Scaffolds". Polymers, 12(7), 1546. DOI: 10.3390/polym12071546 [99].
- **Publication in peer reviewed journal:** Ahlfeld, T., Cubo-Mateo, N., Cometta, S., Guduric, V., Vater, C., Bernhardt, A., ... Gelinsky, M. (2020). "A Novel Plasma-Based Bioink Stimulates Cell Proliferation and Differentiation in Bioprinted, Mineralized Constructs". ACS Applied Materials and Interfaces, 12(11), 12557-12572. DOI: 10.1021/acsami.0c00710 [114].

– **Publication in peer reviewed journal:** Rosales Ibáñez, Raúl, Cubo-Mateo, N., Rodríguez-Lorenzo, L.M., Rodríguez Navarrete, A., Flores Sánchez, M.L.O. (2019). "Potential Benefits from 3D Printing and Dental Pulp Stem Cells in Cleft Palate Treatments: An In Vivo Model Study". Biomedical Journal of Scientific & Technical Research, 16(2), pp 1-4. DOI: 10.26717/bjstr.2019.16.002831 [100].

– **Article in a Scientific Spreading Journal:** Cubo Mateo, Nieves; Rodriguez-Lorenzo, Luis. (2018). "Bioprinting: From a DIY revolution to patients." Biocoder , 13(April), 41. DOI: https://www.oreilly.com/ideas/bioprinting-from-a-diy-revolution-to-patients

REVIEW ▸

– **Review in peer reviewed journal:** Ahlfeld, T., Guduric, V., Duin, S., Akkineni, A. R., Schütz, K., Kilian, D., Emmermacher, J. , N. Cubo-Mateo, N., [...], Gelinsky, M. (2020). "Methylcellulose - a versatile printing material that enables biofabrication of tissue equivalents with high shape fidelity." Biomaterials Science, 8, 2102-2110. DOI: 10.1039/dobm00027b [86].

POSTERS ▸

– **Poster for ESB2018 - 3D Scaffolds session:** "How to print simultaneously cells and thermoplastics and frequently forgotte n parameters of 3D printing that affect the stability, mechanical properties and biological activity of thermoplastic scaffolds" (p. 187).

– **Poster for Biofabrication 2018 - P-36:** "Potentials of 3D Bioprinting for Space Exploration", Nieves Cubo Mateo, Germany - International conference on Biofabrication 2018 Wurzburg (p. 189).

ORAL EXPOSITION ▸

– **Talk at ESB Conference - September 2015 (Oral presentation awarded by the European Society of Biomaterials as best oral presentation.)** - Talk 176 (Sesion 36, Hall 4A, Advance Manufacturing 2: "3D Bioprinting of Functional Fibrin-Based Skin Equivalents. Authors: Nieves Cubo, Marta García, Diego Velasco, Juan Cañizo, Jose Luis Jorcano. Universidad Carlos III, Spain[1]".

1 Proceedings book available at: http://toc.proceedings.com/28321webtoc.pdf

A.2 MATERIALS AND PROTOCOLS

- New plasma-based bioink for multi-purpose tissue regeneration (p. 115).
- How to bioprint using a low cost DIY bioprinter - Firmware and software adaptation (p. 129).

A.3 DEVICES AND LAB EQUIPMENTS

- DIY low/cost Bioprinter (extruder adaptation, p. 125).

A.4 OPEN SOURCE DATA: CITIZEN SCIENCE

- Openbioprinting.org
- GitHub: openbioprinting

Some of the devices designed in first instance as tools for the lab, were used by other as:

1. Low-cost perfusion systems for drugs in Africa (2017)
2. Tools for bioARTs, to create living structures with fungi and algi (2018)
3. Tools for modern cuisine, creating personalized food (2018)
4. Educational tools, as a research platform in schools (2020)

sectionEducation and training imparted

- **Workshops imparted:**
  - **CERN, Switzerland 2017**: BioFabbing Convergence: Fabrications and Fabulations. "Low-cost hydrogels".
  - **MIT, Boston 2017**: Biosummit 2017, Workshop "How to create your own DIY Bioprinter".

- **Zaragoza, 2018**: 7th National Congress of Accessibility technologies - Discussion table.
- **Bilbao, 2019**: 2.5h workshop, "Create your own bioprinter and natural bioinks"
- **ESA (Noordwijk), 2019**:, 1 day Workshop: experts in Bioprinting, invited to debate about the future of this technology at space.

– **Teaching:**

- **Since 2020, VIU:** Teacher in the Master's Degree on Biomedical Engineering. Subject: Regenerative Medicine Engineering .
- **Since 2019, EDDM:** Teacher in the Expert Course in Biomedical 3D Printing - About: Biomaterials, Bioprinting and regenerative medicine. School of Mechanical Design, EDDM. Madrid .
- **Since 2018, EDDM:** Teacher in the Master in 3D Printing and Advanced Manufacturing, MIFA. About: Bioprinting. School of Mechanical Design, EDDM. Madrid.
- **Since 2017, The Valley:** Teacher of Design and 3D Printing and bioprinting in different Training and Specialization programs (EPIOT, IOT, PDE, MDB). The Valley Business School & The Vallue. Madrid.

– **Talks and Lectures:**

- **León (Spain), 2017**. 1h talk - Anual Conference in Biotecnology (BAC León 2017).
- **Mainz (Germany), 2018**. 15 min talk - Towards Osteoarticular Regeneration through Bioprinting: simultaneous deposition of termoplastics, hydrogels and cells.
- **Bilbao, 2018:** 1h technical talk at University Hospital of biocruces, for clinicians and assistant technical staff.

- **Bordeaux, 2019:** 15 min talk at Workshop for INSERM staff.
- **Madrid, 2020:** 15 min talk (Opening), "3D Printing of human Tissues", 1st Virtual Congress of Diabetes, organized by MSD.

A.5 PROJECTS INVOLVED & FUNDING

Project partially funded and developed under the frameworks of:

- **DAAD Research Grant**. Program: Short-Term Grants, 2018 (**57378443**).
- Project "3D Printing of Living Tissue for Space Exploration" funded from the European Space Agency (ESA). Funds came them partially by the University of Dresden via a **contract (No. 4000123640/17/NL/BJ/gp/TUD)** of OHB System AG, Bremen and by OHB System AG itself, under a c**ontract of the European Space Agency ESA (contract No. 4000123640/18/NL/BJ/gp)**.
- "Low intensity ultrasounds for early detection and modulation of tumour and stroma". **Convocatoria Proyecto Retos I+D+i 2017. AEI/FEDER: DPI2017-90147-R.** Entidad financiadora: Agencia Estatal de Investigación, Ministerio de Economía, Industria y Competitividad, Gobierno de España.

B

ETHICAL CONSIDERATIONS AND SOCIO-ECONOMICAL IMPACT

B.1 ETHICAL ISSUES

The experimental part of this thesis (besides the *in vivo* assays) were carried out inside the European union. All the members of the lab comply with the legal and ethical regulations of the European Commission and received a proper instruction prior to any contact with the primary human cells, in order to assure that the research complies with ethical principles and follow all the European and National ethical guidelines (in particular EU Directive 2004/23/EC) regarding the use of human cells and tissues. The same can be applied for welfare and protection of animals used for scientific purposes (Directive 2010/63/EU).

1. **Human plasma:** Fresh frozen human plasma was provided by a local blood bank (Deutsches Rotes Kreuz - Blutspendedienst Nord-Ost, Dresden, Germany). It is blood intended just for research and never for patient use.

2. **Human cells:** Cell culture experiments included the use of primary adult human cells, mesenchymal stromal cells (MSC) isolated from bone marrow. The cells were isolated from donors after obtaining informed consent.

    a) **MSC** were isolated from residual material or removed tissue that would otherwise be discarded: the MSC were isolated from material remaining after bone marrow transplantations (Medical

Clinic I) or from material removed in the course of total hip replacement (University Centre of Orthopaedics and Trauma Surgery). These cells are routinely used for research purposes in the lab of the applicant and the Ethics Commission of the Faculty of Medicine of Technische Universität Dresden has approved the usage of these cells for research.

b) **Human preosteoblasts (hOB)** were isolated from the femoral head of an osteoarthritic patient (female, 56 years) undergoing total hip replacement at the University Hospital Carl Gustav Carus Dresden (Germany) after informed consent (approval by the ethics commission of TU Dresden, EK 303082014).

c) **Human dental pulp stem cells (hDPSC)** were isolated from human wisdom teeth. The ethics commission of TU Dresden approved the application of hDPSC for *in vitro* experiments (EK 106042010).

3. **Animals:** For the *in vivo* studies carried out by Raúl Rosales Laboratory (Mexico), male Vietnamese pig subtype were used. The process was approved by the ethical committee (CE/FESI/052017/1174) for the pilot study.

B.2 SOCIO-ECONOMICAL IMPACT

The use and development of low cost, open-source technologies allows the spreading and access of technology and knowledge.

As reflected previously, the techologies and the knowledge generated in space exploration missions can be translated to isolated areas of the Earth, or those with few available resources.

C

EXTRA DOCUMENTATION

C.1 PAPERS PUBLISHED IN SCIENTIFIC JOURNALS

- **3D printing of skin equivalents with plasma derivatives** (p. 179).
- **Plasma bioink for bone tissue engineering** (p. 180).
- **Study of printing PCL scaffolds properties for bone tissue engineering** (p. 181).
- **Use of 3D printed PCL scaffolds *in vivo*** (p. 182).
- **Methylcellulose minireview** (p. 183).
- **3D Bioprinting as a medical tool for Space exploration** (p. 184).

C.2 POSTERS PRESENTED AT SCIENTIFIC CONFERENCES

- **Poster 3D Scaffolds session:** "How to print simultaneously cells and thermoplastics and frequently forgotten parameters of 3D printing that affect the stability, mechanical properties and biological activity of thermoplastic scaffolds" (p. 187).
- **Poster P-36:** "Potentials of 3D Bioprinting for Space Exploration", Nieves Cubo Mateo, Germany - International conference on Biofabrication 2018 Wurzburg (p. 189).

C.3 DRAWINGS

- **Mechanical sets and subsets for assembly** (p. 191).

Table C.1: Published publications with Impact Factors and Quartiles information.

year	Title	Journal	Cites	Quartile	SJR 2019	SJR Pub. year	JCR 2019
2016	3D bioprinting of functional human skin: production and *in vivo* analysis	Biofabrication, IOP	146	Q1	2.12	1.52	8.21
2019	Potential benefits from 3D Printing and dental pulp stem cells in cleft palate treatments: an *in vivo* model study	Biomedical Journal of Scientific & Technical Research	1	Q2	-	0.55	-
2020	A novel plasma-based bioink stimulates cell proliferation and differentiation in bioprinted, mineralized constructs	ACS Applied Materials & Interfaces	4	Q1	2.57	2.57	8.76
2020	Methylcellulose-a versatile printing material that enables biofabrication of tissue equivalents with high shape fidelity	Biomaterials Science (RSC)	1	Q1	1.44	1.44	6.183
2020	Design of thermoplastic 3D printed scaffolds for bone tissue engineering: influence of parameters of "hidden" importance [...]	Polymers, MPDI	-	Q1	0.72	0.72	3.43
2020	Can 3D bioprinting be a key for exploratory missions and human settlements on the Moon and Mars?	Biofabrication, IOP	-	Q1	2.12	2.12	8.21

C.1 PAPERS

Biofabrication

PAPER

3D bioprinting of functional human skin: production and *in vivo* analysis

Nieves Cubo[1,5], **Marta Garcia**[1,2,3,5], **Juan F del Cañizo**[4], **Diego Velasco**[1,3] **and Jose L Jorcano**[1,2]

[1] Department of Bioengineering and Aerospace Engineering, Universidad Carlos III de Madrid (UC3M), Spain
[2] Division of Epithelial Biomedicine, CIEMAT-CIBERER, Madrid, Spain
[3] Instituto de Investigación Sanitaria de la Fundación Jiménez Díaz, Madrid, Spain
[4] Department of Surgery, Universidad Complutense de Madrid, Experimental Medicine and Surgery, Hospital General Universitario Gregorio Marañón, Madrid, Spain
[5] These authors contributed equally.

E-mail: divelasc@ing.uc3m.es **and** jjorcano@ing.uc3m.es

RECEIVED
27 July 2016

REVISED
11 September 2016

ACCEPTED FOR PUBLICATION
14 September 2016

PUBLISHED
5 December 2016

Keywords: 3D bioprinting, skin bioprinting, artificial skin, skin equivalents, skin tissue engineering, 3D skin culture, fibrin hydrogel

Supplementary material for this article is available online

Abstract

Significant progress has been made over the past 25 years in the development of *in vitro*-engineered substitutes that mimic human skin, either to be used as grafts for the replacement of lost skin, or for the establishment of *in vitro* human skin models. In this sense, laboratory-grown skin substitutes containing dermal and epidermal components offer a promising approach to skin engineering. In particular, a human plasma-based bilayered skin generated by our group, has been applied successfully to treat burns as well as traumatic and surgical wounds in a large number of patients in Spain. There are some aspects requiring improvements in the production process of this skin; for example, the relatively long time (three weeks) needed to produce the surface required to cover an extensive burn or a large wound, and the necessity to automatize and standardize a process currently performed manually. 3D bioprinting has emerged as a flexible tool in regenerative medicine and it provides a platform to address these challenges. In the present study, we have used this technique to print a human bilayered skin using bioinks containing human plasma as well as primary human fibroblasts and keratinocytes that were obtained from skin biopsies. We were able to generate 100 cm^2, a standard P100 tissue culture plate, of printed skin in less than 35 min (including the 30 min required for fibrin gelation). We have analysed the structure and function of the printed skin using histological and immunohistochemical methods, both in 3D *in vitro* cultures and after long-term transplantation to immunodeficient mice. In both cases, the generated skin was very similar to human skin and, furthermore, it was indistinguishable from bilayered dermo-epidermal equivalents, handmade in our laboratories. These results demonstrate that 3D bioprinting is a suitable technology to generate bioengineered skin for therapeutical and industrial applications in an automatized manner.

1. Introduction

Skin injuries caused by burns, chronic ulcers from different etiology, infections, cancer surgery, and other genetic and somatic diseases require effective treatment to prevent morbidity or mortality. The World Health Organization estimates that nearly 11 million burn injuries per year worldwide require medical attention, with approximately 265 000 leading to death [1]. To restore the function of the skin after damage and to facilitate wound-healing, autologous grafts (autografts) obtained from own-patients donor sites are commonly used to repair the skin, while avoiding immune-rejection. Unfortunately, the availability of autografts for wound coverage is insufficient when dealing with large and/or severe wounds [2–4]. As a result, several approaches have been explored for skin replacement therapy, such as cultured autologous epithelial autografts (for a review see [5]), but their results are far from ideal, since they are limited by their fragility and the difficulty of handling, unpredictable take rate and sensitivity to mechanical shearing forces

ACS APPLIED MATERIALS & INTERFACES

www.acsami.org

Research Article

A Novel Plasma-Based Bioink Stimulates Cell Proliferation and Differentiation in Bioprinted, Mineralized Constructs

Tilman Ahlfeld,[‡] Nieves Cubo-Mateo,[‡] Silvia Cometta, Vera Guduric, Corina Vater, Anne Bernhardt, A. Rahul Akkineni, Anja Lode,[*] and Michael Gelinsky[*]

Cite This: https://dx.doi.org/10.1021/acsami.0c00710

Read Online

ACCESS | Metrics & More | Article Recommendations | Supporting Information

ABSTRACT: Extrusion-based bioprinting, also known as 3D bioplotting, is a powerful tool for the fabrication of tissue equivalents with spatially defined cell distribution. Even though considerable progress has been made in recent years, there is still a lack of bioinks which enable a tissue-like cell response and are plottable at the same time with good shape fidelity. Herein, we report on the development of a bioink which includes fresh frozen plasma from full human blood and thus a donor/patient-specific protein mixture. By blending of the plasma with 3 w/v% alginate and 9 w/v% methylcellulose, a pasty bioink (plasma-alg-mc) was achieved, which could be plotted with high accuracy and furthermore allowed bioplotted mesenchymal stromal cells (MSC) and primary osteoprogenitor cells to spread within the bioink. In a second step, the novel plasma-based bioink was combined with a plottable self-setting calcium phosphate cement (CPC) to fabricate bone-like tissue constructs. The CPC/plasma-alg-mc biphasic constructs revealed open porosity over the entire time of cell culture (35 d), which is crucial for bone tissue engineered grafts. The biphasic structures could be plotted in volumetric and clinically relevant dimensions and complex shapes could be also generated, as demonstrated for a scaphoid bone model. The plasma bioink potentiated that bioplotted MSC were not harmed by the setting process of the CPC. Latest after 7 days, MSC migrated from the hydrogel to the CPC surface, where they proliferated to 20-fold of the initial cell number covering the entire plotted constructs with a dense cell layer. For bioplotted and osteogenically stimulated osteoprogenitor cells, a significantly increased alkaline phosphatase activity was observed in CPC/plasma-alg-mc constructs in comparison to plasma-free controls. In conclusion, the novel plasma-alg-mc bioink is a promising new ink for several forms of bioprinted tissue equivalents and especially gainful for the combination with CPC for enhanced, biofabricated bone-like constructs.

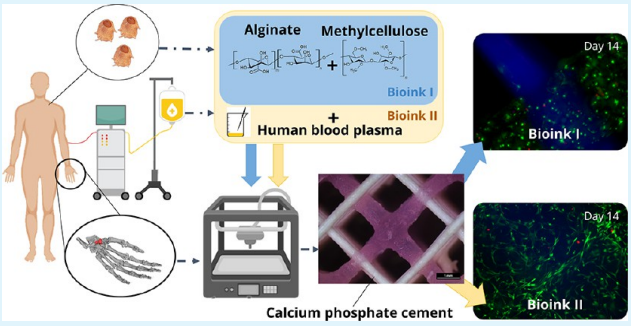

KEYWORDS: *plasma, bioprinting, bone, hydroxyapatite, calcium phosphate cement, alginate, bioink, plotting*

1. INTRODUCTION

Additive manufacturing (AM) has become an intriguing principle for implant fabrication in healthcare. The bottom-up concept allows the manufacturing of implants with patient-specific sizes and shapes, providing better surgical treatment and improved acceptance by the patient.[1] AM was introduced to tissue engineering,[2] combining the patient-specific shape of a scaffold with the patient's autologous cells, improving the biological response and enabling self-healing of the damaged tissues.

One of the most studied AM techniques in biofabrication is extrusion-based bioprinting. The processing in mild conditions, e.g. the absence of unphysiological temperatures like in fused filament fabrication of thermoplastics, is called 3D (bio)-plotting.[3] Bioplotting allows the fabrication of 3D constructs containing temperature sensitive substances, such as growth factors but also cells encapsulated into an artificial extracellular matrix. The plottable cell-matrix mixture is termed bioink.[4] In the past decade, different groups have developed various bioinks based on biopolymers[5−9] or synthetic hydrogels.[10−13]

To further strengthen the patient-specific concept of bioprinting, bioinks which are directly derived from the patient by the use of human plasma were recently introduced.[14−17] Human plasma is the largest component of blood and makes up about 55% of its total volume; it contains over 700 proteins (such as fibrinogen, fibronectin, or albumin as major components but also growth factors, hormones, and cytokines).[18] It has been widely used as base material for tissue engineering to treat skin, bone, muscles, nerves, eye lesions,

Received: January 13, 2020
Accepted: February 24, 2020
Published: February 24, 2020

polymers

MDPI

Article

Design of Thermoplastic 3D-Printed Scaffolds for Bone Tissue Engineering: Influence of Parameters of "Hidden" Importance in the Physical Properties of Scaffolds

Nieves Cubo-Mateo [1,2] and Luis M. Rodríguez-Lorenzo [2,*]

1 Sensors and Ultrasonic Systems Department, Institute for Physical and Information Technologies, ITEFI-CSIC, 28006 Madrid, Spain; nieves.cubo@csic.es
2 Department of Polymeric Nanomaterials and Biomaterials, ICTP-CSIC, 28006 Madrid, Spain
* Correspondence: luis.rodriguez-lorenzo@ictp.csic.es

Received: 4 June 2020; Accepted: 9 July 2020; Published: 13 July 2020

Abstract: Additive manufacturing (AM) techniques are becoming the approaches of choice for the construction of scaffolds in tissue engineering. However, the development of 3D printing in this field brings unique challenges, which must be accounted for in the design of experiments. The common printing process parameters must be considered as important factors in the design and quality of final 3D-printed products. In this work, we study the influence of some parameters in the design and fabrication of PCL scaffolds, such as the number and orientation of layers, but also others of "hidden" importance, such as the cooling down rate while printing, or the position of the starting point in each layer. These factors can have an important impact oin the final porosity and mechanical performance of the scaffolds. A pure polycaprolactone filament was used. Three different configurations were selected for the design of the internal structure of the scaffolds: a solid one with alternate layers (solid) (0°, 90°), a porous one with 30% infill and alternate layers (ALT) (0°, 90°) and a non-alternated configuration consisting in printing three piled layers before changing the orientation (n-ALT) (0°, 0°, 0°, 90°, 90°, 90°). The nozzle temperature was set to 172 °C for printing and the build plate to 40 °C. Strand diameters of 361 ± 26 μm for room temperature cooling down and of 290 ± 30 μm for forced cooling down, were obtained. A compression elastic modulus of 2.12 ± 0.31 MPa for n-ALT and 8.58 ± 0.14 MPa for ALT scaffolds were obtained. The cooling down rate has been observed as an important parameter for the final characteristics of the scaffold.

Keywords: polycaprolactone; 3D printing; scaffolds; bone engineering; thermo-mechanical properties

1. Introduction

Additive manufacturing (AM) techniques are becoming the techniques of choice for the development of scaffolds in tissue engineering (TE). The main advantage of AM over formerly used techniques, such as freeze-drying, particulate-leaching, electrospinning, thermally-induced phase separation or cryopolymerization [1–4], is the ability of designing geometrical parameters of the scaffolds such as pore size, pore strut thickness, pore interconnectivity and pore morphology in advance, and the potential to tailor and scale the manufacturing of scaffolds to each experimental model or patient. In addition, 3D printing has significantly increased the economic feasibility of low volume production runs, because the majority of investment for traditional manufacturing methods like injection moulding is for set up (e.g., fixturing, tooling, and moulds) and costs can only be recouped for high volume production runs [5]. However, the development of 3D printing for tissue

Short Communication

BIOMEDICAL Journal of Scientific & Technical Research

ISSN: 2574 -1241

DOI: 10.26717/BJSTR.2019.16.002831

Potential Benefits from 3D Printing and Dental Pulp Stem Cells in Cleft Palate Treatments: An *In Vivo* Model Study

Rosales Ibáñez Raúl*[1], Cubo Mateo Nieves[2], Rodríguez Lorenzo Luis María[3,4], Rodríguez Navarrete Amairany[1], Flores Sánchez María Leticia Olga[5]

[1]*Laboratorio de Ingeniería Tisular, Fes Iztacala, UNAM, México*

[2]*ITEFI-CSIC, Madrid, Spain*

[3]*ICTP-CSIC, Madrid, Spain*

[4]*CIBER-BBN, Madrid, Spain*

[5]*Bioterio de Fes-Iztacala, UNAM, México*

***Corresponding author:** Rosales Ibáñez Raúl, Laboratorio de Ingeniería Tisular, Fes Iztacala, UNAM, Mexico

ARTICLE INFO

Received: March 13, 2019

Published: March 22, 2019

Citation: Rosales Ibáñez R, Cubo Mateo N, Rodríguez Lorenzo Luis M, Rodríguez Navarrete A, Flores Sánchez María Leticia O. Potential Benefits from 3D Printing and Dental Pulp Stem Cells in Cleft Palate Treatments: An *In Vivo* Model Study. Biomed J Sci & Tech Res 16(2)-2019. BJSTR. MS.ID.002831.

ABSTRACT

Cleft palate is one of the most frequent anomalies in the head and neck region. Different treatments have been used but with each, there are still some disadvantages such as fistulas. The use of a 3D scaffold, with osteoinductive properties, from an easily accessible source, such as dental pulp stem cells, should improve and shorten the treatment of a cleft palate. We conducted a pilot study, in a Vietnamese pig, to evaluate the effectiveness of treating a critical defect of the palate bone, with a 3D Polycaprolactone (PCL) scaffold, in combination with a Beta Tricalcium Phosphate powder (β-TCP) and Pig Dental Pulp Stem Cells (pig DPSC) obtained from the subject pig.

Keywords: Dental Pulp Stem Cells; 3D Scaffold Cleft Palate Regeneration

Introduction

The interest in bone tissue engineering and regeneration therapies, have grown in parallel with the increase in bone fractures due to accidents, musculoskeletal disorders and congenital diseases such as cleft palates [1-3]. Cleft lips and/or palates are the most common congenital malformations of the head and neck and occur in the setting of multiple genetic and environmental factors [4]. In this sense, the repair of the cleft palate intends to establish the division between the oral and nasal cavity, thereby improving feeding, speech, and eustachian tube dysfunction, all while minimizing the negative impact on maxillary growth [5]. For example, although bone healing mediated by iliac crest has been very promising, its efficacy has not always been achieved. Perhaps this is due to the amount of implanted tissue or other factors but whatever the reason is, literature reports that after the treatment palatal wound dehiscence, a residual fistula has an estimated occurrence ranging from 3.4 to 27% [6] and other percentages [7,8]. With the advent of scaffolds printed in three dimensions (3D) [9], we can perhaps overcome those deficiencies. Scaffolds made by a 3D printer, having a microenvironment in three dimensions, may favor the comfort of cells, their survival and proliferation. In this paper the potential of pig dental pulp stem cell in combination with 3D scaffolds for becoming a choice for cleft palate defects treatments is examined in an *in vivo* model.

View Article Online
DOI: 10.1039/D0BM00027B

MINIREVIEW

Methylcellulose – a versatile printing material that enables biofabrication of tissue equivalents with high shape fidelity

Received 00th January 20xx,
Accepted 00th January 20xx

DOI: 10.1039/x0xx00000x

T. Ahlfeld[a,†] & V. Guduric[a,†], S. Duin[a], A.R. Akkineni[a], K. Schütz[a], D. Kilian[a], J. Emmermacher[a], N. Cubo-Mateo[a], S. Dani[a], M. v. Witzleben[a], J. Spangenberg[a], R. Abdelgaber[a], R.F. Richter[a], A. Lode[a], M. Gelinsky[a]

With the aid of biofabrication, cells can be spatially arranged in three dimensions, which offers the opportunity to guide tissue maturation in a better way compared to traditional tissue engineering approaches. A prominent technqiue allowing biofabrication of tissue equivalents is extrusion-based 3D (bio)printing, also called 3D (bio)plotting or robocasting, which comprises cells embedded in the biomaterial (bioink) during the fabrication process. First bioprinting studies introduced bioinks allowing either good cell viability or good shape fidelity. Concepts enabling printing of cell-laden constructs with high shape fidelity were developed only rarely. Recent studies showed the great potential of the polysaccharide methylcellulose (mc) as supportive biomaterial that can be utilized in various ways to enable biofabrication and especially extrusion-based bioprinting of bioinks. This minireview highlights the multiple applications of mc for biofabrication: It was successfully used as sacrifical ink to enable 3D shaping of cell sheets or biomaterial inks as well as as internal stabilizing component of various bioinks. Moreover, a brief overview about first bioprinted functional tissue equivalents is given, which have been fabricated by using mc. Based on these studies, future research should consider mc as an auxiliary materialfor bioinks and biofabricated constructs with high shape fidelity.

Introduction

Bioprinting has emerged as a powerful tool for the fabrication of highly hierarchical, organized tissue equivalents, comprising cells, bioactive molecules and biomaterials in a spatially defined arrangement.[1,2] Previously, it has been postulated that bioprinting of cell-laden (hydrogel) matrices, the bioinks[3], of low polymeric content would be beneficial for the cellular response in bioprinted constructs as the consequential high amount of water is favourable for cell survival, cell migration and diffusion of nutrients, but poor shape fidelity of the fabricated constructs must be expected.[4] The shape fidelity can be defined as the difference of the real printed construct to the related sliced CAD file. For example, poor shape fidelity is a result of fusing of printed features (especially strands fabricated by extrusion-printing), which annihilates the desired inner and outer geometry. Structures fabricated with bioinks of high viscosity resulting from high polymeric content would generate a printed structure of good shape fidelity, since they exhibit a high number of crosslinks, but on the other hand a low cell viability in the bioprinted construct must be expected due to the stiffer and denser hydrogel compromising cellular activities and diffusion processes.[4] However, printing with high shape fidelity is mandatory for most type of tissues, because it allows the fabrication of volumetric and clinically relevant constructs with a controllable spatial distribution of cells. To enable bioprinting of volumetric constructs several approaches have been investigated,[5,6] amongst them visible light-crosslinking,[7] *in situ* UV-crosslinking[8], multichannel printing with stiff and grid-forming materials[9] and FRESH bioprinting (e.g. printing into a gelatin microparticle-based support bath).[10] However, these approaches are limited in the choice of materials and application, due to the high technical efforts which need to be performed, the unclear/potentially harmful effect of photoinitiators on cells[11] or the simple circumstance that stiff (supporting) materials will not be applicable for soft tissues.

As an alternative strategy, many groups investigated blending of hydrogels with additional materials for internal stabilization during fabrication in order to develop novel bioinks, enabling both, enhanced shape fidelity and good cell response. Deducing results from injectable hydrogels, methylcellulose has been coming up as a promising candidate for bioprinting, either alone or in a blend. The following minireview summarises recent advances in the field of biofabrication of tissue constructs using methylcellulose.

Physicochemical properties of methylcellulose

Methylcellulose (mc) is an ether derivative of cellulose, which is synthesized by substitution of the hydrogen atom from the hydroxy group with a methyl group at the positions C-2 and/or C-3 and/or C-6 (Figure 1). The properties of mc were extensively reviewed previously,[12,13] therefore the following section summarises just the most important properties of mc for biofabrication.

MC is a non-toxic and biocompatible polymer, which is an administered food and drug additive in Europe, in the USA and most other countries in the world.[14–16] It is hydrophilic in sol state, but the gelation process increases its hydrophobic properties.[17] In contrast to cellulose (as well as nanocellulose and microfibrillar cellulose), mc is soluble in aqueous media. In the cellulose molecule, hydrogen bonds are formed between the hydroxyl groups.[12] These interactions lead to a very ordered, crystalline structure of cellulose which hinders penetration by water

[a]*Centre for Translational Bone, Joint and Soft Tissue Research University Hospital Carl Gustav Carus and Faculty of Medicine of Technische Universität Dresden, 01307 Dresden, Germany*
Contact: michael.gelinksy@tu-dresden.de
† These authors contributed equally.

1. Introduction

Human spaceflight started almost 60 years ago when Yuri Gagarin flew onboard the Vostok 1 spacecraft as the first human into space and orbited the Earth once. Experience and continuous research have improved technologies for manned space missions, allowing increasing crew size, composition (male/female) and extended duration of spaceflight, making space more and more reachable for humans. In addition, a number of private companies came into play, which offer cheaper and more flexible launch opportunities. Today, manned exploratory missions to the Moon or Mars are widely considered as the next logical steps in human space exploration and, lately, settlement (Ghidini, 2018a, 2018b).

Astronauts exposed to space environmental conditions experience higher radiation and altered gravity levels, which increases the risk of health threatening incidents, such as bone demineralisation, muscles/bones mass reduction, diminished cardiovascular activity, injuries or even cancer. However, in case of serious medical emergencies a fast return to Earth is impossible for far-distant exploratory activities. Thus, crews on these voyages will rely on mission self-sustainability, not only concerning nutrition, oxygen supply or waste removal, but also with respect to medical treatment.

Generally, if the medical events are not too severe, they can be treated onboard with medication and basic first aid kits. However, more severe health incidents, for example extensive burns, bone fractures or even organ failure, can lead to serious emergency situations, and potentially to the death of the astronaut if not treated correctly in time. Therefore, those issues must be considered thoroughly, as in longer and more distant exploratory missions, the probability of these risks increases, while the crew cannot rely on medical infrastructure or support from Earth anymore.

To provide medical treatment on site, new technologies such as additive manufacturing (AM) and bioprinting offer promising perspectives for applications during space exploration missions. In this article, the most probable clinical scenarios are discussed, i.e. the occurrence of medical events during space missions to the Moon or Mars and the potential of 3D (bio)printing technologies to be applied as support for medical interventions in space. Conventional AM can be used to maintain the clinical infrastructure by manufacturing medical tools, splints for medical orthoses, tailored cast and dental equipment, such as implants or fillings.

For direct medical support, 3D bioprinting offers a wide range of potential future applications starting from simple tissue constructs for treating skin lesions and bone defects towards the potential fabrication of complex, vascularized tissue constructs including internal organs, such as kidney and liver. This technology is strongly developing worldwide since few years (Heinrich *et al.*, 2019). However, to accomplish this aim, further improvement of the technology and the materials employed is required to overcome the current limitations. For space applications an adaptation of both, technology and materials, and their maturation to cope with the harsh space environment combined with the necessary reduction of size and weight of all equipment involved are also necessary (Wong and Pfahnl, 2014; Ghidini, Pambaguian and Blair, 2015).

2. Space exploration missions and possible clinical scenarios

Based on previous research on space exploration and on future planned manned missions from national and international space agencies (Horneck *et al.*, 2003, 2006; ISECG, 2018; Woerner and Foing, 2016; Köpping Athanasopoulos 2019), different clinical scenarios including settlement aspects were evaluated to obtain the most probable medical situations that the crew could face (Horneck *et al.*, 2006). These clinical scenarios are composed of a combination of mission scenarios, e.g. short-term close to Earth and long-term distant to Earth, injury and disease incidents, e.g. skin lesions, burns or bone fractures, and potential medical treatment methods, i.e. return to Earth for further treatment or surgery on site etc. Between them, we especially analysed those that have the potential to be medically supported by 3D bioprinting technologies. Table 1 summarises the most important aspects.

2.1 Main health hazards

During a space exploration mission, astronauts are exposed to several health hazards, which can cause injuries, diseases and organ damage that must be treated to save the voyager's life. Major environmental risk factors for human health in space are the impact of radiation and altered gravity levels. Astronauts will be exposed to higher radiation levels than on Earth during space exploration missions to Moon or Mars, as they will be out of the Earth's atmosphere or even, in the latter case, out of the Van Allen belts. Therefore, the risk of developing cancer or any other kind of cell damage is increased (Barcellos-Hoff et al., 2015; Hellweg and Baumstark-Khan, 2007).

Of course, the probability of general injuries, such as burns, cuts, bone fractures or systemic diseases, is also present in space and even increased if the astronaut is involved in exploration activities on a planetary body.

The impact of reduced gravity levels is also relevant, as it decreases exercise capacity and muscle mass (Horneck *et al.*, 2006), leads to bone demineralisation, and influences blood pressure, which can result in multiple organ disorders and also increases the risk of having an accident. Moreover, reduced gravity levels impair also wound healing capability (Davidson *et al.*, 1998).

Generally, medical events in the past during stays on the International Space Station (ISS) or Russian Mir (Horneck *et al.*, 2003; Mcphee and Charles, 2009; Woerner and Foing, 2016) have been harmless and could be treated on-board with

C.2 POSTERS

How to print simultaneously cells and thermoplastics. Frequently forgotten parameters of 3D printing [...]

N. Cubo[1], L.M. Rodríguez-Lorenzo[1,2]

1. Department of Polymeric Nanomaterials and Biomaterials, ICTP-CSIC, Juan de la Cierva 3, 28006 Madrid, Spain
2. CIBER-BBN, Av. Monforte de Lemos 3-5, Pabellón 11, Planta 0, 28029 Madrid, Spain

Abstract

3D Printing allows to build personalized scaffolds through different techniques, materials and parameters to design the printed structures in advance (infill percentage, layer height, temperature, speed, etc.) However, this versatility also comes with huge structural changes that can affect the module and other physical properties of the selected material. The mechanical properties of these scaffolds will determine the short and long-term stability and will be a key point in the regeneration of the tissue. In this work we present some of the most "forgotten/not studied" parameters that must be taken in account when using 3D printing of thermoplastics [1] and new building techniques to print thermoplastics and cells at the same time.

INTRODUCTION

While bioprinting continues its evolution into the development of new and more complex tissues, there are still some limitations to be solved regarding the mechanical behavior of its structures. Temporal scaffolds are normally required to ensure a good stability along the regeneration process, before they are replaced by natural ECM fibers. Hydrogels used as bioinks do not present good mechanical properties, so a reinforcement with other materials (as thermoplastics) is needed. However, thermoplastics present a melting point above the physiological temperature of living cells, which endangers their viability.

Polycaprolactone (PCL) is a widely used biomaterial approved by the FDA & EMA for clinical applications, and its melting point is around 60°C. Some groups have already worked with it in combination with living cells [2,3], however the cell viability is quite affected when exposed at these high temperature. As heat flow and transmission are directly related with the surface area in contact, new structures with smaller contact points and areas must be designed.

In addition, as the cooling down of PCL is very slow at room temperature (RT), its final geometry and internal structure is conditioned with the speed of printing and the use (or not) of coolers (nozzle fan). Changes in RT can highly affect the desired final printed structures. These and other parameters are studied in this work to demonstrate that we can not forget 3D printing basics when working in bioprinting.

MATERIALS AND METHODS

Main studied parameters were:

- Cool down ratio/speed (RT changes)
- Deposition speed
- Layer alternating space (improve isotropic properties)
- Pore filling

Methodology:

- Scaffolds were created using a modified commercial printer (BQ-Witbox 2) and 100% PCL filament (Mw: 84500 ± 1000, 3D4Makers). [Layer height: 0.25 mm, infill: 30%, Tª: 172°C]
- Cool down was controlled with a modulable fan attached to the printer nozzle.
- For composite materials, pores were filled with an hydrogel formed by 3% alginate (Alginic acid sodium salt, Sigma Aldrich). To crosslink it, scaffolds were submerged subsequently on a 1% $CaCl_2$ solution (Calcium chloride dihydrate, Sigma Aldrich) for 10 minutes. Afterwards the excess liquid was removed and scaffolds were stored at RT with controlled humidity conditions.
- For mechanical characterization a QTest 1/L (Elite-MTS) universal test machine in compression mode was used. Samples were printed following the EN ISO 640 [Load cell: 1kN, speed: 5 mm/min].
- Pore morphology was determined by imaging cut samples using a PHILIPS XL30 SEM microcopy operating at 25 kV and coated with Au-Pd using a Polaron SC7640 (Quorum Tech. LTD) sputter coater.

Scaffolds:

(S1)
Alternated layers
(0°, 90°)

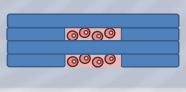

(S2)
Not alternated layers
(0°, 0°, 0°, 90°, 90°,90°)

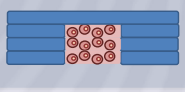

(S3)
Volumetric deposition
(8 layers per cell)

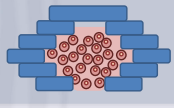

RESULTS AND DISCUSSION

The environmental deposition temperature has been revealed as an important factor for scaffold microstructure. Controlled (slower) cool down of the PCL yield less surface microcracks, which improves the mechanical properties. As the stronger part of the scaffold is the outer PCL, measurements with hydrogel infill did not show any significant change in the modulus. However, because of its elastic nature it is expected to arrest possible cracks produced in the regular structure. Compression module decreased from 4.25 MPa (S1, images A & B) to 2.13 MPa (S2, images C & D) , when changing the alternance of layer direction in the pattern. However, in this last (S2), flow was enhanced because of a bigger pore size (z-axis) and a more homogeneous (isotropic) structure. Higher speeds and slower cooling downs resulted in more chaotic structures (S2, images E & F), which affected the macroporosity (less regular pores) and increased the microporosity, creating random fibers and smaller niches that have a positive effect on cell attachment and differentiation [4].

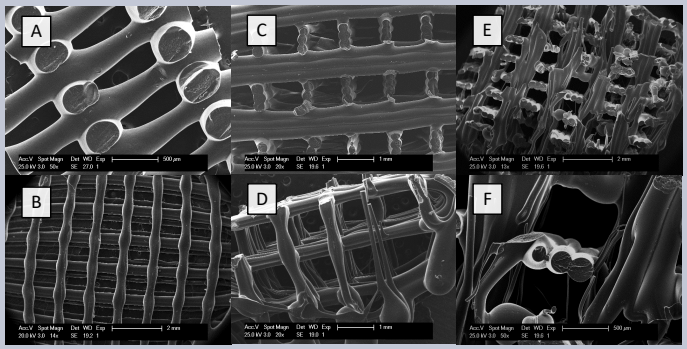

In addition, new simultaneous deposition techniques have demonstrated to improve cell survival when using a combination of thermoplastics and hydrogels (biological studies ongoing) using new geometries (S3, images of the manufacturing procedure below).

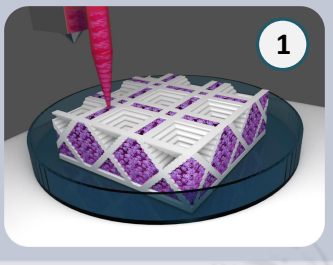

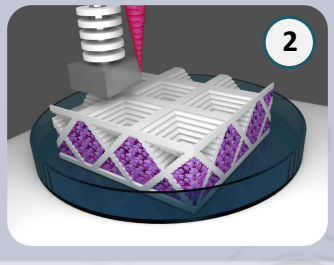

CONCLUSIONS

3D printing approaches needs to be further studied in order to use it along with bioprinting. Some basic parameters (as RT) are frequently forgotten, and can affect even to the mechanical integrity of the scaffolds. Speed and temperature can be modified to obtain more chaotic micropatterns with nanofibers included, without the need of using further devices. This combination of macro and micro pores would enhance cell attachment and regeneration. New deposition strategies can achieve cell survival when printing thermoplastics simultaneously. Pores in the Z axis are important for flow diffusion and tissue ingrowth, allowing a better regeneration and integration.

REFERENCES

[1] Moroni, L. et al., 2006. *Biomaterials*, *27*(7), 974-985
[2] Kundu, J. et. al., 2015. J *Tissue Eng Reg Med, 9(11)*, 1286-1297
[3] Shim, J. H. et al., 2016. Biofabrication, 8(1), 014102
[4] Rodriguez-Lorenzo, L.M., 2012. Et al. *J Tissue Eng Reg Med 6 (6)*, 421-433

ACKNOWLEDGEMENTS

Project partially funded by AEI (Project DPI2017-90147-R)

TECHNISCHE UNIVERSITÄT DRESDEN

OHB

BLUE HORIZON

International Conference on Biofabrication
BIOFABRICATION 2018 WURZBURG

Potentials of 3D Bioprinting for Space Exploration

N. Cubo[1], S. Podhajsky[2], D. Knickmann[2], K. Slenzka[3], T. Ghidini[4], M. Gelinsky[1]

[1] Centre for Translational Bone, Joint and Soft Tissue Research, TU Dresden, Dresden, Germany; [2] OHB System AG, Bremen, Germany; [3] Blue Horizon Sarl, Betzdorf, Luxembourg; [4] European Space Agency, Noordwijk, The Netherlands.

Contact: Nieves Cubo Mateo, Fetscherstr. 74, 01307 Dresden, Germany; e-mail: n.cubo.mateo@gmail.com

Abstract

Today, human exploratory missions to the moon or mars are widely considered as the next logical steps in human space exploration and, ultimately, settlement. Crews on these kind of missions have to be self-sustained, also regarding health issues. Thus, such space exploration missions have to consider a medical infrastructure on-board, so that medical treatment of a wide range of health issues can be provided. The European Space Agency (ESA) identified **3D-bioprinting** as a very promising new technology to support future exploration missions [1] and funded a study to evaluate:

- Scenarios of space exploration (ISS, Moon Village, Mars, etc)
- Main health risk and challenges on those scenarios
- How bioprinting can potentially support medical treatments under these limiting conditions
- Tissues of interest that can be bioprinted
- State-of-the-art bioprinting technologies and its possibility to space adaptation
- New materials and methods to create human tissues in the chosen environments

Health risks + Use of 3D Printing (3DP) and Bioprinting (BP)

During a space exploration mission, astronauts encounter health hazards that can cause injuries and organ damage, which have to be treated on-site to save the astronaut's life and to ensure a successful space exploration mission.

Therefore, it is necessary to assess the most probable/catastrophic health risks and propose contingency actions.

Main health risk factors, contingency actions and Bioprinting			
	Radiation (continuous)	**Microgravity (µg) and altered gravity**	**Accidents (impacts, explosions, etc)**
Effects	• **Cell mutation:** cancer, tumours, etc. • **Tissue damage:** already detected on cornea and skin	• **Blood pressure** increase in the upper part of the body: problems with eyes, heart, strokes, aneurysm, etc. • **Bone and muscle loss**: decalcification, lost of mobility and strength, etc.	• **Bone fractures** – risk of complicate fractures because of decalcified bone • **Skin burns** – different degrees • **Lost of oxygen** because of decompression, CO_2 increase, etc.
Actions to be taken	• Use of protective materials and strategies to skip it • Establish standard procedures to treat most common issues	• Pressurized clothes, rotatory spaces to create gravity, etc. → decrease effects • Future: adaptation, evolution	• Isolate and protect villages • Develop new suits and fabrics • Improve O_2 recycle systems
3DP and BP	• 3DP: medical tools, splints, shields • BP: replace organs damaged by radiation	• 3DP: tailored cast, guides to cut bone, orthosis, dental issues • Bioprinting: bone for replacements, blood vessels, arteries, cardiac tissue	• 3DP: On settlements, shields can be created trough 3DP with the materials of the planet, as it is proposed for the Moon Village and regolith [2]. • BP: skin, bone, cartilage, etc

*Also non-physical, psychological issues can arise because of isolation, but those would not be covered in here.

Bioprinting & Tissue Engineering: challenges on Earth + Space

Printed tissues can also be used to test drugs and other medical procedures, as alternative model to animal experimentation and will be very useful for exploratory missions and on board.

ALTERED GRAVITY	VASCULATURE	BIOMATERIALS	bioPRINTING TECHNOLOGY	SPACE SURGERY	BIOLOGY: n°cells/source
Different gravity conditions for printed tissues, bioprinter and crew	Complex networks of (micro- and marcro-) vascular channels on organs	Mechanical loads, degradation, tissue regeneration and integration, cell damage	fast printing of (big) constructs with high resolution and shorter times	On altered and micro-gravity (liquid leakage, evisceration, etc.)	Volumetric tissue constructs/organs: required cell numbers = new cell sources → further research iPs, MSC,ADSC, etc

Space exploration and settlement scenarios

Different exploratory missions are planned for the incoming years; some of them even propose to settle in the Moon or Mars (see picture below). Therefore, diverse clinical scenarios must be approached as crew will be expose to distinct environments, during different periods of time.

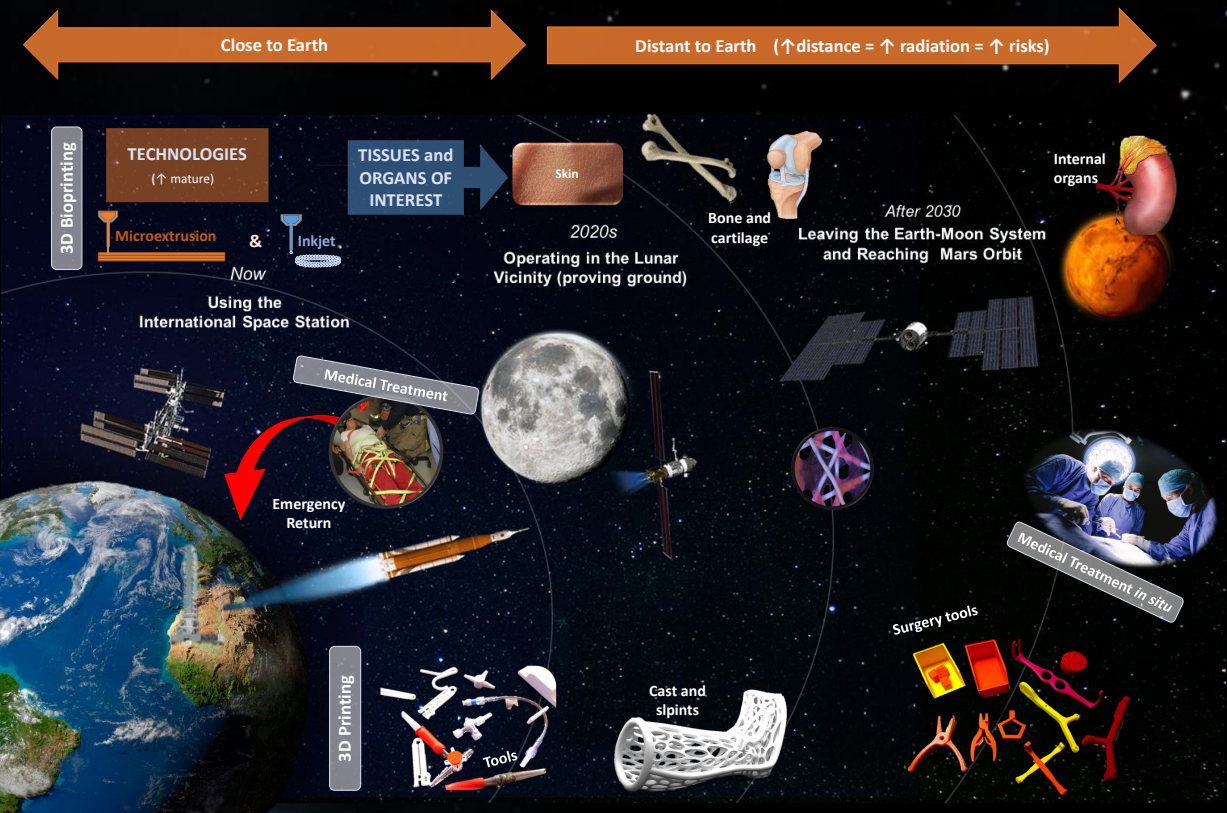

Conclusion

- New solutions are needed to deal with the possible damage astronauts can suffer so they can be **treated autonomously** in almost any scenario.
- Injuries that can be caused because of the loss of muscles and **bone**, as well **as skin injuries** and burns, play a major role in astronauts' health during space flight.
- In this regard, **bioprinting** can be of huge interest as this technology promises that it would be able to reproduce human tissues from patient biopsies and even autologous materials (as human plasma) following established protocols - robotized.
- The most **mature technologies** to do it are microextrusion and inkjet, but the final technology will be a combination of several of them, to cover all the needs.

References

[1] Ghidini, T. (2018) *J Thorac Dis* ***10, S2363-S75***

[2] Woerner, J., and Foing, B. (2016) *Annual Meeting of the Lunar Exploration Analysis Group*. **Vol. 1960**

Acknowledgement

This study is currently funded by the European Space Agency (ESA) within the General Studies Program (GSP).

esa
European Space Agency

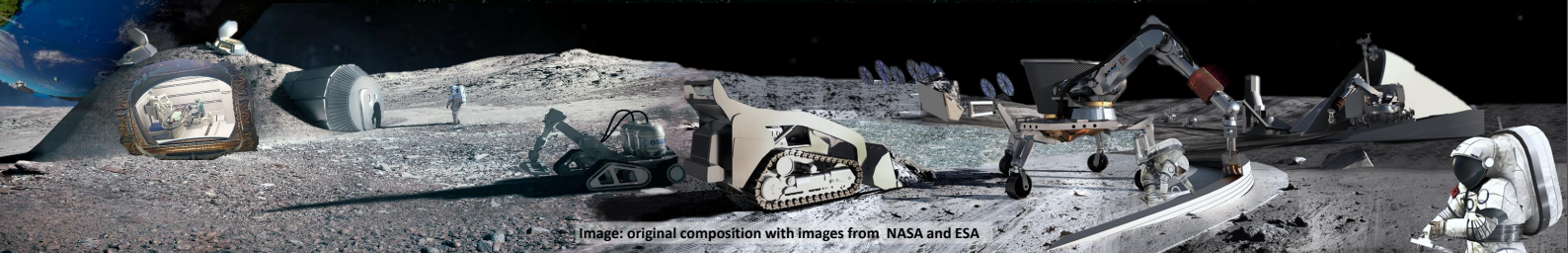

Image: original composition with images from NASA and ESA

C.3 DRAWINGS

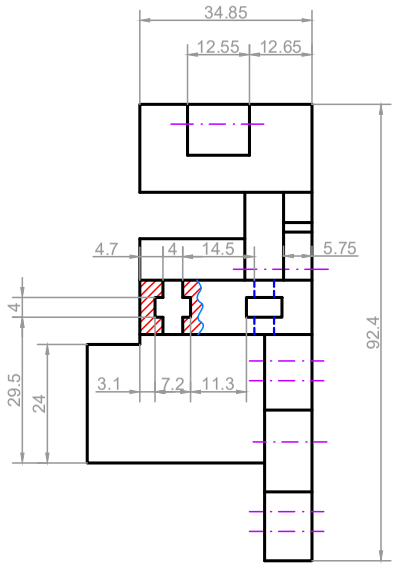

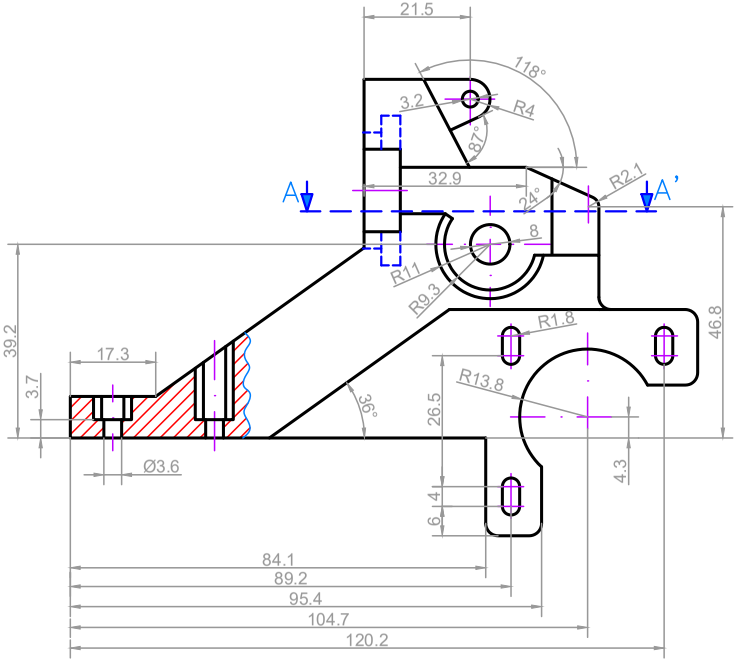

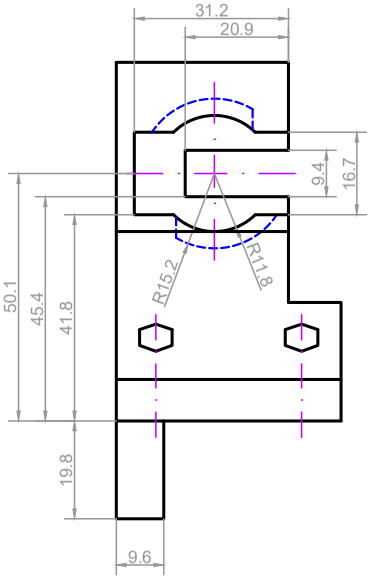

Sección A–A'

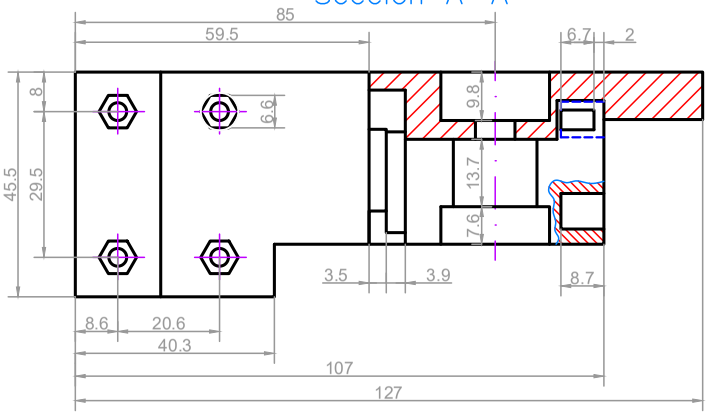

1	BASE_SUPPORT	-	PLA	1	130X95X50
Marca	Denominacion	Norma	Material	N de Piezas	Medidas en bruto

DIBUJADO	22/04/2020	A.PINTO
PROYECTADO	14/04/2017	N.CUBO

ESCALA 1:1

BASE_SUPPORT

PLANO Nº: PEXT-2.1-01

HOJA 1 DE 19

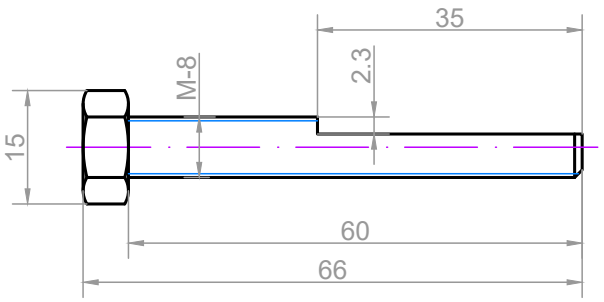

2	Milled Screw	DIN-933	Galv. Steel	1	M-8 x 70
Marca	Denominacion	Norma	Material	N de Piezas	Medidas en bruto

DIBUJADO	22/04/2020	A.Pinto		
PROYECTADO	14/08/2017	N.Cubo		
ESCALA 1:1	Milled Screw		PLANO Nº:	PEXT-2.1-02
			HOJA 2	DE 19

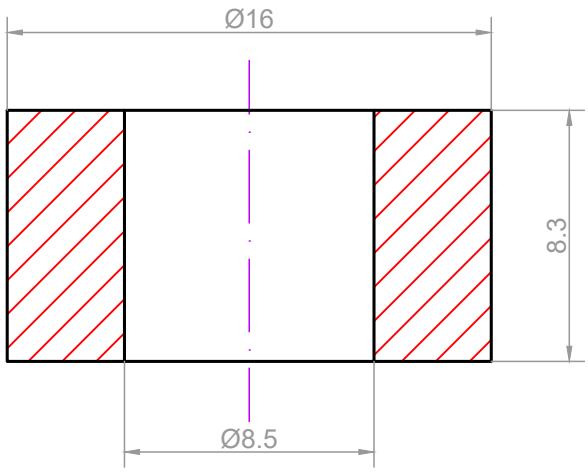

3	Spacer		Steel	1	Ø20 x 15
Marca	Denominacion	Norma	Material	N de Piezas	Medidas en bruto

DIBUJADO	22/04/2020	A.Pinto		
PROYECTADO	14/08/2017	N.Cubo		
ESCALA 4:1	Spacer		PLANO Nº:	PEXT-2.1-03
			HOJA 3	DE 19

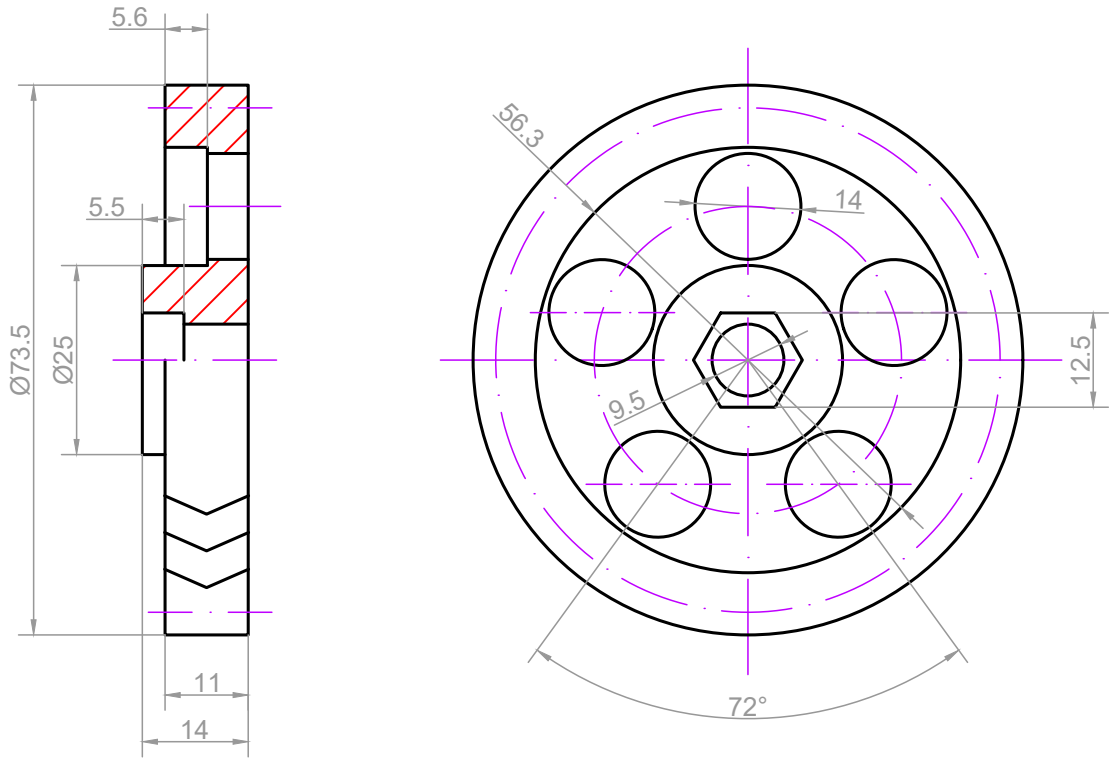

Módulo normal (Mn)	Mn=1.36	
Módulo circular (Mc)	(Mc= Dp / z)	Mc=1.36
Nº Dientes (Z)		Z=47
Diam. Primitivo (Dp)	(Dp= Mn x Z/Cos α)	Dp=69,97
Diam. Exterior (De)	(De= Dp + 2Mn)	De=72.5
Paso normal (Pn)	(Pn= Mn x π)	Pn=4,27
Paso circular (Pc)	(Pc= Mc x π)	Pc=4,67
Altura Diente (H)	(H=2,166 x Mn)	H=2,94
Addendum (a)	(a=Mn)	a=1.36
Dedendum (b)	(b=1.166 x Mn)	b=1,58
Ang. Hélice (α)	α = 24°	

4	Big Gear		PLA	1	Ø73 x 14
Marca	Denominacion	Norma	Material	N de Piezas	Medidas en bruto

DIBUJADO	22/04/2020	A.Pinto		
PROYECTADO	09/08/2015	A.Balsa		
ESCALA 1:1	Big Gear		PLANO Nº:	PEXT-2.1-04
			HOJA 4	DE 19

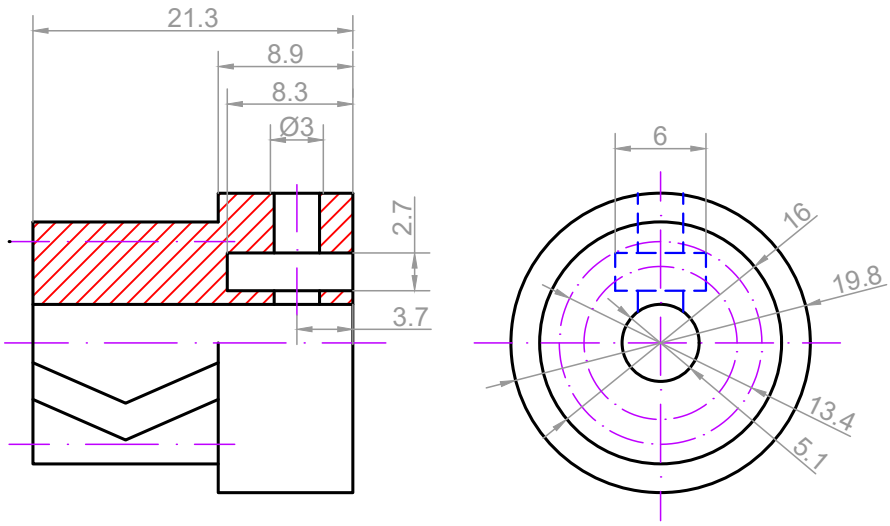

Módulo normal (Mn)	Mn=1.36	
Módulo circular (Mc)	(Mc= Dp / z)	Mc=1.36
Nº Dientes (Z)		Z=9
Diam. Primitivo (Dp)	(Dp= Mn x Z/Cos α)	Dp=13,4
Diam. Exterior (De)	(De= Dp + 2Mn)	De=16
Paso normal (Pn)	(Pn= Mn x π)	Pn=4,27
Paso circular (Pc)	(Pc= Mc x π)	Pc=4,67
Altura Diente (H)	(H=2,166 x Mn)	H=2,94
Addendum (a)	(a=Mn)	a=1.36
Dedendum (b)	(b=1.166 x Mn)	b=1,58
Ang. Hélice (α)	α = 24°	

Marca	Denominacion	Norma	Material	N de Piezas	Medidas en bruto
5	Small Gear		PLA	1	Ø20 x 22

DIBUJADO	22/04/2020	A.Pinto	
PROYECTADO	09/08/2015	A.Balsa	

ESCALA		PLANO Nº:
2:1	Small Gear	PEXT-2.1-05
		HOJA 5 DE 19

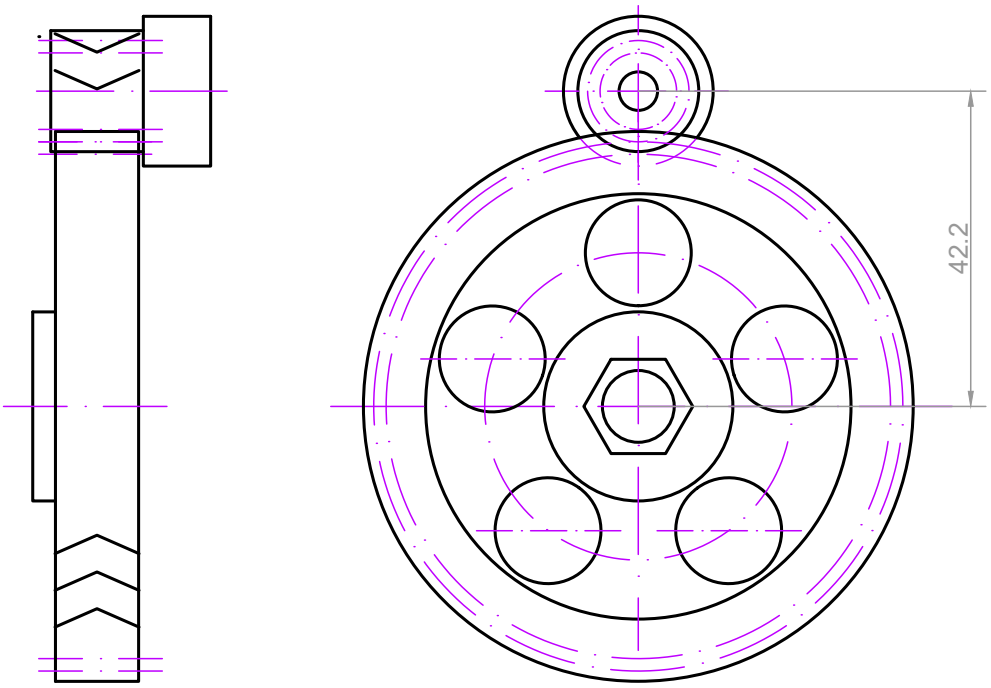

	Motor Transmission				
Marca	Denominacion	Norma	Material	N de Piezas	Medidas en bruto

DIBUJADO	22/04/2020	A.Pinto		
PROYECTADO	09/08/2015	A.Balsa		
ESCALA 1:1	Motor Transmission		PLANO Nº:	PEXT-2.1-06
			HOJA 6	DE 19

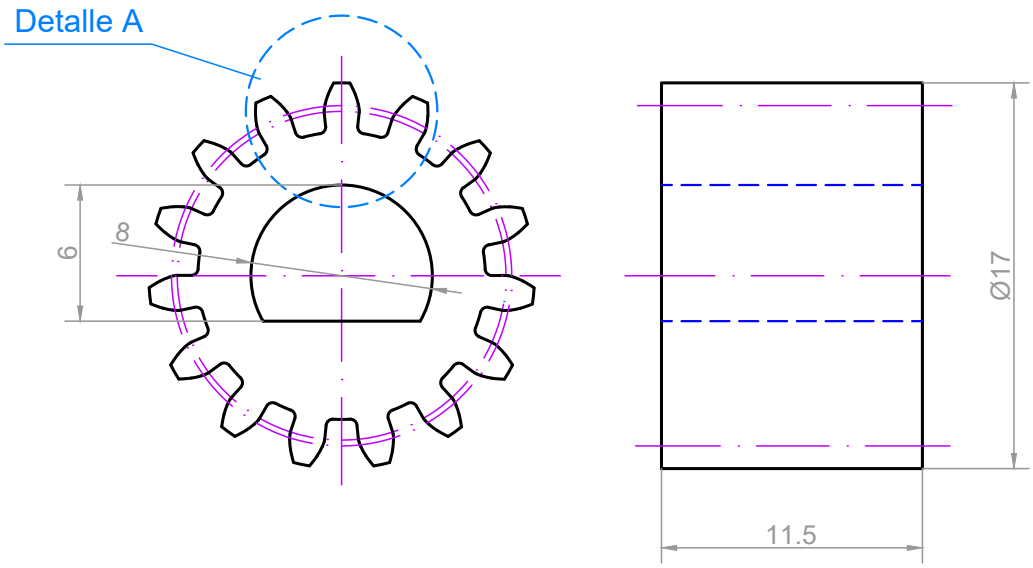

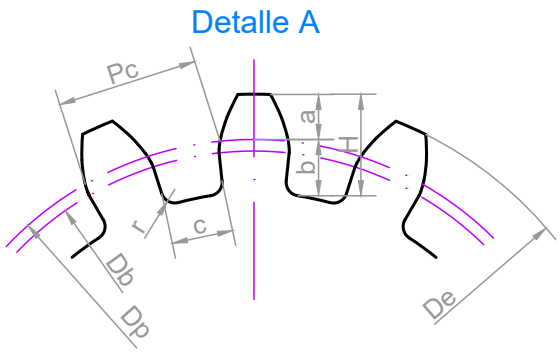

Módulo (m)	m=1	
Nº Dientes (Z)	Z=15	
Diam. Primitivo (Dp)	(Dp= m x Z)	Dp=15
Diam. Exterior (De)	(De= Dp+2m)	De=17
Diam. Base (Db)	(Db= Dp x cos α)	Db=14,49
Paso circular (P)	(P= m x π)	P=3,14
Altura Diente (H)	(H=2,166 x m)	H=2,166
Espesor circular (e)	(e=0,5 x P)	e=1,57
Hueco circular (c)	(c=0,5 x P)	c=1,57
Addendum (a)	(a=m)	a=1
Dedendum (b)	(b=1.166 x m)	b=1,166
Ang. Pres. Crem. (α)	α = 15°	
Radio (r)	(r=0,3xm)	r=0,3

Marca	Denominacion	Norma	Material	N de Piezas	Medidas en bruto
6	Internal Gear		PLA	1	Ø11.5 x 17

DIBUJADO	22/04/2020	A.Pinto	
PROYECTADO	14/08/2017	N.Cubo	

ESCALA		PLANO Nº:
3:1	Internal Gear	PEXT-2.1-07
		HOJA 7 DE 19

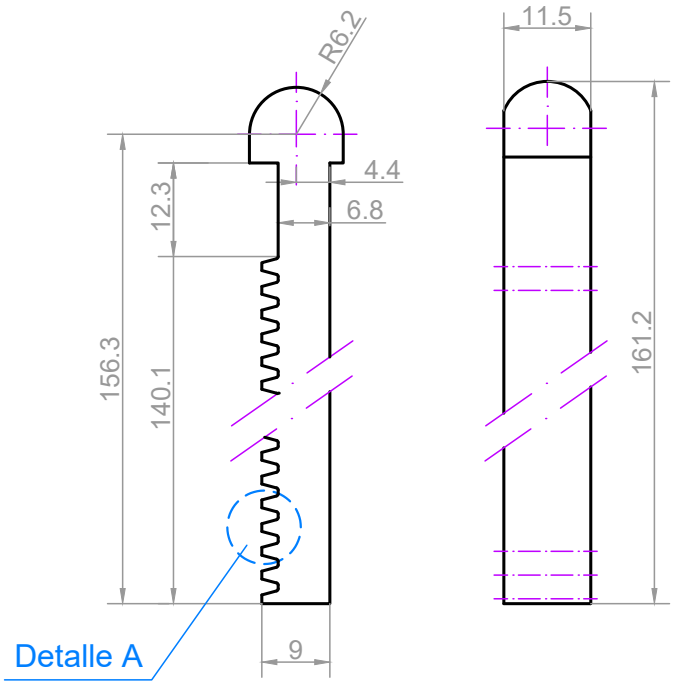

Detalle A

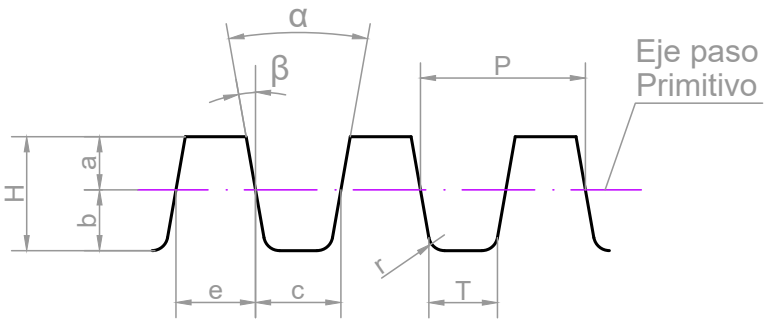

Módulo (m)	m=1	
Paso circular (P)	(P= m x π)	P=3,14
Altura Diente (H)	(H=2,166 x m)	H=2,166
Espesor diente (e)	(e=0,5 x P)	e=1,57
Esp. entre dientes (c)	(c=0,5 x P)	c=1,57
Addendum (a)	(a=m)	a=1
Dedendum (b)	(b=1.166 x m)	b=1,166
Angulo presión (β)	β = 15°	
Radio (r)	(r=0,3xm)	r=0,3

7	Plunge		PLA	1	162 x 11.5 x 9
Marca	Denominacion	Norma	Material	N de Piezas	Medidas en bruto

DIBUJADO	22/04/2020	A.Pinto		
PROYECTADO	14/08/2017	N.Cubo		
ESCALA 1:1	Plunge		PLANO Nº:	PEXT-2.1-08
			HOJA 8	DE 19

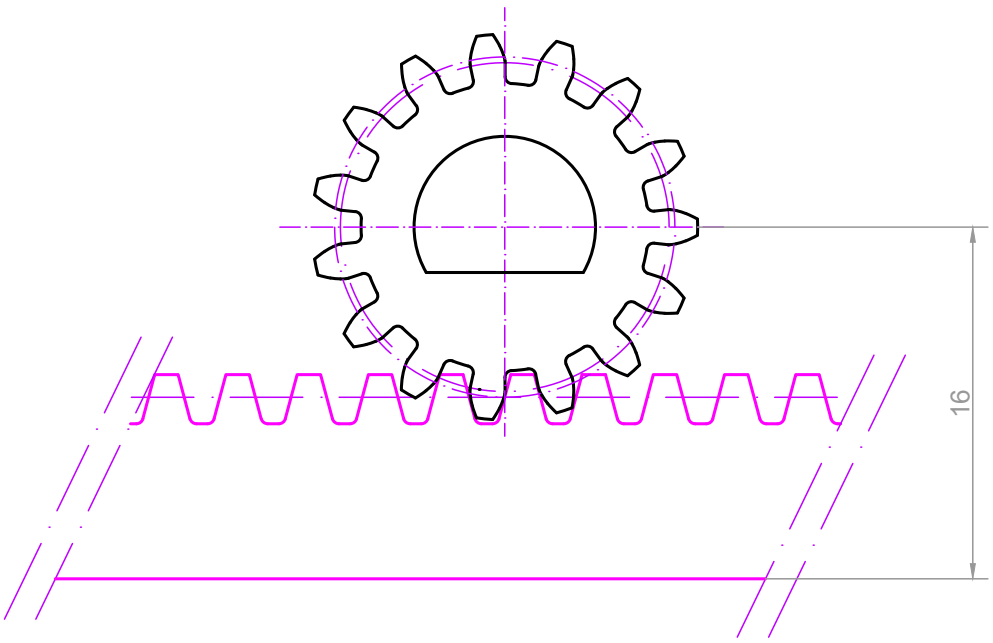

	Rack Transmission				
Marca	Denominacion	Norma	Material	N de Piezas	Medidas en bruto

DIBUJADO	22/04/2020	A.Pinto		
PROYECTADO	14/08/2017	N.Cubo		
ESCALA 3:1	Rack Transmission		PLANO Nº:	PEXT-2.1-09
			HOJA 9	DE 19

Sección B-B'

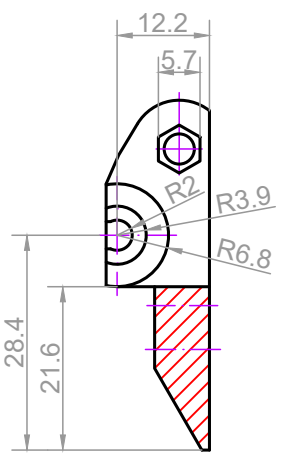

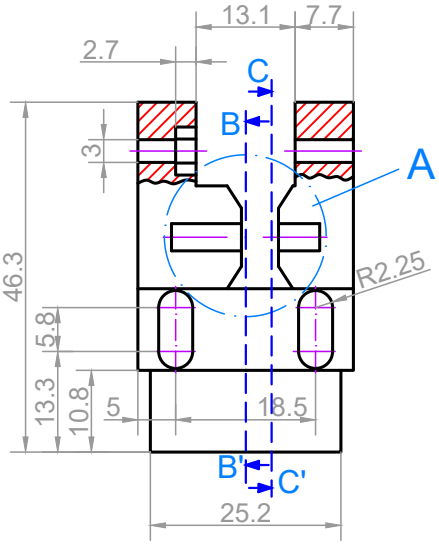

Sección C-C'

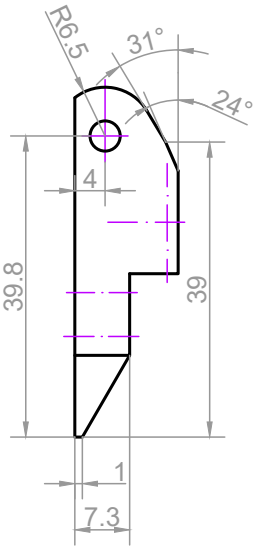

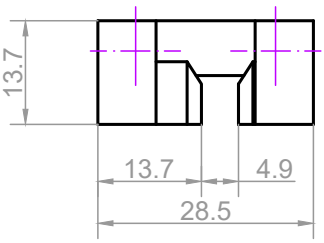

Detalle A

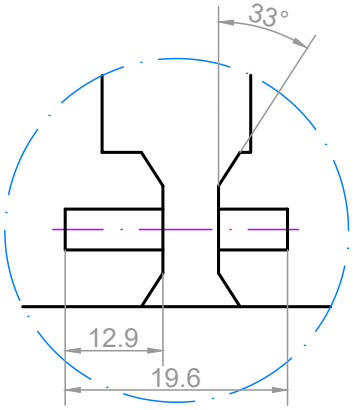

8	Spring Press		PLA	1	47 x 29 x 14
Marca	Denominacion	Norma	Material	N de Piezas	Medidas en bruto

DIBUJADO	22/04/2020	A.Pinto		
PROYECTADO	14/08/2017	N.Cubo		
ESCALA 1:1	Spring Press		PLANO Nº:	PEXT-2.1-10
			HOJA 10	DE 19

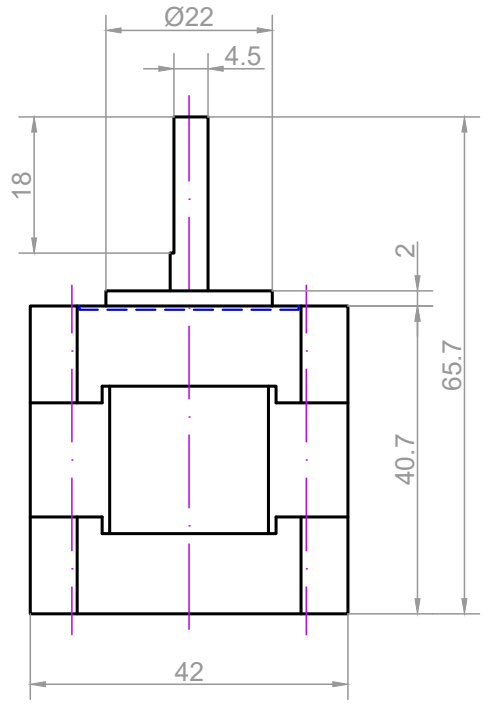

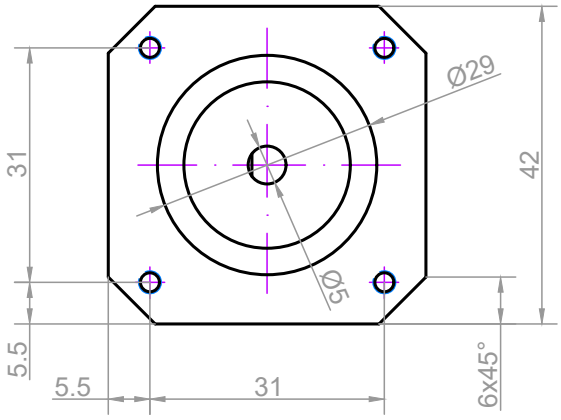

9	Step-By-Step Motor (1.8°)	Nema17		1	66 x 42 x 42
Marca	Denominacion	Norma	Material	N de Piezas	Medidas en bruto

DIBUJADO	22/04/2020	A.Pinto		
PROYECTADO				

ESCALA 1:1	Step-By-Step Motor (1.8°)	PLANO Nº: PEXT-2.1-11
		HOJA 11 DE 19

10

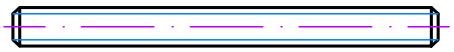

11

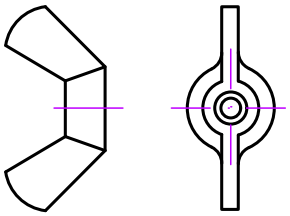

12

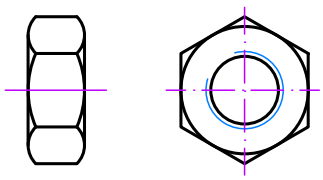

13

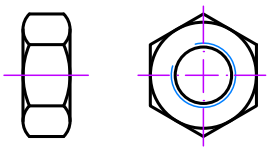

14

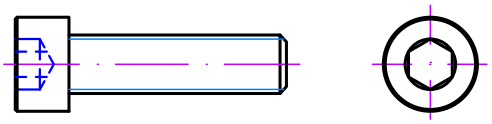

15

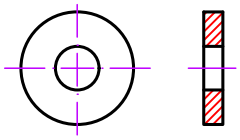

16

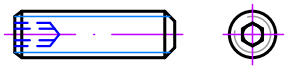

17

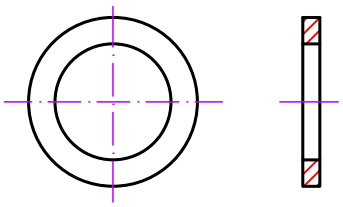

Marca	Denominacion	Norma	Material	N de Piezas	Medidas en bruto
17	Form B Flat whaser	DIN-125-B	Galv.Steel	2	M-8 x 1
16	Set screw	DIN-916	Bluing Steel	1	M-3 x 8
15	Wide flange whaser	DIN-9021	Galv.Steel	2	M-3
14	Cylindrical Head Allen Screw	DIN-912	Galv.Steel	2	M-3 x 15
13	Hex. nut	DIN-934	Galv.Steel	2	M-3
12	Hex. nut	DIN-934	Galv.Steel	2	M-4
11	Wing nut	DIN-315	Galv.Steel	2	M-4
10	Threaded Rod	DIN-976	Galv. Steel	2	M4 x 60

DIBUJADO	22/04/2020	A.Pinto
PROYECTADO	14/08/2017	N.Cubo
ESCALA		

Normalized Elements-1

PLANO Nº: PEXT-2.1-12

HOJA 12 DE 19

18

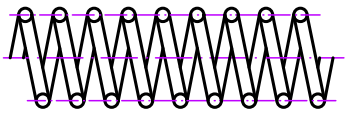

19

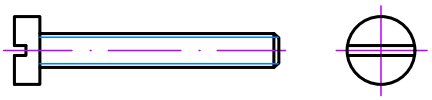

20

21

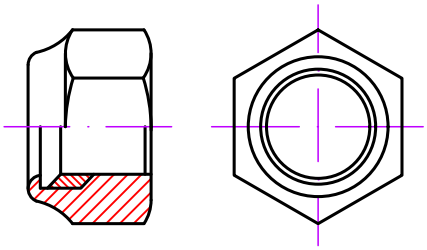

22

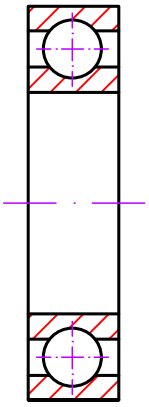

23

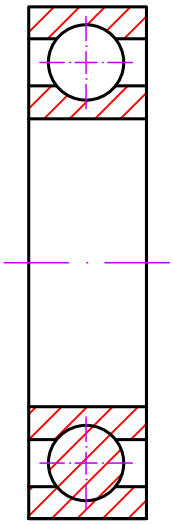

Marca	Denominacion	Norma	Material	N de Piezas	Medidas en bruto
23	Rigid balls bearing 608Z	DIN-625-1	Steel	2	Ø8 x Ø22 x 7
22	Rigid balls bearing 624Z	DIN-625-1	Steel	1	Ø4 x Ø13 x 5
21	Self locking nut	DIN-985	Galv.Steel	1	M-8
20	Threaded Rod	DIN-976	Galv.Steel	1	M-4 x 18
19	Cylindrical sloted head screw	DIN-84	Galv.Steel	1	M-3 x 30
18	Compression Spring	DIN-2095	Zinc-plated steel	2	20 x 5 1,67N/mm

DIBUJADO	22/04/2020	A.Pinto
PROYECTADO	14/08/2017	N.Cubo

ESCALA

Normalized Elements-2

PLANO Nº: PEXT-2.1-13

HOJA 13 DE 19

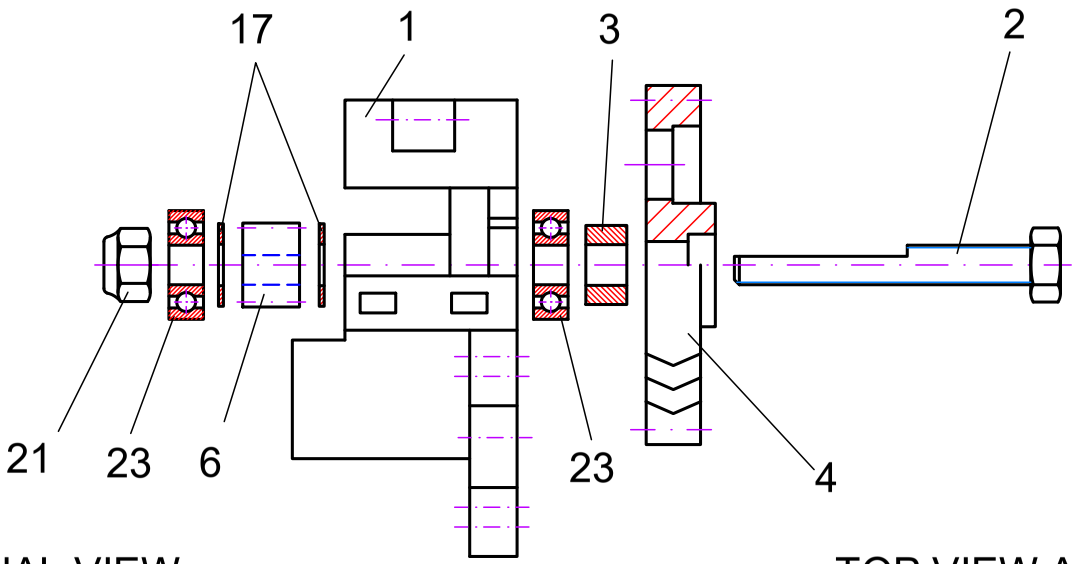

SECTIONAL VIEW

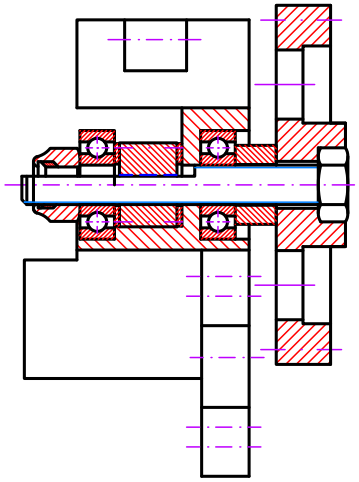

TOP VIEW ASSEMBLY

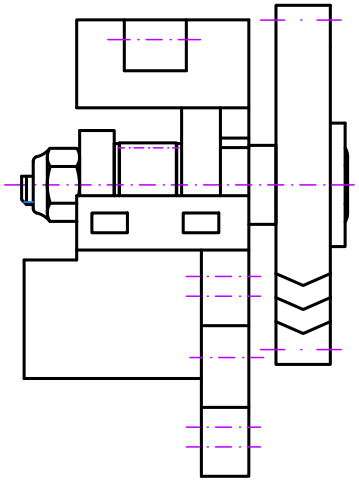

-	SUBSET_1		-	-	-	-
Marca	Denominacion		Norma	Material	N de Piezas	Medidas en bruto
DIBUJADO	22/04/2020	A.PINTO				
PROYECTADO	14/04/2017	N.CUBO				
ESCALA 1:1	SUBSET_1				PLANO N°: PEXT-2.1-14	
					HOJA 14 DE 19	

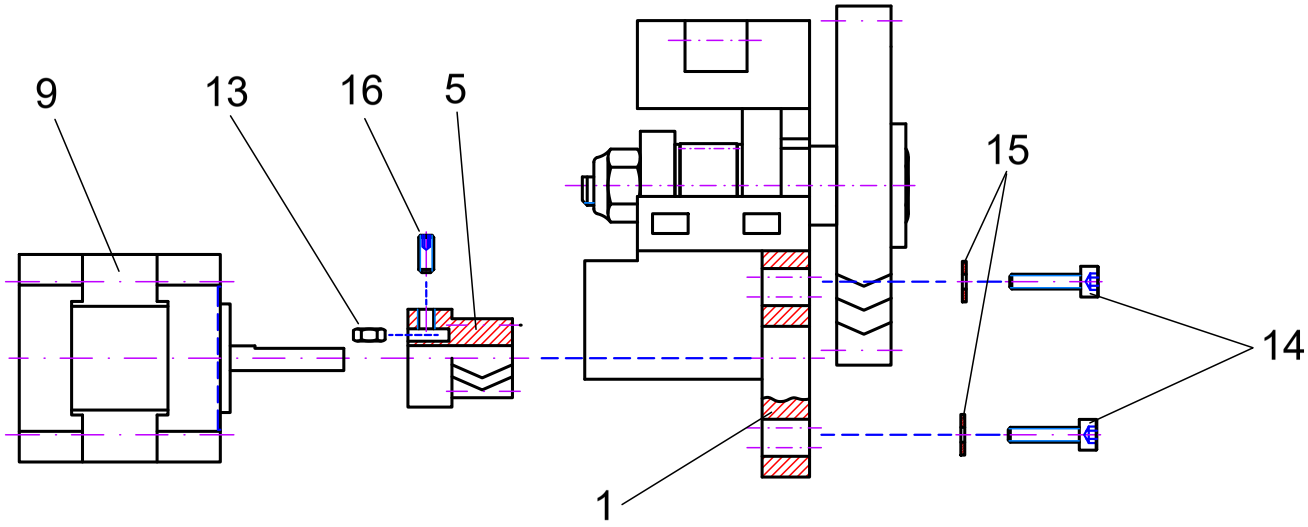

SECTIONAL VIEW

TOP VIEW ASSEMBLY

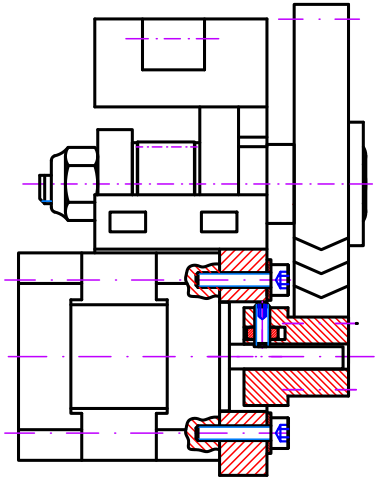

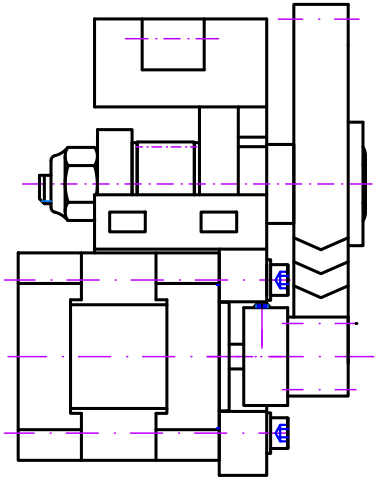

-	SUBSET_2	-	-	-	-
Marca	Denominacion	Norma	Material	N de Piezas	Medidas en bruto

DIBUJADO	22/04/2020	A.PINTO		
PROYECTADO	14/04/2017	N.CUBO		
ESCALA 1:1	SUBSET_2		PLANO N°: PEXT-2.1-15	
			HOJA 15 DE 19	

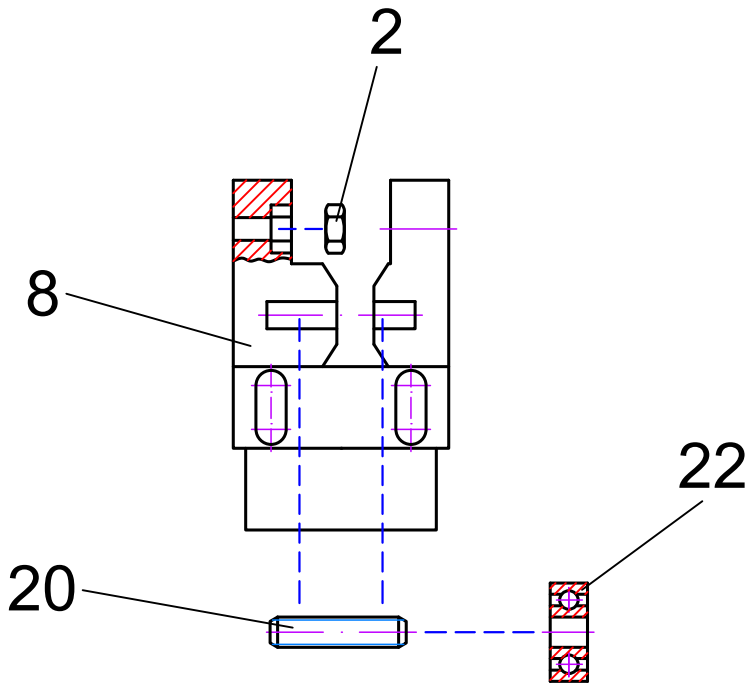

SECTIONAL VIEW

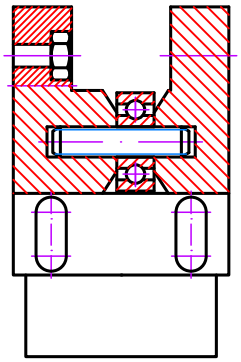

ASSEMBLY

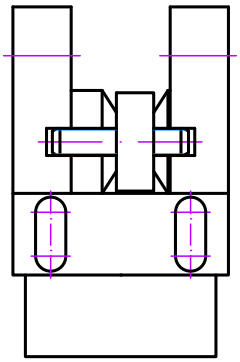

	SUBSET_3				
Marca	Denominacion	Norma	Material	N de Piezas	Medidas en bruto

DIBUJADO	22/04/2020	A.Pinto		
PROYECTADO	14/08/2017	N.Cubo		
ESCALA 1:1	SUBSET_3		PLANO Nº:	PEXT-2.1-16
			HOJA 16	DE 19

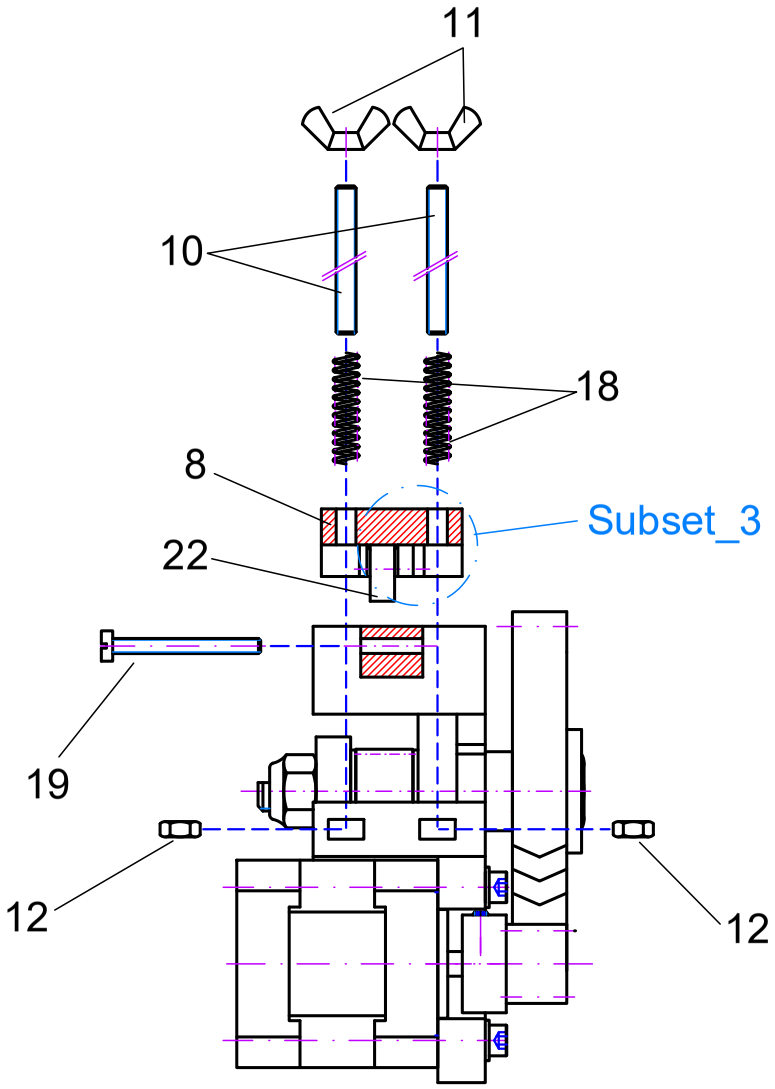

TOP VIEW ASSEMBLY

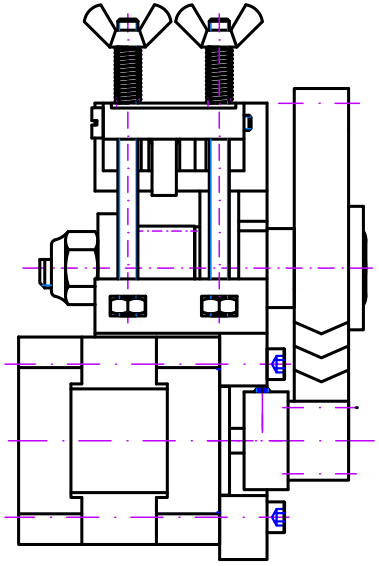

-	SUBSET_4		-	-	-
Marca	Denominacion		Norma	Material	N de Piezas	Medidas en bruto
DIBUJADO	22/04/2020	A.PINTO			
PROYECTADO	14/04/2017	N.CUBO			
ESCALA 1:1	SUBSET_4			PLANO Nº: PEXT-2.1-17	
				HOJA 17 DE 19	

SIDE VIEW OF ASSEMBLY

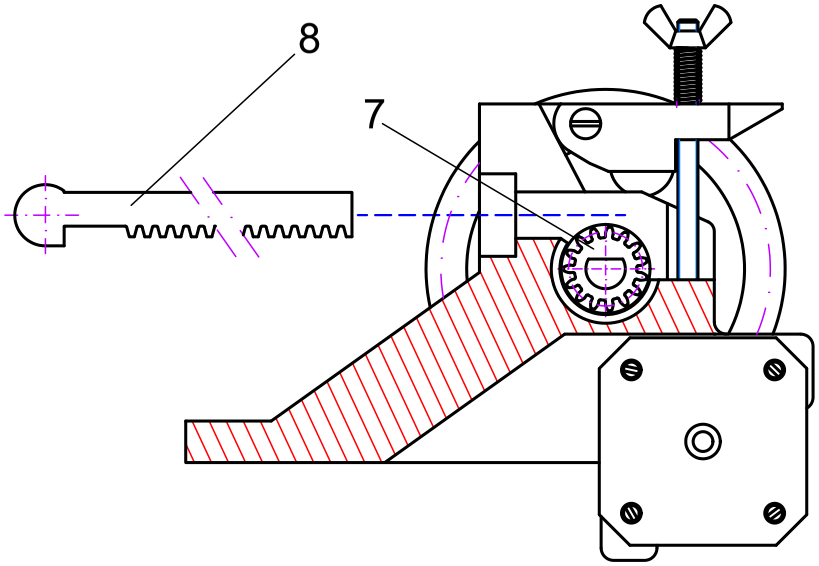

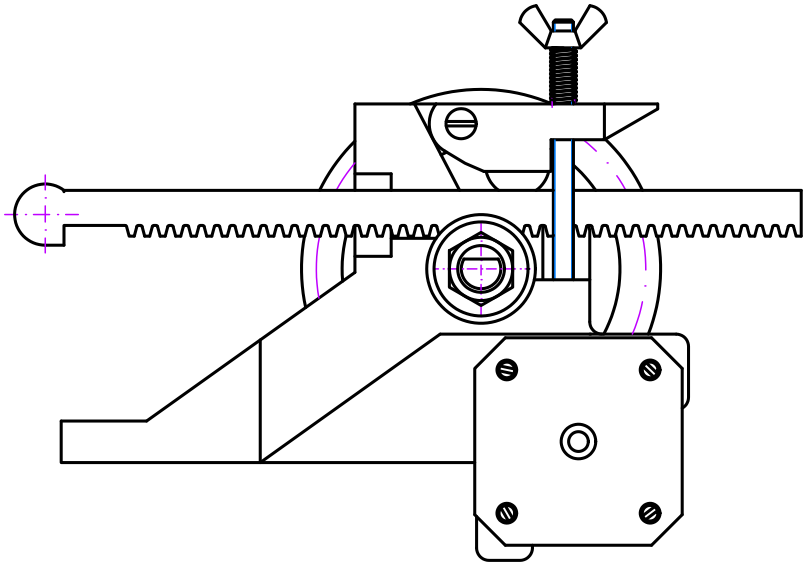

-	SUBSET_5		-	-	-	-
Marca	Denominacion		Norma	Material	N de Piezas	Medidas en bruto
DIBUJADO	22/04/2020	A.PINTO				
PROYECTADO	14/04/2017	N.CUBO				
ESCALA 1:1	SUBSET_5				PLANO Nº: PEXT-2.1-18	
					HOJA 18 DE 19	

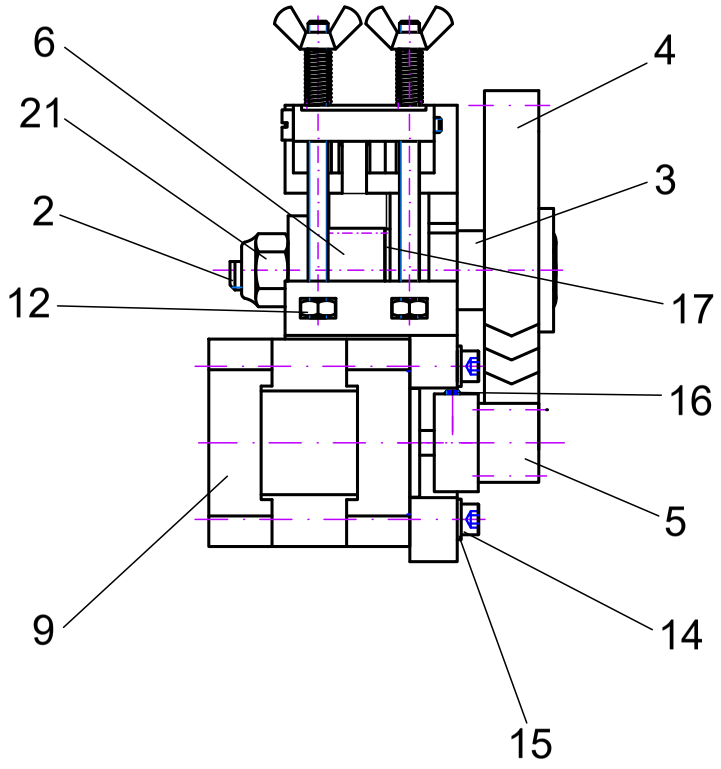

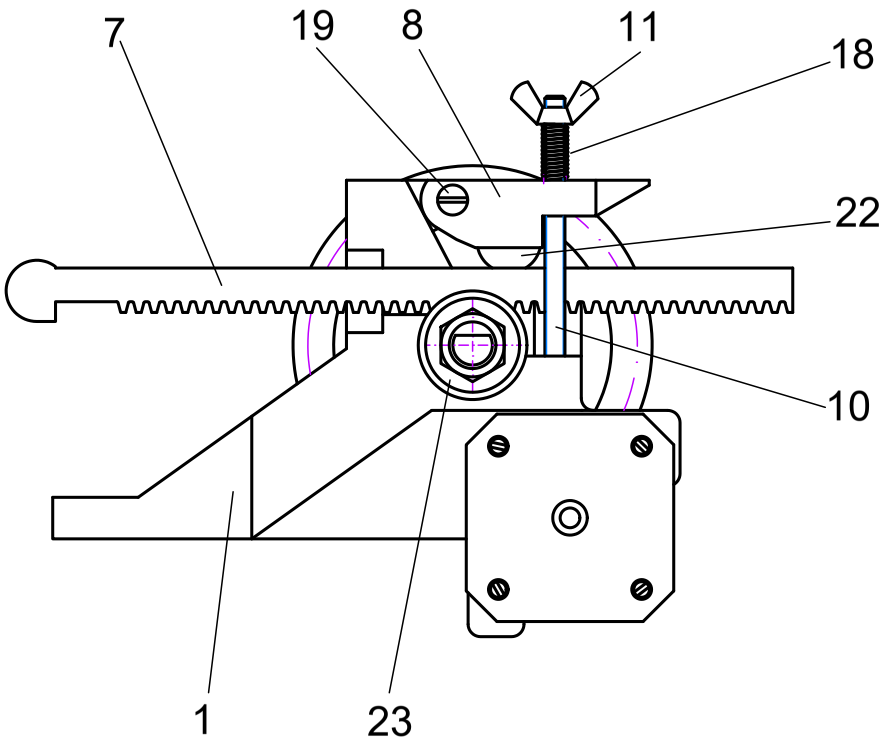

-	EXTRUDER_ASSEMBLY		-	-	-
Marca	Denominacion		Norma	Material	N de Piezas	Medidas en bruto
DIBUJADO	22/04/2020	A.PINTO			
PROYECTADO	14/04/2017	N.CUBO			
ESCALA 1:1	EXTRUDER_ASSEMBLY			PLANO Nº: PEXT-2.1-19	
				HOJA 19 DE 19	

COLOPHON

This document was typeset using an own modified version of the typographical look-and-feel `classicthesis` developed by André Miede. The style was inspired by Robert Bringhurst's seminal book on typography "*The Elements of Typographic Style*". `classicthesis` is available for both LaTeX and LyX:

http://code.google.com/p/classicthesis/

Final Version as of September 14, 2020 (`Nieves Cubo` version 2.0).

DECLARATION OF AUTHORSHIP

I declare that this thesis is an original report of my research, has been written by me and has not been submitted for any previous degree. The experimental work is almost entirely my own work; the collaborative contributions are indicated clearly below and acknowledged. Due references have been provided on all supporting literatures and resources.

I declare that this thesis was composed by myself, that the work contained herein is my own except where explicitly stated otherwise in the text, and that this work has not been submitted for any other degree or professional qualification.

Collaborative work - Authors:

- *NC:* Nieves Cubo (PhD autor)
- *LMR:* Luis María Rodríguez-Lorenzo (PhD Supervisor)
- *ACH:* Aurora Citlalli Hernández (IPN, Mexico)
- *AP:* Alberto Pinto del Corral, ITEFI-CSIC.
- *RR:* Raúl Rosales (UNAM, Mexico)
- *TA:* Tilman Ahlfeld (TU Dresden, Germany)
- *OHB/BH:* Sandra Podhajsky, Daniela Knickmann, Klaus Slenzka
- *ESA:* Tommaso Ghidini, Head of ESA's Structures, Mechanisms and Materials Division

Collaborative work - Writting contributions

- Chapters 1 and 3 were developed as a part of a project funded by the European Space Agency, leaded by OHB/BH team. The part included in this Thesis (except figure 6.1) was developed by myself, if not stated otherwise along the text.
- Chapter 2 contains a review performed jointly by NC and LMR.
- Paste extruder drawings C.3 were made by AP.

Collaborations at experimental level:

- **Alginate:** ACH performed the polymer characterization (molecular weight, polydispersity) and studied autoclaving effect.
- **Biphasic bone:** NC created the plasma-based bioink and performed initial printing test. Investigations on rheology and shape fidelity as well as the study of cell viability and spreading were performed in equal parts by TA and NC. Biphasic plotting of plasma-alg-mc and CPC and analysis of the structures w/o cells (swelling tests, morphology) and w/ cells (studies on cell viability over time) were performed together by NC and TA. Biochemistry was investigated by TA.
- ***In vivo* experiments:** RR and his Lab performed *in vitro* and *in vivo* experiments with the PCL scaffolds provided by us. Work procedures and outcomes at [100].

Previous releases:

Part of the work presented in Chapter 4 was previously published in the PhD Thesis of TA and in *ACS Appl. Mater. Interfaces* as *"A Novel Plasma-Based Bioink Stimulates Cell Proliferation and Differentiation in Bioprinted, Mineralized Constructs"* by *Tilman Ahlfeld, **Nieves Cubo-Mateo**, Silvia Cometta, Vera Guduric, Corina Vater, Anne Bernhardt, A. Rahul Akkineni, Anja Lode, Michael Gelinsky*. This study was conceived by all of the authors.

Part of the work presented in Section 4.3 was previously published in *Polymers, MPDI* as *"Design of Thermoplastic 3D-Printed Scaffolds for Bone Tissue Engineering: Influence of Parameters of "Hidden" Importance in the Physical Properties of Scaffolds"* **by Cubo-Mateo, N.**, & Rodríguez-Lorenzo, L. M. (2020). This study was conceived by all of the authors.

Madrid, September 12, 2020.

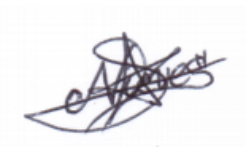

Nieves Cubo Mateo.